

HYBRID ORTHOGONAL CODE SEQUENCES
FOR HIGH-DENSITY SYNCHRONOUS
CDMA SYSTEMS

NYOMAN PRAMAITA

A thesis submitted in partial fulfilment of the
requirements of Liverpool John Moores University
for the degree of Doctor of Philosophy

August 2014

**HYBRID ORTHOGONAL CODE SEQUENCES
FOR HIGH-DENSITY SYNCHRONOUS
CDMA SYSTEMS**

by

Nyoman Pramaita

Liverpool John Moores University

Abstract

One of the primary tasks of the mobile system designers in order to support high density of devices in a CDMA system is to create a code sequence with a capacity for large number of spreading code sequences having low cross-correlation values between them, in order to ensure accommodation of large number of users and to minimise the effect of multiple access interference.

In this research, the design for a novel hybrid orthogonal very large set (HOVLS) code sequence is proposed for high density mobile application scenarios. The design and development of both fixed and variable spreading factor code sequences are presented in this thesis. Both type of code sequences have been implemented via simulation using Matlab/Simulink. The performance of the code sequences has been evaluated and compared with that of existing code sequences. The proposed code sequences are more advantageous for high density mobile networks. The unique feature of the fixed length HOVLS code sequence is that its ACF, CCF, and BER performances are similar to that of orthogonal Gold code sequence and orthogonal m-sequence under Rayleigh flat and frequency selective fading channel conditions while having a significantly higher capacity than those orthogonal code sequences. The proposed HOVLS code sequence could support 134

different cells which is more than twice than that of orthogonal Gold code sequence and orthogonal m-sequence. To the knowledge of the author, this is the largest reported family size in the literature for an orthogonal code sequence for CDMA applications.

In order to support variable data rate, fixed length HOVLS code sequence was developed into orthogonal variable spreading factor code sequence. It is shown that the proposed OVSF code sequence has slightly better CCF than those of OVSF Gold code sequence and m-sequence in terms of CM (correlation margin). The ACF of the proposed OVSF code sequence is similar to those of OVSF Gold code sequence and m-sequence. The proposed OVSF code sequence possesses comparable BER performance to those of orthogonal Gold code sequence and orthogonal m-sequence under flat fading channel condition. Whereas, the BER performance of the proposed OVSF code sequence is slightly better than that of Gold code sequence and OVSF m-sequence under frequency selective fading channel.

Therefore, the proposed HOVLS code sequence is appropriate code sequence in CDMA systems than those of orthogonal Gold code sequence and orthogonal m-sequence for both fixed and variable rate high density network applications.

Acknowledgements

I would like to express the deepest gratitude to my supervisor Dr. Princy Johnson. Her guidance, support, patient advice and encouragement were very valuable throughout my research studies.

I would like to thank all members of LJMU staff for their helpful comments and general enthusiasm to the author.

I also appreciate the financial support from DGHE scholarship for this Ph.D program.

Last but not least, my genuine appreciation to my parents, my wife and my kids, my brother and sisters, and all my family for their support and encouragement to complete my research studies.

Table of Contents

Abstract	i
Acknowledgements	iii
Table of Contents	iv
List of Figures	ix
List of Tables	xii
Acronyms	xiii
Chapter 1 INTRODUCTION	1
1.1 Background	1
1.2 Motivation	2
1.3 Aim and Objectives	4
1.4 Contribution	4
1.5 Thesis Layout	5
Chapter 2 LITERATURE REVIEW ON SPREADING CODE SEQUENCES	6
2.1 Literature Review on Non-Orthogonal Spreading Code Sequences	7
2.2 Literature Review on Orthogonal Spreading Code Sequences	9
Chapter 3 SPREADING CODE SEQUENCES AND SYNCHRONOUS CDMA SYSTEMS	12
3.1 Correlation Properties of Spreading Code Sequence	13
3.1.1 Autocorrelation function	13
3.1.2 Cross-correlation function	13
3.2 Non-orthogonal Spreading Code Sequences	14
3.2.1 Maximal-length sequence	14
3.2.2 Gold code sequence	15

3.2.3 Small set Kasami code sequence	16
3.2.4 Large set Kasami code sequence	17
3.3 Orthogonal Code Sequence	17
3.3.1 Walsh code sequence	17
3.3.2 Orthogonal Gold code sequence	18
3.3.3 Orthogonal m-sequence	18
3.3.4 Orthogonal Small set Kasami code sequence	20
3.3.5 Orthogonal variable spreading factor code sequence	20
3.4 Synchronous CDMA System	23
3.4.1 Differential binary phase shift keying (DBPSK) symbol	24
3.5 Performance Metric	25
3.5.1 Bit error rate	25
Chapter 4 COMMUNICATION CHANNEL	27
4.1 AWGN Channel	27
4.2 Fading Channel	28
4.2.1 Flat fading channel	29
4.2.2 Frequency selective fading channel	31
Chapter 5 DESIGN, IMPLEMENTATION AND ANALYSIS OF FIXED SPREADING FACTOR HYBRID ORTHOGONAL VERY LARGE SET CODE SEQUENCE	33
5.1 Design of HOVLS Code Sequence	33
5.1.1 A Novel method to generate very large set of orthogonal code sequence	36
5.2 Implementation and Analysis of The Proposed HOVLS Code Sequence	42

6.2.1.2 Simulation assumptions for the proposed OVSF HOVLS	
Code sequence of synchronous CDMA system	61
6.2.2 Simulation results and discussions	62
6.2.2.1 Autocorrelation function of the proposed OVSF HOVLS	
code sequence	63
6.2.2.2 Cross-correlation function of the proposed OVSF HOVLS	
code sequence in same groups in the code tree	67
6.2.2.3 Cross-correlation function of the proposed OVSF HOVLS	
code sequence from different groups in the code tree	71
6.2.2.4 BER performance of the proposed OVSF HOVLS code	
sequence under Rayleigh flat fading channel	72
6.2.2.5 BER performance of the proposed OVSF HOVLS code	
sequence under Rayleigh frequency selective	
fading channel for user 2R	75
6.2.2.6 BER performance of the proposed OVSF HOVLS code	
sequence under Rayleigh frequency selective	
fading channel for user R	78
6.2.2.7 Comparison of BER performance of the proposed OVSF	
HOVLS code sequence between user 2R and user R	
under Rayleigh frequency selective fading channel	80
Chapter 7 CONCLUSION AND FUTURE WORK	84
REFERENCES	88
LIST OF CONFERENCES AND JOURNAL SUBMITTED	92
APPENDICES	93
A. The Code Tree for Generation of OVSF Gold Code Sequence	

and OVSF m-Sequence	93
B. Notation of OVSF Gold Code Sequence and OVSF m-Sequence	
in The Code Tree	96
C. Matlab Code and Simulink for The Proposed Code Sequence	99

List of Figures

Figure 3.1	Algorithm for generation of orthogonal small set Kasami code Sequences	21
Figure 3.2	Code tree for generation of OVERSUSF code sequences	22
Figure 4.1	The additive white gaussian noise channel	28
Figure 4.2	Flat fading channel characteristics	30
Figure 4.3	Frequency selective fading channel characteristics	31
Figure 5.1	Block diagram for the simulation of synchronous CDMA System	43
Figure 5.2	ACF of the proposed HOVLS code sequence	47
Figure 5.3	ACF of orthogonal Gold code sequence	47
Figure 5.4	ACF of orthogonal m-sequence	48
Figure 5.5	CCF of the proposed HOVLS code sequence	50
Figure 5.6	CCF of orthogonal Gold code sequence	50
Figure 5.7	CCF of orthogonal m-sequence	51
Figure 5.8	BER versus SNR of the orthogonal code sequences under Rayleigh flat fading channel	52
Figure 5.9	BER versus SNR of the orthogonal code sequences under Rayleigh frequency selective fading channel	54
Figure 5.10	BER versus number of users of the orthogonal code sequences for SNR = 10 dB under Rayleigh frequency selective fading channel	54
Figure 6.1	Code sequence tree for generation of OVSF HOVLS code sequences	58

Figure 6.2	ACF of the proposed OVSF HOVLS code sequence for 128 chip lengths	64
Figure 6.3	ACF of OVSF Gold code sequence for 128 chip lengths	64
Figure 6.4	ACF of OVSF m-sequence for 128 chip lengths	65
Figure 6.5	ACF of the proposed OVSF HOVLS code sequence for 256 chip lengths	65
Figure 6.6	ACF of OVSF Gold code sequence for 256 chip lengths	66
Figure 6.7	ACF of OVSF m-sequence for 256 chip lengths	66
Figure 6.8	CCF of the proposed OVSF HOVLS code sequence in the same groups in the code tree for 128 chip lengths	68
Figure 6.9	CCF of OVSF Gold code sequence in the same groups in the code tree for 128 chip lengths	69
Figure 6.10	CCF of OVSF m-sequence in the same groups in the code tree for 128 chip lengths	69
Figure 6.11	CCF of the proposed OVSF HOVLS code sequence in the same groups in the code tree for 256 chip lengths	70
Figure 6.12	CCF of OVSF Gold code sequence in the same groups in the code tree for 256 chip lengths	70
Figure 6.13	CCF of OVSF m-sequence in the same groups in the code tree for 256 chip lengths	71
Figure 6.14	BER versus SNR of the OVSF code sequences under Rayleigh flat fading channel for user 2R	74
Figure 6.15	BER versus SNR of the OVSF code sequences under Rayleigh flat fading channel for user R	74
Figure 6.16	BER versus SNR of the OVSF code sequences	

	under Rayleigh frequency selective fading channel for user 2R	76
Figure 6.17	BER versus number of users of the OVSF code sequences under Rayleigh frequency selective fading channel for SNR = 10 dB for user 2R	77
Figure 6.18	BER versus SNR of the OVSF code sequences under Rayleigh frequency selective fading channel for user R	79
Figure 6.19	BER versus number of users of the OVSF code sequences under Rayleigh frequency selective fading channel for SNR = 10 dB for user R	79
Figure 6.20	BER versus SNR of the proposed OVSF HOVLS code sequence under Rayleigh frequency selective fading channel between 16 user 2Rs and 16 user Rs	81
Figure 6.21	BER versus SNR of OVSF Gold code sequence under Rayleigh frequency selective fading channel between 16 user 2Rs and 16 user Rs	81
Figure 6.22	BER versus SNR of OVSF m-sequence under Rayleigh frequency selective fading channel between 16 user 2Rs and 16 user Rs	82

List of Tables

Table 3.1	Encoding and decoding operation of DBPSK symbol	25
Table 5.1	Capacity and peak cross-correlation value of the proposed and selected orthogonal code sequences	45
Table 5.2	Merit factor of the proposed HOVLS code sequence	46
Table 5.3	CM of the proposed HOVLS code sequence	49
Table 6.1	MF of the proposed OVSF HOVLS code sequence	63
Table 6.2	CM of the proposed OVSF HOVLS code sequence	68

Acronyms

AWGN	Additive white gaussian noise
ACF	Autocorrelation function
BER	Bit error rate
CCF	Cross-correlation function
CM	Correlation margin
CDMA	Code division multiple access
DS-CDMA	Direct-sequence code division multiple access
HOVLS	Hybrid orthogonal very large set
ISI	Intersymbol interference
MAI	Multiple access interference
MF	Merit figure
OVSF	Orthogonal variable spreading factor
SF	Spreading factor
SNR	Sinal to noise ratio
WCDMA	Wide band code division multiple access

Chapter 1

INTRODUCTION

1.1 Background

Spread spectrum signals for digital communication were originally developed and used for military communication either (1) to provide resistance to hostile jamming, (2) to hide a signal by transmitting it at low power and thus, making it difficult for an unintended listeners to detect its presence in noise, or (3) to make it possible for multi user to communicate through the same channel. Today, however spread spectrum signals are being used for commercial applications including vehicular communications and interoffice wireless communications (Proakis and Salehi, 1998).

Spread spectrum can be defined as a transmission technique using code sequences having bit rate much higher than that of the information signal. The effect of this is to significantly increase the bandwidth of the signal to be transmitted. This transformation is called spreading and the code sequence used to spread the information signal is known as spreading code sequence. The term chip rate is used to describe the rate of the spreading code sequence while the term symbol rate is used to represent the rate of information signal (Fazel and Kaiser, 2008).

Each end user terminal has its own spreading code sequence. The identical spreading code sequence is used in both transformations on each end of radio channel, spreading the original signal, producing wideband signal, and despreading wide band signal back to the original narrowband signal (Korhonen, 2001).

Code division multiple access (CDMA) system is one of the applications based on spread spectrum requiring a unique spreading code sequence for each user

(Hoshyar, et.al, 2008; Cheng, et.al., 2009; Nikjah and Beaulieu, 2008). In a synchronous CDMA system or in the downlink of a mobile network, a signal transmitted by the base station will contain the component intended for the desired user and parts of components intended for other users sharing the same frequency in the cell. From the perspective of the desired user, the signal components intended for other users contribute to noise components known as multiple access interference (MAI) (Jatunov and Madisetti, 2006; Van-Houtum, 2001). This MAI arising from the cross-correlation between the spreading code sequences assigned to different users, limits the performance of a CDMA based wireless system under multiple access interference limited channel conditions (Adeola, et.al, 2011).

There is a growing need for the design of mobile networks that support high density of devices, for example users of national mobile networks in urban areas, in a CDMA system. One of the primary objectives of the mobile system designers in this case is to create a code sequence with a capacity for large number of spreading code sequences having low cross-correlation values between them, in order to ensure accommodation of large number of users and to minimise the effect of multiple access interference (Kedia, et.al, 2010).

In this research, the design of hybrid orthogonal very large set (HOVLS) code sequence is proposed to minimise the effect of MAI and accommodate larger number of users. In order to support variable data rate, fixed spreading factor HOVLS code sequence was developed into orthogonal variable spreading factor code sequence.

1.2 Motivation

Binary spreading code sequence can be divided into two categories, namely, orthogonal and non-orthogonal code sequences. Walsh code sequence has proven its

existence as a popular orthogonal code sequence, whereas m-sequence, Gold and Kasami code sequences have established themselves as popular non-orthogonal binary code sequences (Pal and Chattopadhyay, 2010; Akansu and Poluri, 2007).

There are orthogonal spreading code sequences that are created from non-orthogonal spreading code sequences, namely orthogonal Gold code sequence which is generated from non-orthogonal Gold code sequence (Tachikawa, 1992) and orthogonal m-sequence which is generated from non-orthogonal m-sequence (Donelan and O'Farrell, 1999). These orthogonal spreading code sequences have large family size and can minimise the effect of multiple access interference under flat fading channel condition; however the effect of multiple access interference under frequency selective fading channel condition is worse than that of under flat fading channel condition.

Recently, Chandra and Chattopadhyay in 2009 demonstrated that non-orthogonal small set Kasami code sequence can be converted into orthogonal code sequence, however this orthogonal small set Kasami code sequence only possesses a small family of code sequences compared to the orthogonal Gold code sequence and orthogonal m-sequence.

This research work gets inspiration from the research works described above, and proposes hybrid orthogonal very large set code sequence that minimises the effect of multiple access interference and has a very large family size to accommodate large number of users. This hybrid orthogonal very large set (HOVLS) code sequence is generated from two different non-orthogonal code sequences, namely non-orthogonal m-sequence and large set Kasami code sequence.

1.3 Aim and Objectives

The aim of this research is to design very large sets of orthogonal fixed and variable spreading factor code sequences for multi user wireless mobile networks based CDMA systems and to evaluate their performance against other orthogonal code sequences namely orthogonal Gold and orthogonal m-sequences.

The objectives of this proposed research can be summarised as follows:

1. To design orthogonal code sequence for CDMA applications
2. To develop the orthogonal code sequence into orthogonal variable length code sequence for wide band application
3. To evaluate the performance of the proposed orthogonal fixed spreading factor code sequence including auto-correlation function (ACF), cross-correlation function (CCF) and bit error rate (BER) under various channel conditions namely Rayleigh flat and frequency selective fading channels.
4. To evaluate the performance of the proposed orthogonal variable spreading factor code sequence against the metrics such as CCF and ACF and BER under Rayleigh flat and frequency selective fading channels.

1.4 Contribution

In this research work, hybrid orthogonal code sequences have been designed for fixed and variable spreading factor. It has been shown that for fixed spreading factor, the proposed code sequence has comparable ACF, CCF, and BER performance under flat and frequency selective fading channel conditions to those of orthogonal Gold code sequence and orthogonal m-sequence; however family size of the proposed code sequence is much larger (more than twice) than that of orthogonal Gold code sequence and orthogonal m-sequence.

BER performance of the proposed code sequence for variable spreading factor is comparable to those of orthogonal Gold code sequence and orthogonal m-sequence under flat fading channel condition. However, the proposed orthogonal variable spreading factor (OVSF) code sequence has slightly better BER performance than those of OVSF Gold code sequence and m-sequence under frequency selective fading channel condition.

Besides, the proposed OVSF code sequence has slightly better CCF than those of OVSF Gold code sequence and m-sequence in terms of CM (correlation margin), however ACF of the proposed OVSF code sequence is similar to those of OVSF Gold and m-sequences.

1.5 Thesis Layout

The layout of this PhD thesis is as follows: Chapter 1 shows an introduction of this research work. Literature review on spreading code sequences is presented in Chapter 2. Chapter 3 presents non-orthogonal and orthogonal spreading code sequences and CDMA systems. AWGN, flat and frequency selective fading channels used to evaluate BER performance of the spreading code sequences are presented in Chapter 4. Chapter 5 presents the design and evaluation of fixed spreading factor hybrid orthogonal very large set code sequence. Chapter 6 presents the design and evaluation of variable spreading factor hybrid orthogonal very large set code sequence. Conclusion and future work are presented in Chapter 7. Finally, references and appendices are included.

Chapter 2

LITERATURE REVIEW ON SPREADING CODE SEQUENCES

Binary spreading code sequence can be divided into two categories, i.e. orthogonal and non-orthogonal code sequences. Each of these spreading code sequences has its own unique parameter including autocorrelation, cross-correlation, and family size or number of different spreading code sequences in a chip set (Mollah and Islam, 2012).

When the cross-correlation value between any two spreading code sequences from same chip set is not zero, spreading code sequences in that chip set are called non-orthogonal code sequences. While orthogonal code sequences have zero cross-correlation value between any two spreading code sequences from same chip set (Ziani and Medouri, 2012).

Maximal-sequence (m-sequence), Gold and Kasami code sequences (three families of binary spreading code sequences) have established themselves as popular non-orthogonal binary code sequences. Walsh code sequence, which is generated by mapping code word rows of special square matrices called Hadamard matrices has proven its existence as a popular orthogonal code sequence (Pal and Chattopadhyay, 2010; Dinan and Jabbari, 1998). However, orthogonal Gold code sequence, orthogonal m-sequence, and orthogonal small set Kasami code sequence are orthogonal code sequences generated from their non-orthogonal counter parts (Tachikawa, 1992; Chandra and Chattopadhyay, 2009; Donelan and O'Farrell, 1999).

The orthogonal spreading code sequence used in the code division multiple access (CDMA) and wideband CDMA systems could be divided into fixed-length

and variable-length orthogonal code sequences respectively (Dinan and Jabbari, 1998).

2.1 Literature Review on Non-Orthogonal Spreading Code Sequences

According to (Golomb, 1967) the theory of maximal-sequence (m-sequence) was developed. As the name suggests, these are precisely the code sequences of maximum possible period (which is $N = 2^n - 1$) from n -stage binary shift register with linear feedback. These code sequences possess ideal autocorrelation function (ACF) close to the noise impulse function property, i.e. it can take only two values, N and -1 . However, the code sequences have poor cross-correlation function (CCF) and do not have a large family size. Therefore, these code sequences are inadequate for spread spectrum multiple access communication application requiring much larger number of code sequences and low cross-correlation values to accommodate larger number of user and mitigate the effect of multiple access interference (MAI) respectively.

One important class of periodic code sequences which provides large number of code sequences with good cross-correlation function is Gold code sequence. Therefore, Gold code sequences are more appropriate to be implemented in applications such as spread spectrum multiple access communications in that they can mitigate the effect of MAI and accommodate a large number of users. However, the autocorrelation function of Gold code sequences is not as good as that of the m-sequences, therefore synchronisation at the receiver will be more difficult. These code sequences were proposed by Gold in the late 1960's (Gold, 1968).

Kasami code sequence proposed by Kasami (1966) can be divided into small set and large set Kasami code sequences. Small set Kasami code sequence sets are one of the important types of binary code sequence sets as they are able to mitigate the

effect of MAI in multi user applications due to their very low cross-correlation values. However, this code sequence generates the smallest number of code sequences compared to any other binary spreading code sequence, therefore small set Kasami code sequence is not appropriate for large number of users within the spread spectrum multiple access communications environment. The autocorrelation function (ACF) of small set Kasami code sequence is better than that of Gold code sequence, however is worse than that of m-sequence, and hence synchronisation is more difficult at the receiver than that of m-sequence due to more than two values in the autocorrelation function unlike m-sequence. The point in time, when the receiver can detect sufficiently high signal strength indicates that the starting point of the code sequence is found or synchronised.

Small set Kasami code sequences have better correlation properties compared to Gold code sequences. However, the family size contains less number of code sequences. The number of code sequences can be increased by making some relaxation on the correlation values of the code sequences. The new set of code sequences is called large set Kasami code sequences. These code sequences have the largest family size among binary spreading code sequence. However, autocorrelation and cross-correlation properties are the worst for the code sequence. These code sequences can be implemented in CDMA system or any other multi-user communication system that needs to accommodate a large number of users. However, due to the high value of cross-correlation between the code sequences, the contribution to the effect of MAI by these codes will be significant.

2.2 Literature Review on Orthogonal Spreading Code Sequences

Walsh code sequences are obtained from the Hadamard matrix which is a square matrix where each row in the matrix is orthogonal to all other rows, and each column in the matrix is orthogonal to all other columns (Thompson et.al., 1986). Each column or row in the Hadamard matrix corresponds to a Walsh code sequence of length N . These code sequences are used in synchronous downlink CDMA systems. They can maintain orthogonality (zero cross-correlation function) and thus cause zero MAI in CDMA systems. Even though these code sequences can maintain orthogonality, since the length of the code sequence is directly related to the family size of the code sequence, when the demand from more users arises in CDMA systems, these code sequences are not effective in accommodating those large number of users. Also, ACF of Walsh code sequence is not impulsive, therefore synchronisation is more difficult at the receiver.

Orthogonal spreading code sequence proposed in (Tachikawa, 1992) is generated from non-orthogonal Gold code sequence. This orthogonal code sequence has larger number of distinct code sequences than that of Walsh code sequence. Orthogonal Gold code sequence has N (length of non-orthogonal Gold code sequence) groups where each group has $(N + 1)$ members of length $(N + 1)$ chips. For same length of code sequence, orthogonal Gold code sequence has much more number of distinct code sequences than that of Walsh code sequence, however CCF of orthogonal Gold code sequence is not zero in any group. Moreover, any member in a group of orthogonal Gold code sequences is not orthogonal to other members in other groups. Therefore, orthogonal Gold code sequence is not adequate to minimize the effect of multiple access interference in CDMA systems. However,

synchronisation of orthogonal Gold code sequence at the receiver is easier than that of Walsh code sequence, due to impulsive ACF of orthogonal Gold code sequence.

H. Donelan and T. O'Farrell in 1999 proposed a method to generate sets of orthogonal code sequences. This orthogonal code sequence is generated using two different non-orthogonal m-sequences. The total number of code sequence sets and distinct code sequences can be generated are N (length of non-orthogonal m-sequence) and $N(N + 1)$ respectively, thus orthogonal m-sequence has similar number of different code sequences to that of orthogonal Gold code sequence, but much more number of different code sequences to that of Walsh code sequence for same code length. This orthogonal m-sequence possesses an impulsive ACF similar to that of orthogonal Gold code sequence, therefore synchronisation of orthogonal m-sequence at the receiver is easier than that of Walsh code sequence. However, the cross-correlation function (CCF) of orthogonal m-sequence in a group is worse than that of Walsh code sequence, since CCF of orthogonal m-sequence in a group is not zero. Therefore, the orthogonal m-sequence is not effective to minimise the effect of multiple access interference in multi users spread spectrum application such as CDMA systems. Also, the property of orthogonality in m-sequence applies only within a group of code sequences, the code sequences from different groups are not orthogonal to each other.

However, orthogonal small set Kasami code sequence proposed by (Chandra and Chattopadhyay, 2009) has much smaller number of distinct code sequences than those of orthogonal Gold code sequence and orthogonal m-sequence, whereas, its correlation properties are similar to those of orthogonal Gold code sequence and orthogonal m-sequence.

The target for mobile communication provider in order to improve capabilities of multimedia communications is to provide services of a blend of data types such as audio, data, image and video transfer at high data rates from their customers. One way to flexibly provide data services of different rates from low to very high bit rates is to assign orthogonal code sequences with different lengths (orthogonal code sequence used for different bit rate is called orthogonal variable spreading factor (OVSF) code sequence) in the forward link to each user according to the data rate requested. This will ensure constant chip rate after spreading of variable data rate (Adachi, et.al., 1997). The authors proposed tree structure generation of orthogonal spreading code sequences for different code sequence lengths of different data rates in CDMA mobile radio where generated code sequences of the same layer constitute a set of Walsh code sequences and they are orthogonal. This method of tree structure generation can be used for orthogonal Gold code sequence and orthogonal m-sequence to generate OVSF Gold and OVSF m-sequences.

Based on the literature review presented above, it becomes apparently clear that there is no research work that generates orthogonal code sequences using two different types of non-orthogonal code sequences (non-orthogonal m-sequence and large set Kasami code sequence). Therefore, I have decided to research into the novel design that generates a large set code sequence from two different code sequences. This research work has successfully generated a set of orthogonal code sequence that has the largest number of distinct code sequences and can reduce the effect of multiple access interference (MAI) in CDMA systems.

Chapter 3

SPREADING CODE SEQUENCES AND SYNCHRONOUS CDMA SYSTEMS

Binary spreading code sequence can be divided into two categories, i.e. orthogonal and non-orthogonal code sequences. Walsh code sequence has proven its existence as a popular orthogonal code sequence, whereas m-sequence, Gold and Kasami code sequences have established themselves as popular non-orthogonal binary code sequences (Pal and Chattopadhyay, 2010).

Walsh code sequences are generated from mapping of Hadamard matrix, however the orthogonal code sequences such as orthogonal Gold code sequence, orthogonal m-sequence and orthogonal small set Kasami code sequence have been generated using their non-orthogonal versions.

In order to support a large number of users in CDMA system, one of the primary tasks of the mobile system designers is to create a large number of spreading code sequences while maintaining low cross-correlation values between them to mitigate the effect of multiple access interference (Kedia et. al., 2010).

Moreover, to support a variety of data services from low to very high bit rates, orthogonal variable spreading factor (OVSF) code sequence is generated to keep constant chip rate after spreading (Adachi, 1997; Dinan and Jabbari, 1998; Kedia, et.al., 2010).

Evaluation of spreading code sequence in CDMA system includes evaluating their performance metrics such as autocorrelation function, cross-correlation function, and bit error rate performance.

3.1 Correlation Properties of Spreading Code Sequence

Correlation is a measure of the similarity between two signals (spreading code sequences) as one is shifted with respect to the other (Abu-Rgheff, 2007).

3.1.1 Autocorrelation function

Correlation of a spreading code sequence with a copy of itself is called autocorrelation of that spreading code sequence. Autocorrelation function ($R_{xx}(\tau)$) of a spreading code sequence is given by (Duhan, 2010):

$$R_{xx}(\tau) = \sum_{n=1}^N a_n a_{n+\tau} \quad (3-1)$$

where a_n is the elements of a spreading code sequence with period N .

Another parameter used in designing a spreading code sequence in terms of the autocorrelation function is called merit factor (MF). The merit factor (MF) is defined by the ratio of the energy of autocorrelation at zero time shift to the total energy of autocorrelation at non zero time shifts (Abu-Rgheff, 2007; Golay, 1982). Mathematically, MF is represented by:

$$M_F = \frac{|R_{xx}(0)|^2}{2 \sum_{\tau=1}^{N-1} |R_{xx}(\tau)|^2} \quad (3-2)$$

Where, $R_{xx}(0)$ and $R_{xx}(\tau)$ are autocorrelation at zero time shift and non-zero time shifts respectively.

3.1.2 Cross-correlation function

Cross-correlation of spreading code sequence is correlation between two different spreading code sequences. Cross-correlation function ($R_{xy}(\tau)$) of spreading code sequence is mathematically represented as (Huda and Islam, 2009; Dinan and Jabbari, 1998):

$$R_{xy}(\tau) = \sum_{n=1}^N a_n b_{n+\tau} \quad (3-3)$$

Where, a_n and b_n are the elements of two spreading code sequences with period N .

In a multi users environment, in terms of cross-correlation function, there is a parameter called correlation margin (CM) used to design a spreading code sequence.

CM is defined by (Lotter and Linde, 1994) the following expression:

$$CM = 10 \log \left(\frac{R_{xx}(0)}{\max_{\tau} |R_{xy}(\tau)|} \right) - 10 \log(P) \quad (3-4)$$

where $R_{xx}(0)$ = autocorrelation value at zero time shift, $R_{xy}(\tau)$ = cross-correlation function values, and P = number of users transmitting simultaneously.

3.2 Non-orthogonal Spreading Code Sequences

3.2.1 Maximal-length sequence

Maximal-length sequence is a form of pseudo noise (PN) sequence. Pseudo noise sequence is a periodic binary sequence with a noise-like waveform that is generated by using a linear feedback shift register (Lee and Miller, 1998; Ziani and Medouri, 2012). The period of a PN sequence produced by a linear feedback shift register of length n cannot exceed the value $2^n - 1$. When the period is exactly $2^n - 1$, the PN sequence is called a maximal-length sequence or simply m-sequence (Xinyu, 2011). The autocorrelation function $R_{xx}(\tau)$ of m-sequence is defined as:

$$R_{xx}(\tau) = \begin{cases} N & \text{for } \tau = 0 \\ -1 & \text{for } \tau \neq 0 \end{cases} \quad (3-5)$$

The cross-correlation function $R_{xy}(\tau)$ of these sequences could have three values, four values or many values (Abu-Rgheff, 2007). There is no standard formula for the family size of m-sequence.

3.2.2 Gold code sequence

Gold code sequences are generated by the modulo-2 operation of a preferred pair of m-sequences of same length (Gold, 1967; Meel, 1999; Xinyu, 2011). From a pair of preferred m-sequences, the Gold code sequences are generated using a modulo-2 sum of the first pair with the shifted version of the second pair or vice versa. Since preferred pair of m-sequences has equal length N , the generated Gold code sequence is of length N as well. For a period of $N = 2^r - 1$, there are N possible circular shifts where r is the number of registers. Thus, one can get N code sequences with two preferred pairs of m-sequences, and the family size (M) will be $N + 2$ code sequences. If u and v are preferred pairs of m-sequences, then the set of Gold code sequences generated is given as (Yong-Hwan and Seung-Jun, 2000; Mitra, 2008):

$$G(u, v) = \{u, v, u \oplus v, u \oplus T.v, u \oplus T^2.v, \dots, u \oplus T^{N-1}.v\} \quad (3-6)$$

where, T is the cyclic shift operator and \oplus is the XOR operation. The autocorrelation function of Gold code sequences is not as good as that of the m-sequences. Apart from two original code sequences, the others are not m-sequences. Hence the autocorrelation function is not two-valued. The autocorrelation function $R_{xx}(\tau)$ and the cross-correlation function $R_{xy}(\tau)$ of Gold code sequences are represented by equations (3-7) and (3-8) respectively (Babadi et. al., 2011):

$$R_{xx}(\tau) = \begin{cases} N & \text{for } \tau = 0 \\ (-1, -t(r), t(r) - 2) & \text{for } \tau \neq 0 \end{cases} \quad (3-7)$$

$$R_{xy}(\tau) = (-1, -t(r), t(r) - 2) \quad (3-8)$$

$$\text{where } t(r) = \begin{cases} 1 + 2^{\frac{r+1}{2}} & \text{for } r \text{ odd} \\ 1 + 2^{\frac{r+2}{2}} & \text{for } r \text{ even} \end{cases}$$

3.2.3 Small set Kasami code sequence

Small set Kasami code sequence is a non-orthogonal code sequence and generated from m-sequence by using a set of algorithms as explained below.

Let u be an m-sequence of length N generated by a generator polynomial of length n , and let w be a code sequence obtained by decimating u by $2^{n/2} + 1$, where n is an even number and $N = 2^n - 1$. Then, the code sequence w is also an m-sequence of length $2^{n/2} - 1$. The small set Kasami code sequence is then given by (Chandra and Chattopadhyay, 2009):

$$K_s = (u, u \oplus w, u \oplus Tw, \dots, u \oplus T^{2^{n/2}-2} w) \quad (3-9)$$

where, K_s is a small set Kasami code sequence of length $N = 2^n - 1$; T denotes cyclic shift operator; \oplus denotes XOR operation, and $2^{n/2} - 2$ is the shift parameter for w . Since w and u have different code sequence lengths, we must first perform $N/(2^{n/2} - 1)$ repetitions of the code sequence w before performing the XOR operation.

These code sequences have a family size (M) of $2^{n/2}$ binary code sequences, each of length $N = 2^n - 1$. The autocorrelation function $R_{xx}(\tau)$ of small set Kasami code sequence is given as (Dinan and Jabbari, 1998):

$$R_{xx}(\tau) = \begin{cases} N & \text{for } \tau = 0 \\ (-1, -s(n), s(n) - 2) & \text{for } \tau \neq 0 \end{cases} \quad (3-10)$$

where $s(n) = 2^{n/2} + 1$ and n is even.

The cross-correlation function $R_{xy}(\tau)$ of this code sequence is given by (Dinan and Jabbari, 1998):

$$R_{xy}(\tau) = (-1, -s(n), s(n) - 2) \quad (3-11)$$

3.2.4 Large set Kasami code sequence

Let v be the sequence formed by decimating the sequence u (m-sequence) by $2^{\frac{n}{2}+1} + 1$ where $n = 2 \pmod{4}$, then a large set Kasami code sequence is defined by the following set of expressions (Tsai and Li, 2007):

$$K_L = \begin{cases} u & k = 0, \dots, 2^n - 2 \\ v & k = 0, \dots, 2^n - 2 \\ u \oplus T^k v & k = 0, \dots, 2^n - 2 \\ u \oplus T^m w & m = 0, \dots, 2^{\frac{n}{2}} - 2 \\ v \oplus T^m w & m = 0, \dots, 2^{\frac{n}{2}} - 2 \\ u \oplus T^k v \oplus T^m w & k = 0, \dots, 2^n - 2; m = 0, \dots, 2^{\frac{n}{2}} - 2 \end{cases} \quad (3-12)$$

where, k and m are the shift parameter. These code sequences have a family size (M) of $2^{n/2} (2^n + 1)$ binary code sequences, each of length $N = 2^n - 1$. The autocorrelation function $R_{xx}(\tau)$ of the large set Kasami code sequence is given as:

$$R_{xx}(\tau) = \begin{cases} N & \text{for } \tau = 0 \\ \left(-1, -1 \pm 2^{\frac{n}{2}}, -1 \pm 2^{\frac{n}{2}} + 1 \right) & \text{for } \tau \neq 0 \end{cases} \quad (3-13)$$

The cross-correlation function $R_{xy}(\tau)$ of this code sequence is given by:

$$R_{xy}(\tau) = \left(-1, -1 \pm 2^{\frac{n}{2}}, -1 \pm 2^{\frac{n}{2}} + 1 \right) \quad (3-14)$$

3.3 Orthogonal Code Sequence

3.3.1 Walsh code sequence

Walsh code sequences are orthogonal spreading code sequences that are generated by mapping code word rows of special square matrices called Hadamard matrices (Woo, 2002). These matrices contain one row of all zeros, and the remaining rows will have an equal number of ones and zeroes for each. These code sequences are used in synchronous downlink CDMA systems (Akansu and Poluri,

2007). A Walsh code sequence set of length N can provide a maximum of N number of distinct orthogonal spreading code sequences (Dongwook, et.al., 1998).

3.3.2 Orthogonal Gold code sequence

The orthogonal Gold code sequences are developed from a set of non-orthogonal Gold code sequences, which contain elements of the alphabet $\{1, -1\}$, by appending an additional “1” to the end of each code sequence. The set orthogonal Gold (*OGold*) code sequence of $N + 1$ code sequences of length $N + 1$ chips is given by (Tachikawa, 1992):

$$OGold(A, B) = (U, V_0, V_1, \dots, V_{N-1}) \quad (3-15)$$

Where, $U = (A, 1)$, $V_j = (A \oplus T^j B, 1)$, and $A = (a_0, a_1, \dots, a_{N-1})$ and $B = (b_0, b_1, \dots, b_{N-1})$ are preferred pairs of m-sequences of length N . $T^j B$ is sequence B after j chip cyclic shift and \oplus is XOR operation.

3.3.3 Orthogonal m-sequence

Orthogonal m-sequences generated by the multiplication of one m-sequence with all shifts of a second m-sequence, after mapping bit 0 to 1 and bit 1 to -1 of these two m-sequences, since multiplication is equal to modulo-2 addition for such mapping (Donelan and O’Farrel, 1999).

Two m-sequences with zero chip shifts of lengths N are represented by $\{a_i\}_0$ and $\{b_i\}_0$, where

$$\{a_i\}_0 = (a_0, a_1, \dots, a_{N-2}, a_{N-1}) \quad (3-16)$$

$$\{b_i\}_0 = (b_0, b_1, \dots, b_{N-2}, b_{N-1}) \quad (3-17)$$

Use of the Gold construct method on these two m-sequences forms the set of code sequences given by:

$$\{g_i^{(k)}\}_0 = \begin{cases} \{a_i\}_0 \times T^k\{b_i\}_0 & \text{for } 0 \leq k < N \\ \{a_i\}_0 & \text{for } k = N \\ 0 & \text{otherwise} \end{cases} \quad (3-18)$$

Where, $T^k\{b_i\}_0$ represents a cyclic shift of $\{b_i\}_0$ by k chips. As can be seen in equation (3-18), $\{a_i\}_0$ for $k = N$ is the original m-sequence, $\{a_i\}_0$.

Performing the following procedure on equation (3-18) produces a set of orthogonal code sequences:

Step 1: make the first chips of the code sequences all '1s'.

Step 2: if the first chips of the code sequences were already '1s' and have not, therefore, been altered by step 1 then affix '-1s' on the end of the code sequences

Step 3: if the first chips of the code sequences were '-1s' and have, therefore, been altered by step 1 then affix '1s' on the end of the code sequences

Step 4: repeat steps 1-3 for all code sequences in the equation (3-18).

The procedure to produce a set of orthogonal code sequences can be mathematically represented as follows:

$$\{v^{(k)}\}_0 = (1^{(k)}, \{u^{(k)}\}_0, (-g_0^{(k)})_0) \quad (3-19)$$

Where, $\{u^{(k)}\}_0$ be the set of code sequences $\{g^{(k)}\}_0$ with the first chip, $(g_0^{(k)})_0$, of every code sequence removed.

The set of code sequences $\{v^{(k)}\}_0$ is a set of $N + 1$ code sequences of length $N + 1$ that are orthogonal to each other. By following the same procedure with the same m-sequences but with the m-sequences in a different initial chip shift to those of initial zero chip shift as presented in equations (3-20) and (3-21), an entirely different set of orthogonal code sequences is generated.

$$\{a_i\}_1 = (a_{N-2}, a_0, a_1, \dots, a_{N-1}) = T^1\{a_i\} \quad (3-20)$$

$$\{b_i\}_1 = (b_{N-2}, b_0, b_1, \dots, b_{N-1}) = T^1\{b_i\} \quad (3-21)$$

For each of the initial chip shift of the m-sequences, where the circular shift is the same on both m-sequences, there is a different orthogonal code sequence set. Therefore, for two m-sequences of length N , there exists N sets of $N + 1$ code sequences of length $N + 1$ chips, and hence, the total number of different code sequences that can be generated using this process is given by:

$$M = N(N + 1) \quad (3-22)$$

3.3.4 Orthogonal small set Kasami code sequence

Orthogonal small set Kasami code sequences are generated from non-orthogonal small set Kasami code sequence using the set of algorithms presented in the flowchart shown in figure 3.1 (Chandra and Chattopadhyay, 2009).

Orthogonal small set Kasami code sequence is capable to produce $(\sqrt{N + 1}) N$ number of distinct code sequences, each of length $N + 1$ chips, where $\sqrt{N + 1}$ is number of code sequence sets and N is number of members in each code sequence set.

3.3.5 Orthogonal variable spreading factor code sequence

The target for mobile communications in order to improve capabilities of multimedia communication is to meet a huge demand for transmitting a blend of data types such as audio, data, image and video transfer at high data rates from their customers.

One way to flexibly provide data services of different rates from low to very high bit rates is to assign orthogonal code sequence with different lengths or orthogonal variable spreading factor (OVSF) code sequence in the forward link to each user according to the data rate requested, in order to ensure constant chip rate after spreading of variable data rate (Adachi, et.al., 1997).

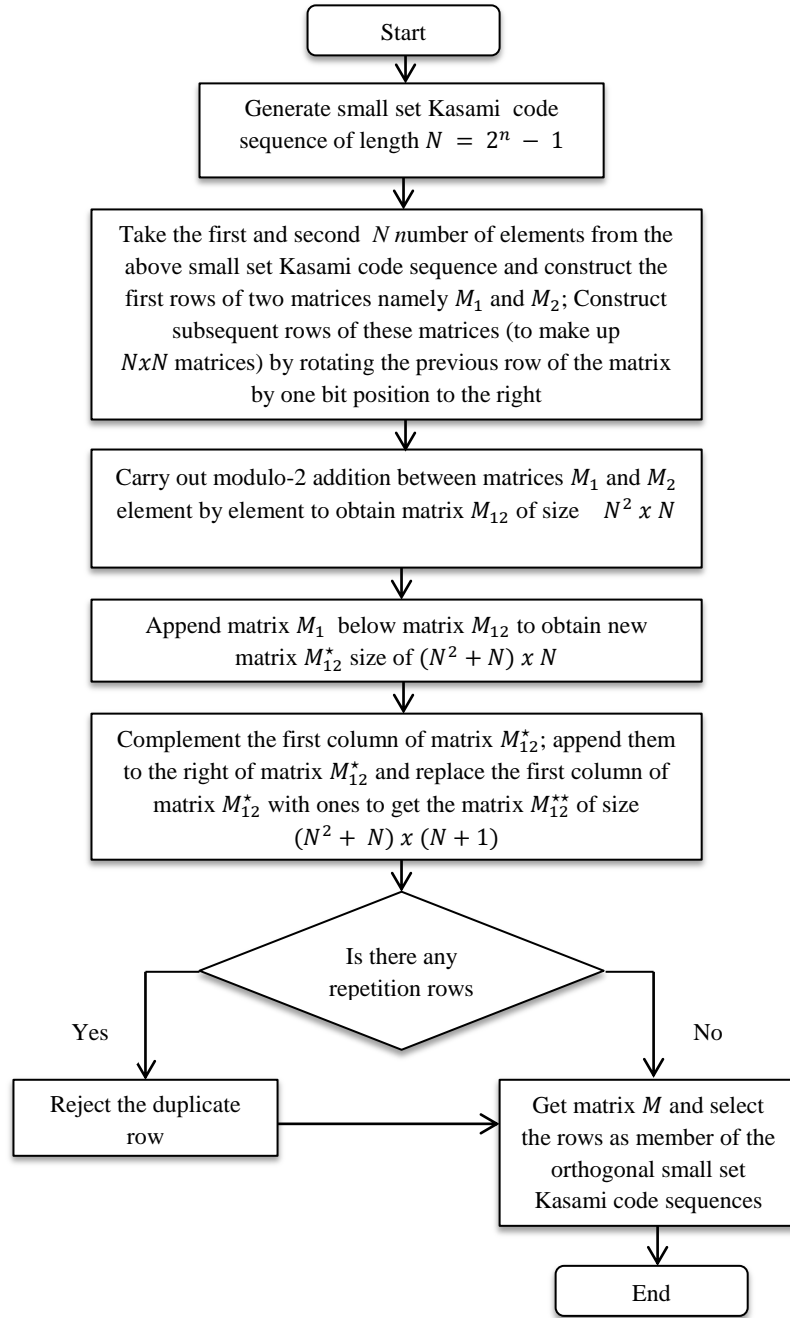


Figure 3.1 Algorithm for generation of orthogonal small set Kasami code sequences

The code tree for generation of OVVSF code sequence is shown in figure 3.2. Here the generated code sequences of the same layer form a set of Walsh code sequences and these are orthogonal. Also, any two code sequences of different layers are orthogonal except for the case that one of the two code sequences is in a mother-child relationship.

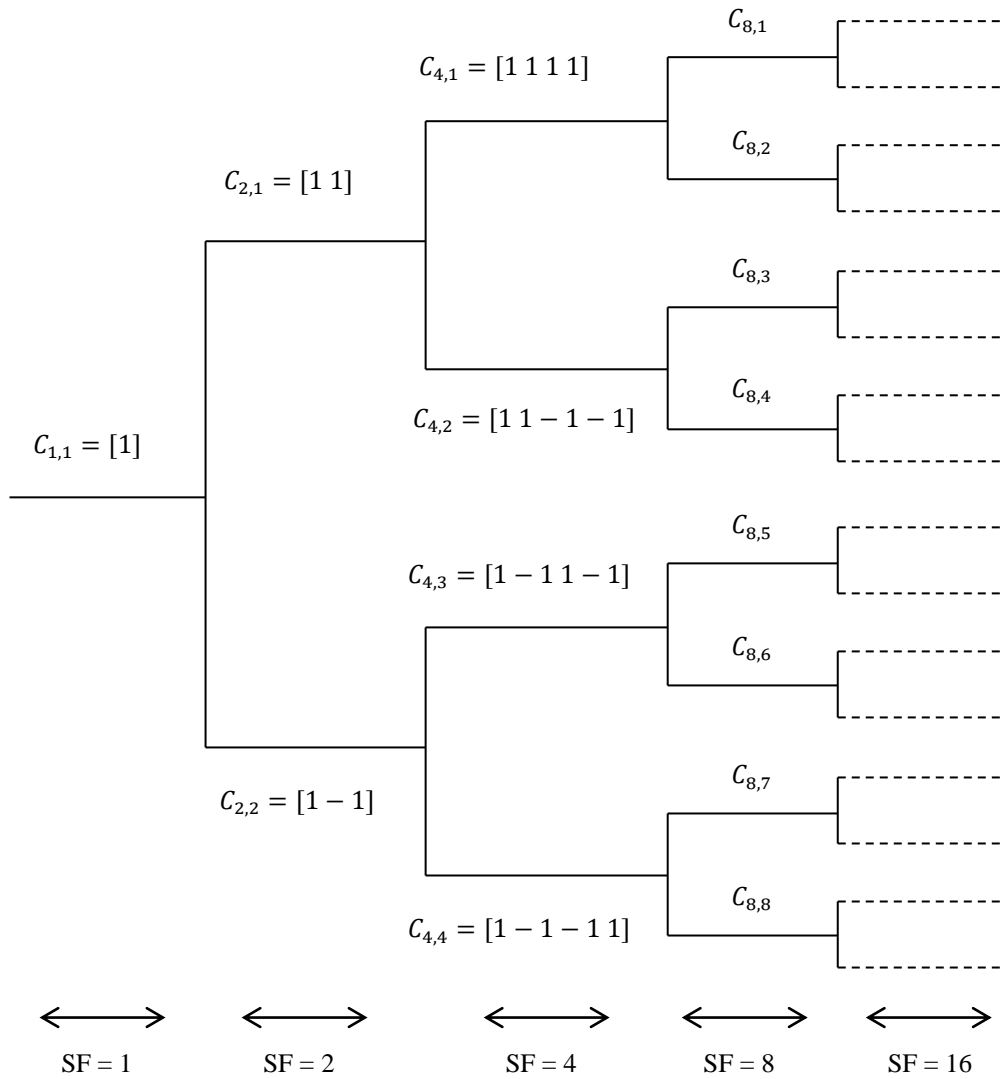


Figure 3.2 Code tree for generation of OVSF code sequences

One can choose appropriate spreading code sequences according to the transmission rate. However, a code sequence in the code tree can be used by a mobile station *iff* no other code sequence in the path from the specific code sequence to the root of the tree or in the sub-tree below the specific code is used by other mobile stations. Such code sequences do not fulfil the orthogonality condition and thus their usage is avoided for variable data rate communication. In this case, if $C_{4,1}$ is used by a mobile station then $C_{2,1}$ and $C_{1,1}$ can not be used by other mobile stations since $C_{2,1}$ is located in the sub-tree below $C_{4,1}$ while $C_{1,1}$ is the root of the tree.

3.4 Synchronous CDMA System

CDMA is mainly being used in wireless communication systems at present. The system model considered for this investigation is synchronous CDMA system which is employed for the downlink transmission from the base station to the mobile receivers. This system uses direct-sequence code division multiple access (DS-CDMA) (Tarek, et.al., 2010).

The principle of DS-CDMA is to spread a data symbol with a spreading code sequence $c^{(k)}(t)$ of length L which is given as (Fazel and Kaiser, 2008; Luna-Rivera and Campos-Delgado, 2009; Masouros and Alsusa, 2010).

$$c^{(k)}(t) = \sum_{l=0}^{L-1} c_l^{(k)} p_{T_c}(t - lT_c) \quad (3-23)$$

assigned to user k , $k = 0, \dots, K - 1$, where K is the total number of active users.

The rectangular pulse $p_{T_c}(t)$ is equal to 1 for $0 \leq t < T_c$ and zero otherwise. T_c is the chip duration and $c_l^{(k)}$ are the chips of the user specific spreading code sequence $c^{(k)}(t)$. Elements of $c_l^{(k)}$ takes on values $\left\{ +1/\sqrt{L}, -1/\sqrt{L} \right\}$. After spreading, the signal $x^{(k)}(t)$ of user k is given by:

$$x^{(k)}(t) = d^{(k)} \sum_{l=0}^{L-1} c_l^{(k)} p_{T_c}(t - lT_c), \quad 0 \leq t < T_d \quad (3-24)$$

for one data symbol duration $T_d = LT_c$ where $d^{(k)}$ is the transmitted data symbol of user k . Data symbol of user k in this investigation is differentially binary phase shift keying modulated (DBPSK). The multiplication of the information sequence with the spreading code sequence is done bit-synchronously and the overall transmitted signal $x(t)$ of all K synchronous users (downlink of a cellular system) results in:

$$x(t) = \sum_{k=0}^{K-1} x^{(k)}(t) \quad (3-25)$$

The signal received by a user is the convolution of the transmitted signal $x(t)$ with the channel ($h(t)$), plus additive white Gaussian noise ($n(t)$) as given by (Turkmani and Goni, 1993; Wang and Chen, 2011):

$$r(t) = x(t) * h(t) + n(t)$$

$$r(t) = \sum_{k=0}^{K-1} r^{(k)}(t) + n(t) \quad (3-26)$$

where $r^{(k)}(t) = x^{(k)}(t) * h(t)$ is the noise-free received signal of user k , $n(t)$ is the additive white Gaussian noise (AWGN), and $*$ denotes the convolution operation.

The receiver recovers the transmitted data symbol by correlating $r(t)$ with the local spreading code sequence of a desired user to form decision statistics Z given by (Turkmani and Goni, 1993):

$$Z^{(k)} = \int_0^{T_d} r(t) c^{(k)}(t) \quad (3-27)$$

The decision statistics is used to form an estimate of the transmitted data symbol based on threshold.

3.4.1 Differential binary phase shift keying (DBPSK) symbol

In DPSK scheme, the phase reference for demodulation is derived from the phase of carrier during the preceding signalling interval, and the receiver decodes the digital information based on the differential phase.

The differential encoding and decoding operation performed by DBPSK is explained in table 3.1 (assuming noise free). The encoding process starts with an arbitrary first bit (say bit 1), and thereafter the encoded bit stream d_k is generated by the following equation (Shanmugam, 1979):

$$d_k = d_{k-1} b_k \oplus \overline{d_{k-1}} \overline{b_k} \quad (3-28)$$

Table 3.1 Encoding and decoding operation of DBPSK symbol

Input sequence (b_k)	1	1	0	1	0	0	0	1	1
Encoded sequence (d_k)	1^a	1	1	0	0	1	0	1	1
Transmitted phase	0	0	0	π	π	0	π	0	0
Received phase	0	0	0	π	π	0	π	0	0
Output bit sequence	1	1	0	1	0	0	0	1	1

a = arbitrary starting reference bit

The transmitted phase is zero if encoded sequence is bit 1, and if the encoded sequence is bit 0 then the transmitted phase is π . With an initial angle of 0 (for the reference bit), the receiver output is bit 1 if the carrier phase is the same during two successive bit intervals. If the phase angles are different, the receiver output is bit 0.

3.5 Performance Metric

Performance metric used for evaluation of the proposed HOVLS code sequence in this CDMA system include ACF, CCF, and bit error rate (BER). ACF and CCF have given in detail in section 3.1. In this section, BER is outlined.

3.5.1 Bit error rate

In digital transmission, when bit data is transmitted over a communication channel, there is a possibility of errors being introduced into the bit data. Number of bit errors is the number of received bits of a data stream over a communication channel that have been altered due to impairment of communication channel such noise, interference and fading. If errors are introduced into the data, then the integrity of the system may be compromised. As a result, it is necessary to assess the performance of the system, and bit error rate (BER) provides a way in which this can be achieved (Proakis, 2000; Sklar, 1994).

Bit error rate is defined as the rate at which errors occur in a transmission system and mathematically is given as (Lathi, 1998):

$$BER = \frac{\text{number of error bits}}{\text{number of bits sent}} \quad (3-29)$$

BER is a unit less performance measure. BER curves are plotted to describe the functionality of a digital communication system. In digital wireless communication system, BER is plotted as a function of signal to noise ratio (SNR). SNR is defined as the ratio between the power of wanted signal (P_R) and the noise power (N_R). SNR is usually expressed in decibel (dB) defined as (Oberger, 2001):

$$SNR = 10 \log \left(\frac{P_R}{N_R} \right) \quad (3-30)$$

where P_R and N_R are both in Watt (W).

Chapter 4

COMMUNICATION CHANNEL

Communication channel is a physical medium that is used to send a signal from a transmitter to a receiver. In wireless transmission, the channel may be the atmosphere or free space. On the other hand, telephone channels usually employ a variety of physical media including wire lines, optical fiber and wireless media (microwave radio) (Lathi, 1998; Proakis, 2000).

Whatever the physical medium used for transmission of the information, the essential feature is that the transmitted signal is corrupted in a random manner by contamination source such as additive thermal noise generated by electronic devices. Another contamination to the transmitted signal is fading due to multipath propagation encountered in wireless communication systems. (Cho, et.al., 2010).

4.1 AWGN Channel

The noise is commonly encountered in most communication systems and is appropriately called thermal noise. The thermal noise process is defined by Gaussian distribution and it has power spectral density which is almost constant over a very large frequency spectrum and hence is called white Gaussian noise. In communication systems, the received signal at the channel output is the sum of the information signal plus white Gaussian noise, therefore called additive white Gaussian Noise (AWGN).

The AWGN of a communication channel could be represented by a model shown in figure 4.1. Physically, AWGN arises from electronic component at the receiver of the communication system (Proakis, 2000).

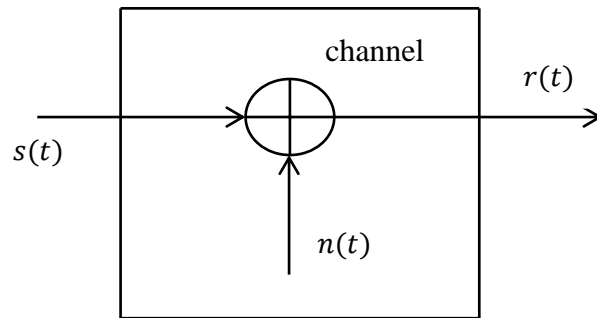


Figure 4.1 The additive white gaussian noise channel

As seen in figure 4.1, $s(t)$ is a transmitted signal, $n(t)$ is additive white gaussian noise and signal output ($r(t)$) is given by (Proakis, 2000):

$$r(t) = s(t) + n(t) \quad (4-1)$$

4.2 Fading Channel

In any wireless communication system there could be more than one path over which the signal can travel between the transmitter and receiver antennas. The presence of multiple paths is due to atmospheric scattering and refraction, or reflections from buildings and other objects (Jeruchim, 2002).

The transmitted signal follows many different paths before arriving at the receiving antenna, and it is the aggregate of these paths that constitutes the multipath radio propagation channel. These waves called multipath waves, combined at the receiver antenna to give resultant signal. The resulting signal strength will undergo fluctuations that results in a fade (Jeruchim, 2002; Rappaport, 1996).

Small scale fading or simply fading is caused by interference between two or more versions of the transmitted signal which arrive at the receiver at slightly different times due to multipath radio propagation channel (Rappaport, 1996).

For mobile radio applications, the channel is time-varying because the motion between the transmitter and receiver results in propagation path changes. The time variation of the channel (t in equation (4-3)) is characterised by the Doppler frequency (Doppler shift) which is given by (Jeruchim, 2002):

$$f_d = \frac{v f_c}{c} \quad (4-2)$$

Where, f_d = Doppler shift (Hz), v = velocity (m/sec), f_c = carrier frequency (Hz) and c = light velocity (m/sec). Time varying wireless channel (fading channel), $h(t, \tau)$ is represented by the following equation (Jeruchim, 2002):

$$h(t, \tau) = \sum_n a_n(t, \tau) \delta(\tau - \tau_n(t)) \quad (4-3)$$

where, $a_n(t, \tau)$ and $\tau_n(t)$ are path gains and path delays respectively of n_{th} multipath component at time t .

For an input signal $s(t)$, the output of fading channel ($r(t)$) is given by (Proakis, 2000):

$$r(t) = s(t) * h(t, \tau) \quad (4-2)$$

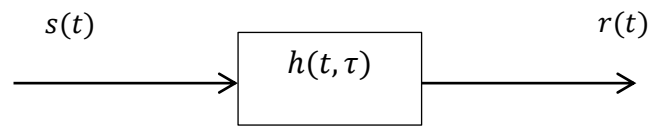
Where, $h(t, \tau)$ is fading channel and $*$ is convolution operator.

Time dispersion (τ in equation (4-3)) due to multipath causes the transmitted signal to undergo either flat or frequency selective fading (Rappaport, 1996).

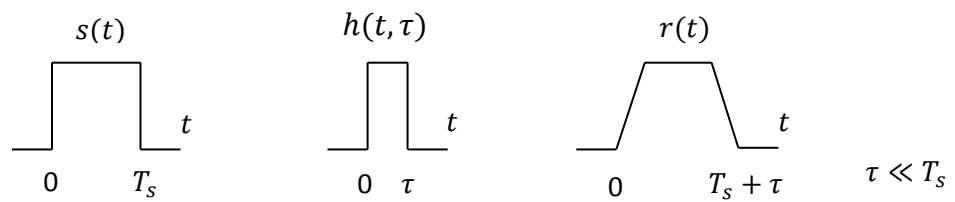
4.2.1 Flat fading

If the bandwidth of fading channel is greater than the bandwidth of the transmitted signal, then the received signal will undergo flat fading. The characteristics of a flat fading channel are illustrated in figure 4.2. Fading channel, time and frequency domains of a flat fading channel are presented in figure 4.2(a), 4.2(b) and 4.2(c) respectively (Rappaport, 1996; Tse, 2005).

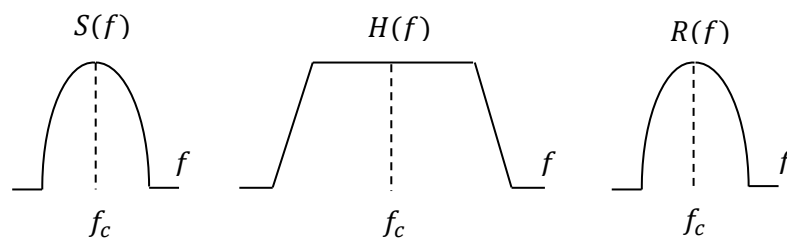
In a flat fading channel, the reciprocal bandwidth of the transmitted signal is much larger than time delay spread of the channel (time between the first and the last arriving of multipath components), and $h(t, \tau)$ can be approximated as having no excess delay (single delta function with $\tau = 0$) as seen in figure 4.2(b) (Rappaport, 1996). Excess delay is the delay of n -th multipath component as compared to the first arriving component. As shown in figure 4.2(c), the spectrum of the transmitted signal is preserved at the output of flat fading channel.



(a) Fading channel

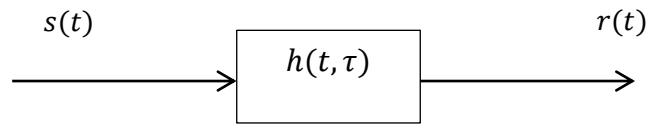


(b) Time domain of flat fading channel

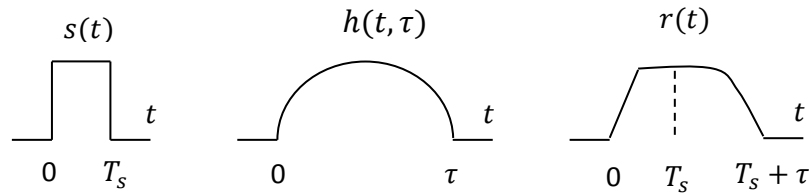


(c) Frequency domain of flat fading channel

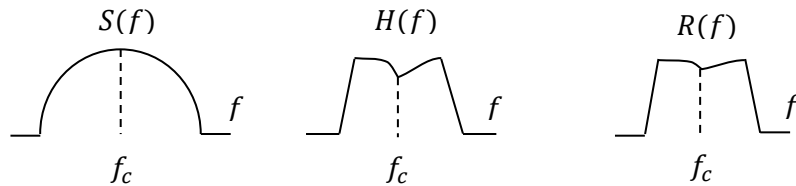
Figure 4.2 Flat fading channel characteristics



(a) Fading channel



(b) Time domain of frequency selective fading channel



(c) Frequency domain of frequency selective fading channel

Figure 4.3 Frequency selective fading channel characteristics

4.2.2 Frequency selective fading

If the bandwidth of fading channel is smaller than the bandwidth of the transmitted signal, then the channel creates frequency selective fading on the received signal. Characteristics of a frequency selective fading channel is illustrated in figure 4.3 (Rappaport, 1996; Tse, 2005). Figure 4.3(a), 4.3(b), and 4.3(c) present fading channel, time and frequency domains of a frequency selective fading channel.

As shown in figure 4.3(b), frequency selective fading channel has a multipath delay spread which is greater than the reciprocal bandwidth of the transmitted signal.

When this occurs, the received signal includes multiple versions of the transmitted signal which are attenuated and delayed in time, and hence the received signal is distorted. Frequency selective fading is due to time dispersion of the transmitted symbols within the channel. Thus, the channel induces intersymbol interference (ISI). Viewed in frequency domain, certain frequency components in the received signal spectrum have greater gains than others as presented in figure 4.3(c).

Chapter 5

DESIGN, IMPLEMENTATION AND ANALYSIS OF FIXED SPREADING FACTOR HYBRID ORTHOGONAL VERY LARGE SET CODE SEQUENCE

Fixed spreading factor (fixed length) orthogonal Gold code sequence, orthogonal m-sequence and orthogonal small set Kasami code sequence have been designed from their non-orthogonal counter parts.

The method used by Donelan and O'Farrell in 1999, for generating orthogonal m-sequence has been adapted to the design of fixed spreading factor hybrid orthogonal very large set (HOVLS) code sequence in this research work. My research work applies this principle to two different types of spreading code sequences namely large set Kasami code sequence and m-sequence, instead of using two m-sequences (thus the name hybrid).

The proposed HOVLS code sequence is implemented in a synchronous CDMA system, via simulation using Simulink/Matlab programming. The ACF, CCF, and BER performance of the proposed HOVLS code sequence is evaluated and compared to those of fixed spreading factor (fixed length) orthogonal Gold code sequence and orthogonal m-sequence.

5.1 Design of HOVLS Code Sequence

The method used by Donelan and O'Farrell, 1999 in generating orthogonal m-sequence has been adapted to design the proposed HOVLS code sequence in this research work.

Let large set Kasami code sequence and m-sequence, each of length N ($N = 2^n - 1$ for $n = 2 \bmod 4$) and generated using the same generator polynomial, be

represented by $\{k_i\}$ and $\{u_i\}$ respectively. These two code sequences can be represented as:

$$\{k_i\}_a = T^a\{k_i\} = T^a(k_0, k_1, k_2, \dots, k_{N-2}, k_{N-1}) \quad (5-1)$$

$$\{u_i\}_a = T^a\{u_i\} = T^a(u_0, u_1, u_2, \dots, u_{N-2}, u_{N-1}) \quad (5-2)$$

Where $a = (0, 1, 2, \dots, N - 1)$ denotes shift parameter; $T^a\{k_i\}$ and $T^a\{u_i\}$ represent cyclic shift of large set Kasami code sequence and m-sequence respectively.

$\{k_i\}$ and $\{u_i\}$ in equation (5-1) and (5-2) are binary digits. By replacing bit 0 by 1 and bit 1 by -1, hybrid code sequences are obtained by multiplying the large set Kasami code sequence with all resulting m-sequence shifted by one chip. This is expressed mathematically as below:

$$\{h_i^{(j)}\}_a = \begin{cases} \{k_i\}_a \times T^j\{u_i\}_a & \text{for } 0 \leq j < N \\ \{k_i\}_a & \text{for } j = N \\ 0 & \text{otherwise} \end{cases} \quad (5-3)$$

where $T^j\{u_i\}_a$ represents a cyclic shift of $\{u_i\}_a$ by j chips. As can be seen in equation (5-3), $\{k_i\}_a$ for $j = N$ is the original large set Kasami code sequence.

The following steps describe the procedure to convert the hybrid code sequences resulting from equation (5-3) to be a set of orthogonal code sequences (Donelan and O'Farrell, 1999):

Step 1: replace the first column (the first chips) by '1s'.

Step 2: if the first chips were already all '1s' and therefore have not been altered by step 1 then append '-1s' at the end of the code sequences (column).

Step 3: if the first chips were all '-1s' and therefore have been altered by step 1 then append '1s' at the end of the code sequences.

Step 4: repeat step 1 to 3 for all the code sequences represented in equation (5-3).

These steps in obtaining the proposed orthogonal code sequence can be mathematically represented as below:

$$\{o^{(j)}\}_a = \left(1^{(j)}, \{s^{(j)}\}_a, (-h_0^{(j)})_a\right) \quad (5-4)$$

where $\{s^{(j)}\}_a$ is the resulting $\{h_i^{(j)}\}_a$ matrix with the first chip (column) $(h_0^{(j)})_a$ removed.

The set of code sequence $\{o^{(j)}\}_a$ is a set of code sequences of $(N + 1) \times (N + 1)$ matrix whose rows are orthogonal to each other.

Each value of 'a' in equation (5-1) and (5-2), by the process explained above i.e. applying equation (5-3) and (5-4), generates one set of orthogonal code sequence. Therefore, one set of orthogonal code sequence will be generated for each value of 'a' using this process. As a result, there will be N different sets of orthogonal code sequences. Each set contains $(N + 1)$ code sequences (rows) of length $(N + 1)$ chips (columns). No two rows either in the same set or across the sets have the same code sequence. Therefore, total number of different code sequences that can be generated using this process is given by:

$$M = N(N + 1) \quad (5-5)$$

Referring to large set Kasami code sequence for $n = 2 \bmod 4$, smallest value of n equals to 6 and hence $N = 2^n - 1 = 63$. Therefore, 63 different sets of orthogonal code sequences can be generated where each set contains 64 code sequences of length 64 chips. Hence, total number of different code sequences is $63 \times 64 = 4032$ code sequences. These numbers (63 different sets of orthogonal code sequences and 4032 number of different code sequences) for 64 chip length are the same as the result that has been demonstrated by Donelan and O'Farrell, 1999.

5.1.1 A Novel method to generate very large set of orthogonal code sequence

If this hybrid method as presented by equation (5-3) is applied to the large set Kasami code sequences shown in expression (3-12) and m-sequence, a very large set of orthogonal code sequence can be generated. The derivation of the different components of the code sequence design is given below:

a. The first component

By substituting '0' for 'a' in equation (5-3), a set of hybrid code sequence generated as shown below:

$$\{h_i^{(j)}\}_0 = \begin{cases} \{u_i\}_0 \times T^j\{u_i\}_0 & \text{for } 0 \leq j < N \\ \{u_i\}_0 & \text{for } j = N \\ 0 & \text{otherwise} \end{cases}$$

where $\{u_i\}_0$ is an m-sequence for $a = 0$.

Applying equation (5-4) to this set of hybrid code sequence, one set of orthogonal code sequence is generated:

$$\{o^{(j)}\}_0 = (1^{(j)}, \{s^{(j)}\}_0, (-h_0^{(j)})_0)$$

where $\{o^{(j)}\}_0$ has $(N + 1)$ code sequences (rows) of length $(N + 1)$ chips (columns).

By substituting '1' for 'a' in equation (5-3), another set of hybrid code sequence is generated and given by:

$$\{h_i^{(j)}\}_1 = \begin{cases} \{u_i\}_1 \times T^j\{u_i\}_1 & \text{for } 0 \leq j < N \\ \{u_i\}_1 & \text{for } j = N \\ 0 & \text{otherwise} \end{cases}$$

where $\{u_i\}_1$ is an m-sequence for $a = 1$.

Applying equation (5-4) as above, another set of orthogonal code sequence is generated:

$$\{o^{(j)}\}_1 = (1^{(j)}, \{s^{(j)}\}_1, (-h_0^{(j)})_1)$$

where $\{o^{(j)}\}_1$ has $(N + 1)$ code sequences (rows) of length $(N + 1)$ chips (columns).

Using the same process as above, for all values of a , N sets of orthogonal code sequences, each of $(N + 1)$ code sequences of length $(N + 1)$ chips can be obtained. In this case, sets of orthogonal sequences are generated from the original and the shifted versions of an m-sequence, $\{u_i\}$. Since an m-sequence is multiplied by a cyclic shifted version of the same sequence, N identical sets of orthogonal code sequences are generated. Therefore the number of orthogonal code sequence sets with a unique set of members in the sequences is 1.

b. The second component

For $a = 0$, equations (5-1) and (5-2) are given by:

$$\{k_i\}_0 = T^0\{v_i\} = (v_0, v_1, v_2, \dots, v_{N-2}, v_{N-1})$$

$$\{u_i\}_0 = T^0\{u_i\} = (u_0, u_1, u_2, \dots, u_{N-2}, u_{N-1})$$

and the set of hybrid code sequences shown in equation (5-3) is given by:

$$\{h_i^{(j)}\}_0 = \begin{cases} \{v_i\}_0 \times T^j\{u_i\}_0 & \text{for } 0 \leq j < N \\ \{v_i\}_0 & \text{for } j = N \\ 0 & \text{otherwise} \end{cases}$$

Applying equation (5-4) to this set of hybrid code sequences, one set of orthogonal code sequences is generated:

$$\{o^{(j)}\}_0 = (1^{(j)}, \{s^{(j)}\}_0, (-h_0^{(j)})_0)$$

where $\{o^{(j)}\}_0$ has $(N + 1)$ code sequences (rows) of length $(N + 1)$ chips (columns).

Similarly, for $a = 1$, equations (5-1) and (5-2) are given by:

$$\{k_i\}_1 = T^1\{k_i\} = (v_{N-1}, v_0, v_1, v_2, \dots, v_{N-2})$$

$$\{u_i\}_1 = T^1\{u_i\} = (u_{N-1}, u_0, u_1, u_2, \dots, u_{N-2})$$

and the corresponding set of hybrid code sequences referring to equation (5-3) is given by:

$$\{h_i^{(j)}\}_1 = \begin{cases} \{v_i\}_1 \times T^j\{u_i\}_1 & \text{for } 0 \leq j < N \\ \{v_i\}_1 & \text{for } j = N \\ 0 & \text{otherwise} \end{cases}$$

Applying equation (5-4), another set of orthogonal code sequences is generated:

$$\{o^{(j)}\}_1 = (1^{(j)}, \{s^{(j)}\}_1, (-h_0^{(j)})_1)$$

Using the same process as above, for all values of a , there exists N sets of orthogonal code sequences, each of $(N + 1)$ code sequences of length $(N + 1)$ chips.

As can be seen from this process, sets of orthogonal code sequences are generated from $\{u_i\}$ and $\{v_i\}$ code sequences. Since $\{u_i\}$ and $\{v_i\}$ are different code sequences, combination of m-sequence and the second component of expression (3-12) of large set Kasami code sequence generate N different sets of orthogonal code sequences.

c. The third component

Let us take the first sequence of the third component of expression (3-12). This component is given by:

$$u_i \oplus v_i = u_i \times v_i$$

XOR operator is the same as multiply operation if bit 0 in a code sequence is replaced by 1 and bit 1 by -1 (Donelan and O'Farrell, 1999). Following this operation the equations (5-1) and (5-2) are given as below:

$$\{k_i\}_a = T^a\{u_i \times v_i\} = (u_0 \times v_0, u_1 \times v_1, u_2 \times v_2, \dots, u_{N-2} \times v_{N-2}, u_{N-1} \times v_{N-1})$$

$$\{u_i\}_a = T^a\{u_i\} = (u_0, u_1, u_2, \dots, u_{N-2}, u_{N-1})$$

and the corresponding set of hybrid code sequences shown in equation (5-3) is given by:

$$\{h_i^{(j)}\}_a = \begin{cases} T^a\{u_i \times v_i\} \times T^j\{u_i\}_a & \text{for } 0 \leq j < N \\ T^a\{u_i \times v_i\} & \text{for } j = N \\ 0 & \text{otherwise} \end{cases}$$

As can be seen in this equation, sets of hybrid code sequences are constructed from $\{u_i\}$ and $\{v_i\}$ code sequences. Using the same process as above, since u_i and v_i represent different code sequences, combination of m-sequence and the third component of the expression (3-12) for large set Kasami code sequence generate N different sets of orthogonal code sequences.

d. The fourth component

Let us now consider the first code sequence of the fourth component of expression (3-12). This component is given by:

$$u_i \oplus w_i = u_i \times w_i$$

and therefore, the corresponding representation of equations (5-1) and (5-2) is given below:

$$\{k_i\}_a = T^a\{u_i \times w_i\} = (u_0 \times w_0, u_1 \times w_1, u_2 \times w_2, \dots, u_{N-2} \times w_{N-2}, u_{N-1} \times w_{N-1})$$

$$\{u_i\}_a = T^a\{u_i\} = (u_0, u_1, u_2, \dots, u_{N-2}, u_{N-1})$$

and the corresponding set of hybrid code sequences shown in equation (5-3) is given by:

$$\{h_i^{(j)}\}_a = \begin{cases} T^a\{u_i \times w_i\} \times T^j\{u_i\}_a & \text{for } 0 \leq j < N \\ T^a\{u_i \times w_i\} & \text{for } j = N \\ 0 & \text{otherwise} \end{cases}$$

As can be seen in this equation, sets of hybrid code sequences are constructed from $\{u_i\}$ and $\{w_i\}$ code sequences. Using the same process as above, N sets of orthogonal code sequences can be generated.

However, since the code sequence w must be first repeated $N/(2^{n/2} - 1)$ times before performing the XOR operation as explained in section 3.2.3, there are $N/(2^{n/2} - 1)$ identical sets of orthogonal code sequences. Therefore, combination of

m-sequence and the fourth component of equation (3-12) generates $(2^{n/2} - 1)$ different sets of orthogonal code sequences.

e. The fifth component

Let us consider the first code sequence of the fifth component of expression (3-12). This component is given by:

$$v_i \oplus w_i = v_i \times w_i$$

and hence, equations (5-1) and (5-2) are given as follows:

$$\{k_i\}_a = T^a\{v_i \times w_i\} = (v_0 \times w_0, v_1 \times w_1, v_2 \times w_2, \dots, v_{N-2} \times w_{N-2}, v_{N-1} \times w_{N-1})$$

$$\{u_i\}_a = T^a\{u_i\} = (u_0, u_1, u_2, \dots, u_{N-2}, u_{N-1})$$

and the resulting set of hybrid code sequences shown in equation (5-3) is given by:

$$\{h_i^{(j)}\}_a = \begin{cases} T^a\{v_i \times w_i\} \times T^j\{u_i\}_a & \text{for } 0 \leq j < N \\ T^a\{v_i \times w_i\} & \text{for } j = N \\ 0 & \text{otherwise} \end{cases}$$

As can be seen in this equation, sets of hybrid code sequences are constructed from $\{u_i\}$, $\{v_i\}$ and $\{w_i\}$ code sequences.

Using the same process as above, since $\{u_i\}$, $\{v_i\}$, and $\{w_i\}$ are different code sequences, combination of m-sequence and the fifth component of expression (3-12) of large set Kasami code sequence generate N different sets of orthogonal code sequences.

f. The sixth component

Let us consider the first code sequence of the sixth component of expression (3-12). This component is given by:

$$u_i \oplus v_i \oplus w_i = u_i \times v_i \times w_i$$

and therefore, equivalent of equations (5-1) and (5-2) is given as follows:

$$\{k_i\}_a = T^a\{u_i \times v_i \times w_i\} = (u_0 \times v_0 \times w_0, u_1 \times v_1 \times w_1, u_2 \times v_2 \times$$

$$w_2, \dots, u_{N-2} \times v_{N-2} \times w_{N-2}, u_{N-1} \times v_{N-1} \times w_{N-1})$$

$$\{u_i\}_a = T^a\{u_i\} = (u_0, u_1, u_2, \dots, u_{N-2}, u_{N-1})$$

and the corresponding set of hybrid code sequences shown in equation (5-3) is given by:

$$\{h_i^{(j)}\}_a = \begin{cases} T^a\{u_i \times v_i \times w_i\} \times T^j\{u_i\}_a & \text{for } 0 \leq j < N \\ T^a\{u_i \times v_i \times w_i\} & \text{for } j = N \\ 0 & \text{otherwise} \end{cases}$$

As can be seen in this equation, sets of hybrid code sequences are constructed from $\{u_i\}$, $\{v_i\}$ and $\{w_i\}$ code sequences.

Using the same process as above, since $\{u_i\}$, $\{v_i\}$, and $\{w_i\}$ are different sequences, combination of m-sequence and the fifth component of expression (3-12) of large set Kasami sequence generate N different sets of orthogonal code sequences.

The orthogonal code sequence sets resulting from the fifth component are same as that from the sixth component, as they were generated by this hybrid method using the same code sequences. Also, similar sets of orthogonal code sequences will result from the second and third components, for the reason stated above. Hence, to obtain dissimilar sets of orthogonal code sequences, the fifth or the sixth component and the second or the third component must be eliminated. Therefore, total number of orthogonal code sequence sets (N_s) can be obtained by adding sets obtained from the first component to the sixth component by selecting only one set from the similar sets as mentioned above:

$$N_s = 1 + 2N + \left(2^{\frac{n}{2}} - 1\right) \quad (5-6)$$

And the total number of different code sequences (M_{total}) that can be generated is obtained by multiplying the total number of orthogonal code sequence sets (N_s) by the number of members in a set ($N + 1$):

$$M_{total} = N_s (N + 1)$$

$$M_{total} = (N + 1) + 2N(N + 1) + \left(2^{\frac{n}{2}} - 1\right) (N + 1) \quad (5-7)$$

5.2 Implementation and Analysis of The Proposed HOVLS code sequence

The proposed HOVLS code sequence is implemented in a synchronous CDMA system, via simulation using Simulink/Matlab programming to analysis the performance metrics such as family size or capacity, autocorrelation function, cross-correlation function, and bit error rate (BER) performance. BER performance of the proposed HOVLS code sequence is analysed under two different channel conditions namely Rayleigh flat and frequency selective fading channels. The performance of the proposed HOVLS code sequence is compared to that of orthogonal Gold code sequence and orthogonal m-sequence.

5.2.1 Simulation of the proposed HOVLS code sequence

A set of assumptions have been made for the simulation of the synchronous CDMA system, which are given in section 5.2.1.2. The block diagram and the rationale behind the blocks used to simulate the synchronous CDMA system are given in section 5.2.1.1. Number of Monte Carlo simulations used for this system is five times.

5.2.1.1 Block diagram of the synchronous CDMA system

The block diagram of the simulation model used is shown in figure 5.1. This simulation is performed under Rayleigh flat and frequency selective fading channel conditions.

At the input of the system, randomly generated binary digit (bit) information is modulated using DBPSK modulator to produce DBPSK symbols. The CDMA

system assigns each user different spreading code sequence from a set of code sequences that are from the same family to spread the DBPSK symbols. The spread spectrum signal is then radiated into the channel. At the AWGN channel output, the received signal is de-spread using a correlation receiver. This process will reject the interfering signals and pass the desired signal to DBPSK demodulator. The desired signal is then demodulated to obtain the desired bit information.

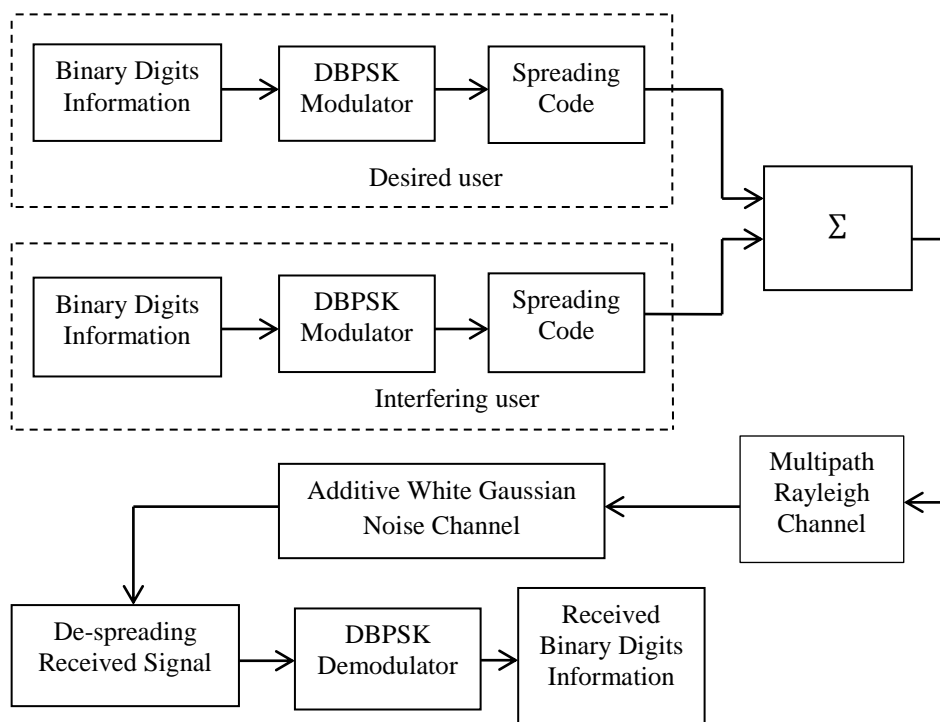


Figure 5.1 Block diagram for the simulation of synchronous CDMA system

5.2.1.2 Assumptions for the simulation of the synchronous CDMA system

Based on the block diagram of the simulation model shown in figure 5.1, the assumptions for the simulations are as follows:

- The input considered is binary bit sequence with Bernoulli distribution with same probability between bit 0 and 1.
- The total number of bits for the entire simulation is 300 Kbits.

- Sampling time = 0.001 second.
- Modulation is DBPSK.
- The number of users is 64.
- The average power transmitted by each user's signal at the base station is 1 Watt.
- Spreading code sequence lengths is 64 chips.
- The receiver is a correlation receiver.
- The desired signal and MAI signals are chip synchronized at the receiver.
- There is no interference from other cells.
- Rayleigh flat fading channel is modeled by one path with a path gain equal to 0 dB.
- Rayleigh frequency selective fading channel is modeled with four path time delays (0 , 1 chip duration, 2 chips duration, 3 chips duration) and four path gains (0 dB, -3 dB, -6 dB -9 dB). One chip duration = $\frac{0.001}{64} = 0.000016$ second.
- To represent mobile radio channel, it is assumed a desired user (a pedestrian user) moving with speed of 5 km/hour. Since carrier frequency used in CDMA systems is 2.11 GHz (Rao and Dianat, 2005), based on equation (4-2), Doppler shift is 10 Hz.

5.2.2 Simulation results and discussion

In the following section, the performance metrics of the proposed HOVLS code sequence simulated using Simulink/Matlab programming is compared to those of orthogonal Gold code sequence and orthogonal m-sequence.

5.2.2.1 Capacity and peak cross-correlation value of the proposed HOVLS code sequence

As shown in table 5.1, the proposed code sequence has the largest code sequence set. These sets can be used simultaneously if the peak cross-correlation value between the code sequences (from different groups) is less than half of the code sequence length (Donelan and O'Farrel, 1999). Since the peak cross-correlation value of the proposed code sequence of length 64 chips is 16, which is one quarter of 64, 134 groups of the proposed code sequence can be used simultaneously. This means, this code sequence set could support 134 different cells in a synchronous CDMA system.

Table 5.1 Capacity and peak cross-correlation value of the proposed and selected orthogonal code sequences

Orthogonal code sequence	Length of code sequence (chips)	Number of sets	Capacity of code sequence (users)	Peak cross-correlation value
The proposed HOVLS code	64	134	8676	16
Orthogonal Gold	64	63	4032	16
Orthogonal m-sequence	64	63	4032	16

5.2.2.2 Autocorrelation function of the proposed HOVLS code sequence

Autocorrelation function of the proposed HOVLS code sequence, orthogonal Gold code sequence and orthogonal m-sequence for 64 chip lengths are presented in figures 5.2 to 5.4 respectively. As seen in the figures 5.2 to 5.4, at zero time shifts the orthogonal code sequences have maximum autocorrelation values (the same as the length of the code sequences) since the values were obtained from correlation between the code sequence with a copy of itself that has the same chips structure as the original one. Whereas, at non-zero time shifts, the autocorrelation values are

much lower than that of zero time shift due to different chips structure between the two code sequences. The autocorrelation value at zero time shift represents desired user's signal strength while that at non-zero time shifts represent inter-symbol interference (ISI) signal strengths.

Based on these autocorrelation functions, merit factor (MF) of the proposed HOVLS code sequence, orthogonal Gold code sequence and orthogonal m-sequence is tabulated in table 5.2.

Since MFs of these orthogonal code sequences are similar, the proposed HOVLS code sequence has autocorrelation function values comparable to those of orthogonal Gold code sequence and orthogonal m-sequence.

Table 5.2 Merit factor of the proposed HOVLS code sequence

Orthogonal code sequence	Length of code sequence (chips)	MF
The proposed HOVLS code	64	0.68
Orthogonal Gold	64	0.82
Orthogonal m-sequence	64	0.59

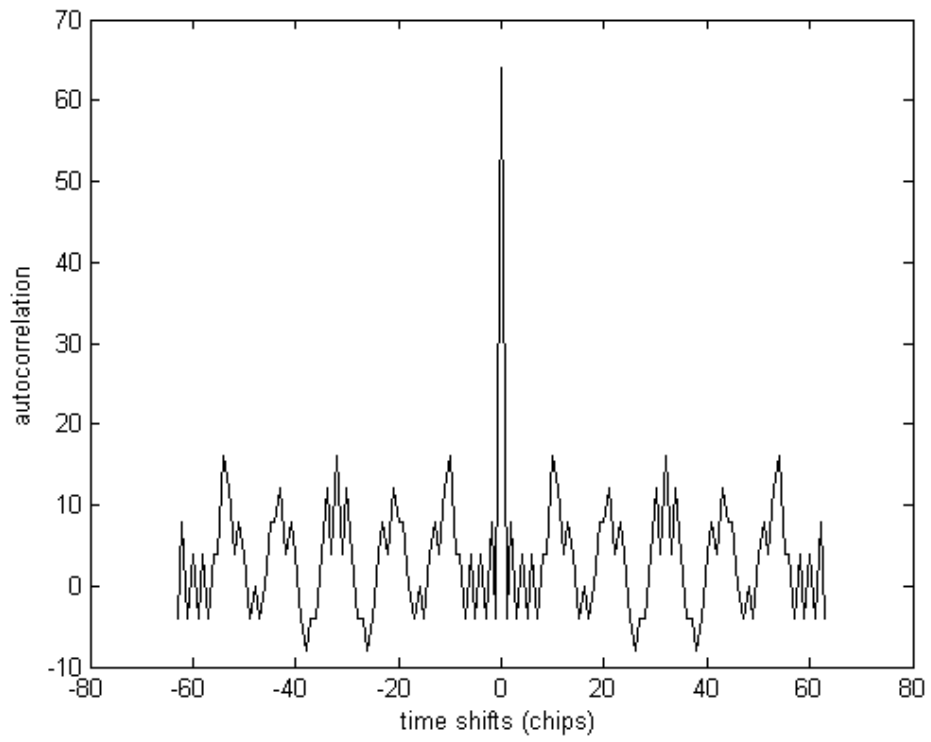


Figure 5.2 ACF of the proposed HOVLS code sequence

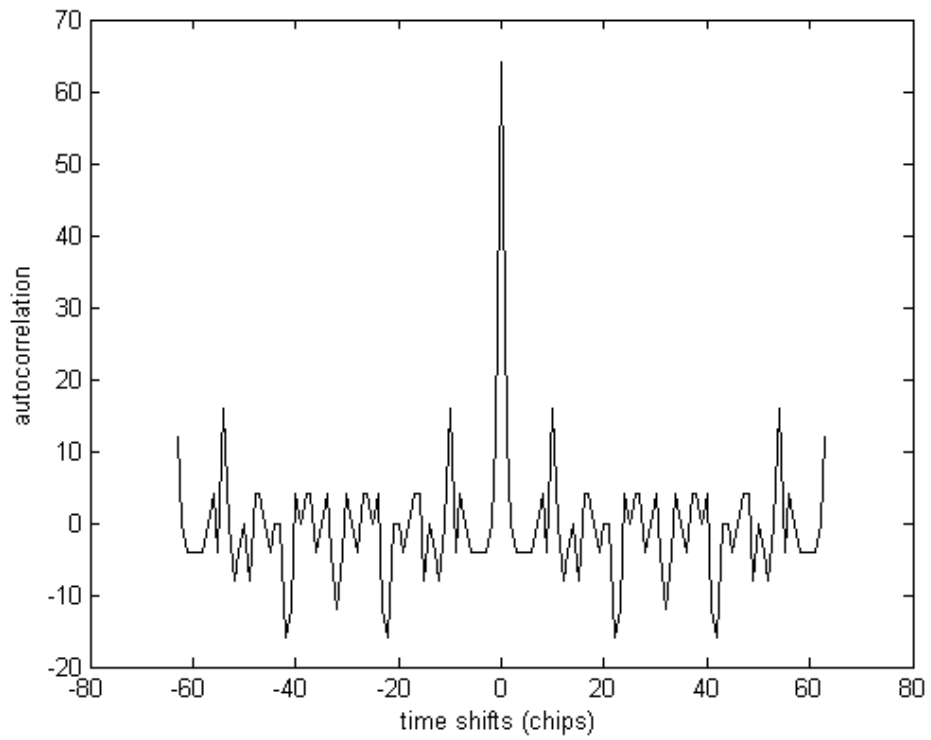


Figure 5.3 ACF of orthogonal Gold code sequence

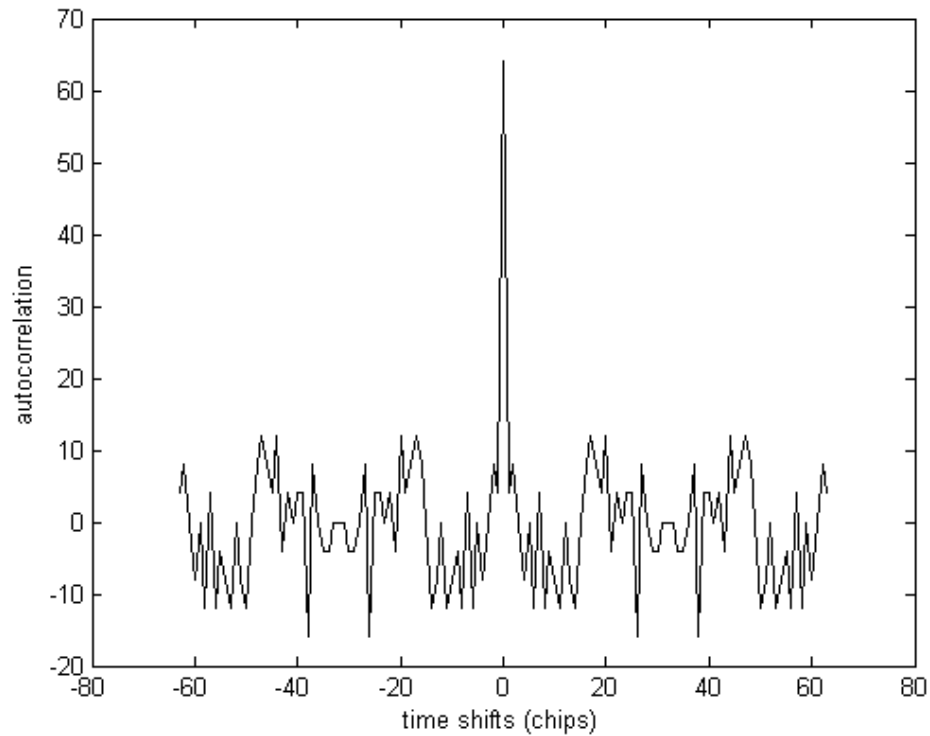


Figure 5.4 ACF of orthogonal m-sequence

5.2.2.3 Cross-correlation function of of the proposed HOVLS code sequence

Cross-correlation functions of the proposed HOVLS code sequence, orthogonal Gold code sequence and orthogonal m-sequence for 64 chip lengths are presented in figures 5.5 to 5.7. As seen in figures 5.5 to 5.7, the cross-correlation values of the orthogonal code sequences at zero time shifts are zero. Zero cross-correlation value at zero time shift means that the code is orthogonal (zero MAI signal strength). However, some cross-correlation values are non-zero at non-zero time shifts since the chips' structure of the orthogonal code sequence has been changed when the orthogonal code sequence was shifted. Non-zero cross-correlation values at non-zero time shifts represent non-zero MAI signal strengths.

Based on these cross-correlation functions, correlation margin (CM) of the proposed HOVLS code sequence, orthogonal Gold code sequence and orthogonal m-sequence for 64 chip lengths is tabulated in table 5.3.

As seen in table 5.3, the proposed HOVLS code sequence has CM comparable to those of orthogonal Gold code sequence and orthogonal m-sequence. Therefore, in terms of CM, the proposed HOVLS code sequence has comparable CCF to those of orthogonal Gold code sequence and orthogonal m-sequence.

Table 5.3 CM of the proposed HOVLS code sequence

Spreading code sequence	Length of code sequence (chips)	CM(dB)
The proposed HOVLS code	64	-13.01
Orthogonal Gold	64	-13.01
Orthogonal m-sequence	64	-12.04

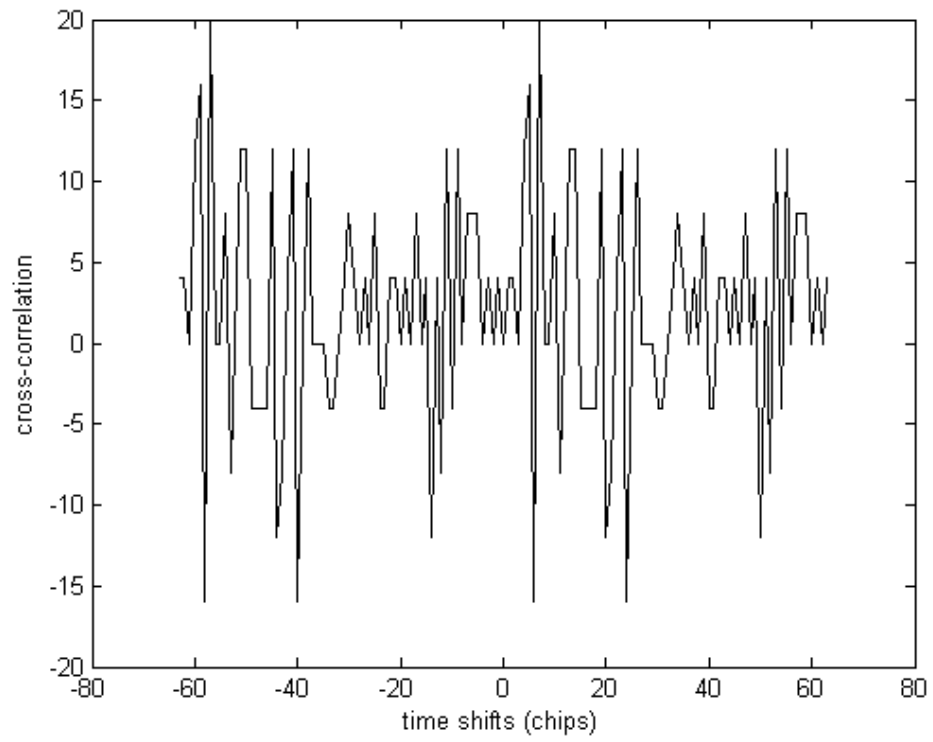


Figure 5.5 CCF of the proposed HOVLS code sequence

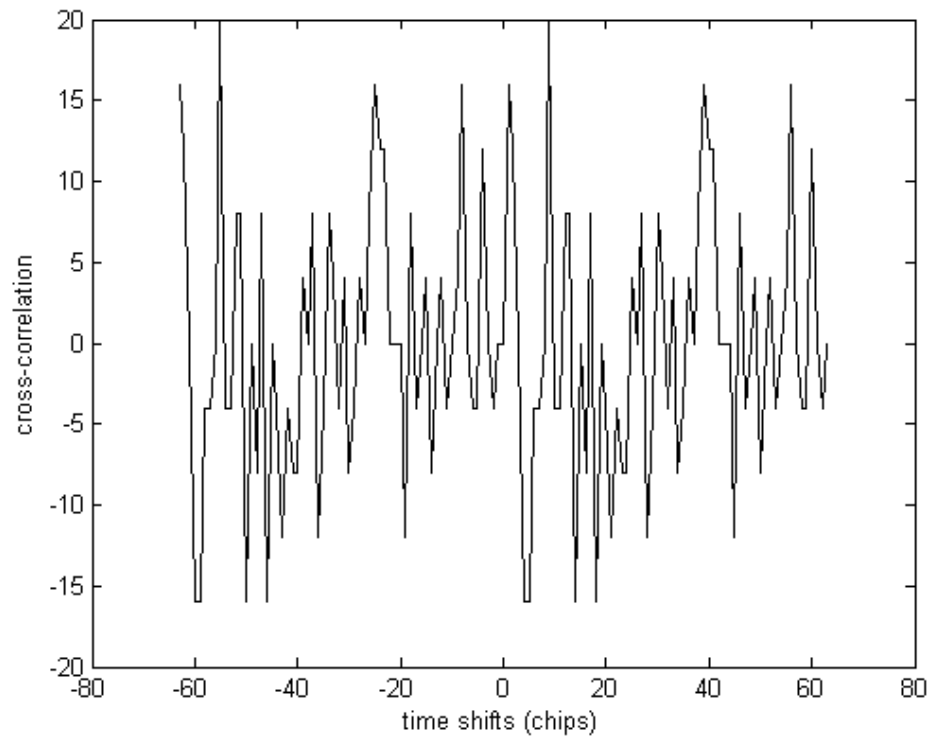


Figure 5.6 CCF of orthogonal Gold code sequence

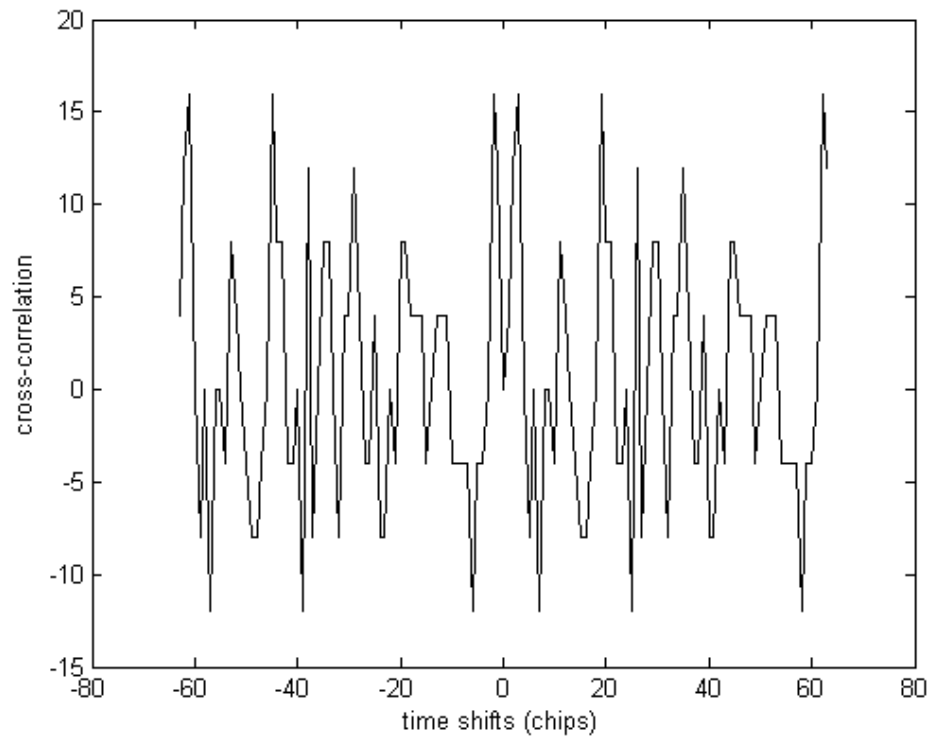


Figure 5.7 CCF of orthogonal m-sequence

5.2.2.4 BER performance of the proposed HOVLS code sequence under Rayleigh flat fading channel condition

In any digital communication system, BER values decrease for increasing SNR value, since increasing SNR value means the desired signal power becomes higher than the noise power. When the desired signal power increases, the number of bits corrupted by the noise becomes smaller, therefore BER values decrease (Proakis, 2000). Evaluation of the BER performance of the proposed HOVLS code sequence demonstrates that the BER values decrease as SNR value increases, as seen in subsections 5.2.2.4, 5.2.2.5, 6.2.2.4, 6.2.2.5, 6.2.2.6 and 6.2.2.7.

As can be seen from figure 5.8, the proposed HOVLS code sequence has similar BER performance to those of orthogonal Gold code sequence and orthogonal m-sequence in a synchronous CDMA system under Rayleigh flat fading channel. The reasons for this performance behaviour are discussed in the following paragraphs.

In flat fading channel condition there is no excess delay, and hence when de-spreading the received signal, both the autocorrelation (ACF) and cross-correlation functions (CCF) of the orthogonal spreading code sequences will be at zero time shift as shown in figures 5.2 to 5.7. Therefore, there is no Inter-symbol interference (ISI) and multiple access interference (MAI) at the receiver, and hence BER value is constant for increasing number of users. However, as seen in figure 5.8, BER values of the orthogonal code sequences decrease only for increasing SNR value, therefore the orthogonal code sequences are operating under noise limited condition.

Since these code sequences are under noise limited condition (MAI does not exist), and have similar desired user's signal strength represented by ACF at zero time shift due to the absence of ISI, therefore these orthogonal code sequences have similar BER performance.

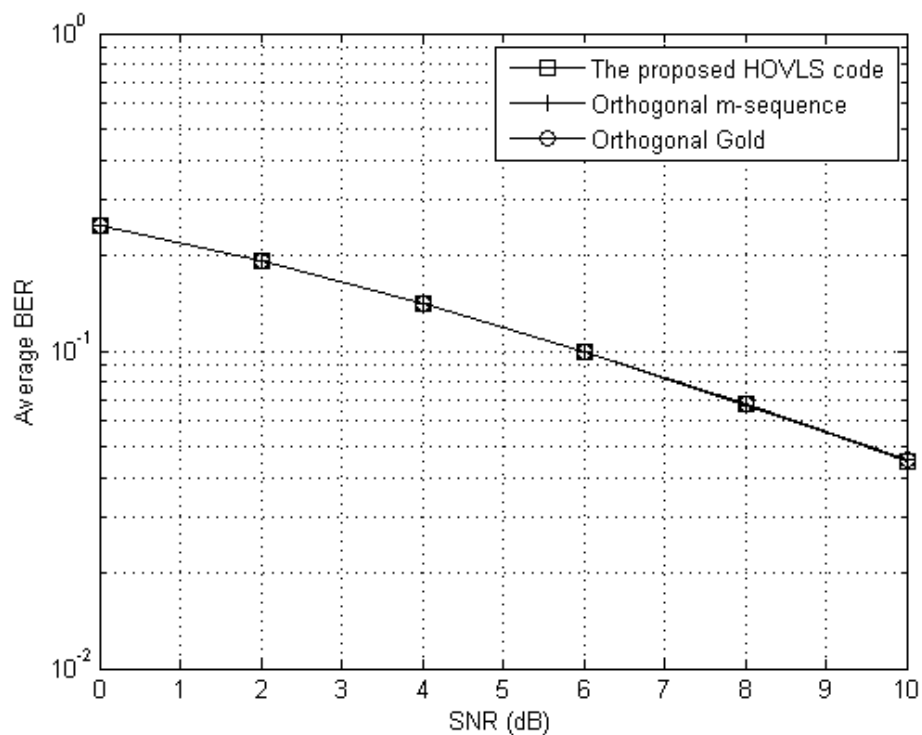


Figure 5.8 BER versus SNR of the orthogonal code sequences under Rayleigh flat fading channel

5.2.2.5 BER performance of the proposed HOVLS code sequence under Rayleigh frequency selective fading channel condition

As seen from figure 5.9, the proposed HOVLS code sequence has BER performance similar to that of orthogonal Gold code sequence and orthogonal m-sequence in a synchronous CDMA system under Rayleigh frequency selective fading channel conditions. The reason behind this performance is discussed below.

In frequency selective fading channel, the received signal includes multiple versions of the transmitted signal which are attenuated and delayed in time. Therefore, ISI and multiple access interference (MAI) occur when de-spreading the received signal, due to the non-zero values of ACF and CCF of the orthogonal code sequences at non-zero time shifts. This is presented in figures 5.2 to 5.7. Under this condition, the desired user's signal is distorted and BER value increases with increasing number of users as seen in figure 5.10. However, BER values of the orthogonal code sequences as shown in figure 5.9 decrease with increasing SNR value, therefore these orthogonal code sequences are under both noise and multiple access interference (MAI) limited conditions. Since these orthogonal code sequences are under similar conditions and have comparable ACF (similar BER value for one user) and CCF (similar BER value for increasing number of users), their BER performance is similar as shown in figure 5.9.

Comparison between BER performances of the orthogonal code sequences under flat fading channel condition to that of under frequency selective fading channel is shown in figures 5.8 and 5.9 respectively.

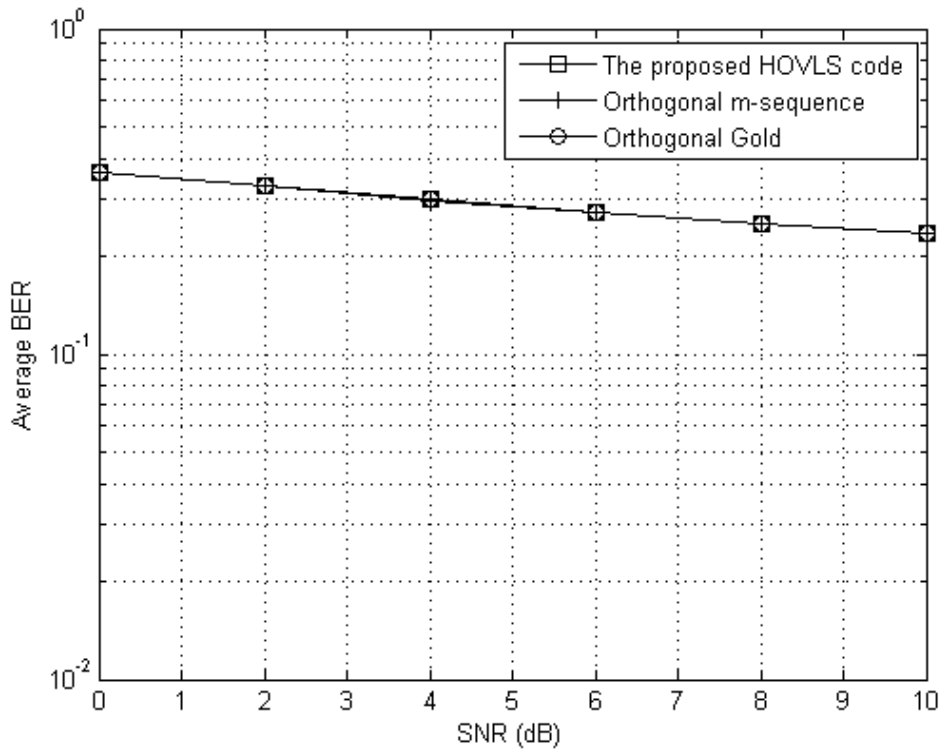


Figure 5.9 BER versus SNR of the orthogonal code sequences under Rayleigh frequency selective fading channel

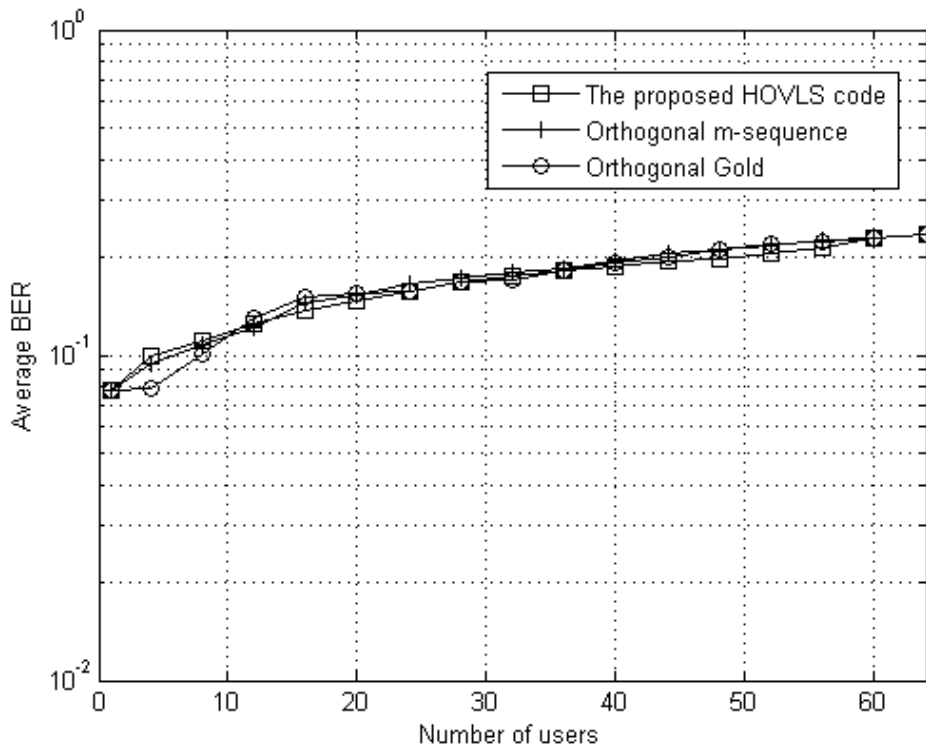


Figure 5.10 BER versus number of users of the orthogonal code sequences for SNR = 10 dB under Rayleigh flat fading channel

BER performances of the orthogonal code sequences under frequency selective fading channel are worse than that of under flat fading channel, due to MAI and ISI under frequency selective fading channel conditions. However, there is no ISI and MAI when implementing orthogonal code sequences in synchronous CDMA system under flat fading channel condition.

The proposed HOVLS code sequence has similar BER performance to those of orthogonal code sequence and orthogonal m-sequence under Rayleigh frequency selective fading channel. This means that the proposed HOVLS code sequence has levels of effect from MAI similar to that of the orthogonal Gold code sequence and orthogonal m-sequence in CDMA systems. However, the proposed HOVLS code sequence fairs much better than those existing codes in terms of its capacity. This means, the proposed HOVLS code sequence can accommodate very large number of users, which is more than twice than that of orthogonal code sequence and orthogonal m-sequence.

Chapter 6

DESIGN, IMPLEMENTATION AND ANALYSIS OF VARIABLE SPREADING FACTOR HYBRID ORTHOGONAL VERY LARGE SET CODE SEQUENCE

Nowadays, cellular phone operators are in a scramble to meet huge demands from their customers for transmitting a blend of data types such as audio, data, image and video transfer at high data rates. This is the target for mobile phone operators in order to improve capabilities of multimedia communications. One way to flexibly provide data services of different rates from low to very high bit rates is to assign orthogonal code sequences with different lengths in the forward link to each user according to the data rate requested. This will ensure constant chip rate after spreading at variable data rate. An orthogonal code sequence used for different bit rates is called an orthogonal variable spreading factor (OVSF) code sequence (Adachi, et.al., 1997; Feng, et.al., 2007; Wang, et.al., 2008).

Since an orthogonal code sequence must have the capability to support variable data rate, a novel design was developed to adapt the fixed length HOVLS code sequence for variable data rate.

The BER performance of the proposed OVSF HOVLS code sequence is evaluated and compared to OVSF Gold code sequence and OVSF m-sequence in synchronous CDMA system, using Rayleigh flat and frequency selective fading channels. Besides ACF and CCF of the OVSF code sequences are also evaluated. This evaluation is performed via simulation using Simulink/Matlab programming.

6.1 Design of the proposed OVSF HOVLS code sequence

In a CDMA system providing services of differing bit rates, consider that each bit of the lowest bit rate service (R_{min}) is spread by a code sequence length $N = 2^n$ ($n > 0$ where n is a positive integer number). A code sequence with a bit rate twice that of the lowest bit rate ($2R_{min}$) code sequence will have half the code sequence length of the lowest bit rate ($N/2 = 2^{n-1}$) code sequence, since the bit duration for $2R_{min}$ rate is half the duration of a bit with minimum rate (Dinan and Jabbari, 1998; Karakayali et. al., 2006; Amico et. al., 2002):

$$R_{min} = \frac{1}{T_b} \quad (1)$$

where T_b is bit duration. In such a system, OVSF code sequences such as the proposed OVSF HOVLS code sequence could accommodate applications ranging across different bit rate values such as audio, data, image and video represented by different spreading factor (SF). However, for simplicity, only two different bit rates were considered. In this case two different SFs (128 and 256) are used to evaluate the performance of the proposed OVSF HOVLS code sequence.

Adapting the method demonstrated by (Adachi et. al., 1997), the code tree for the OVSF HOVLS code sequence has been designed as shown in figure 6.1. The minimum spreading factor for the proposed OVSF HOVLS code sequence is 64, since the minimum length of the proposed fixed length HOVLS code sequence is 64. Therefore, the different spreading factors that can be generated using the code tree are 64, 128, 512, etc., as shown in figure 6.1. K_{64} denotes a set of the proposed OVSF HOVLS code sequences having 64 members, each of length 64, while \bar{K}_{64} represents binary complement of the K_{64} code sequence set.

The code tree shown in figure 6.1 starts from the root of the code tree i.e. the K_{64} HOVLS code sequence of length 64 chips (the proposed fixed length

HOVLS code sequence) as a mother with a spreading factor of 64. This mother has two child code sequences denoted by $K_{64}K_{64}$ and $K_{64}\bar{K}_{64}$ each having a spreading factor of 128. Each of these child code sequences will be a mother in turn for two child code sequences with a spreading factor of 256 each. The same process is performed to obtain higher spreading factor code sequences.

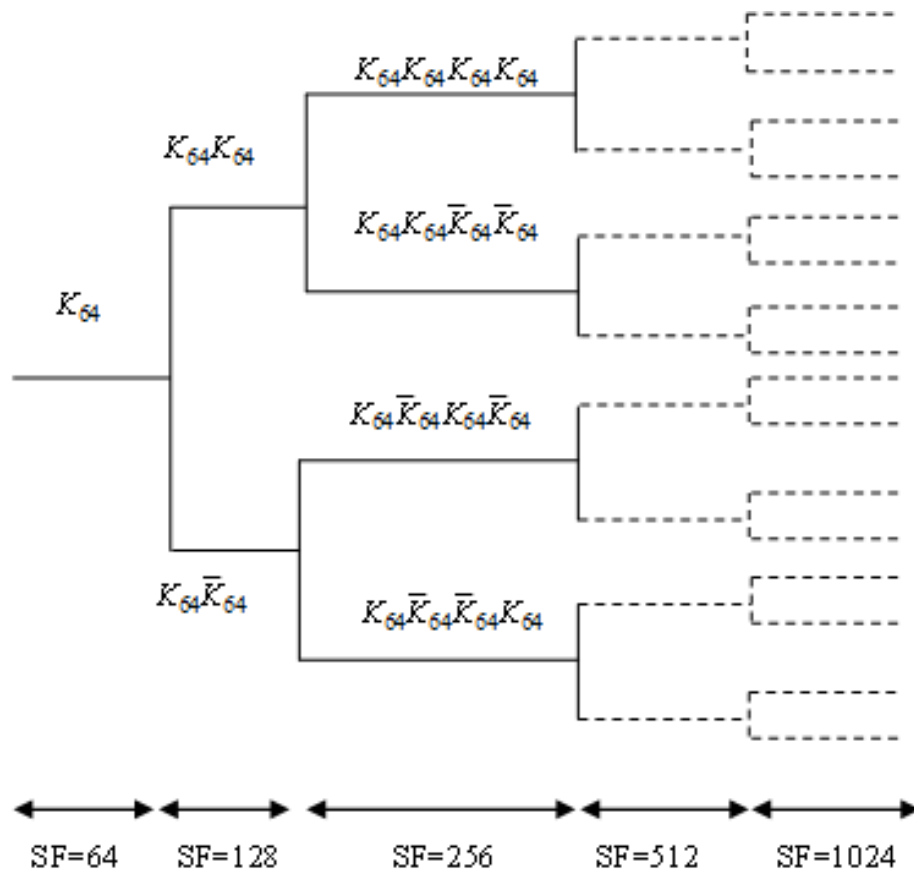


Figure 6.1 Code sequence tree for generation of OVSF HOVLS code sequences

The proposed OVSF HOVLS code sequences belonging to the same layer (i.e. same SF in figure 6.1) of the code tree form a set of orthogonal code sequences with zero cross-correlation values. Also, the code sequences belonging to different layers (i.e. different SFs in figure 6.1) are orthogonal, provided these code sequences do not have mother-child relationship. In fact, a code sequence in the code tree can be used by a mobile station *iff* (if and only if) no other code sequence on the path from

the specific code sequence to the root of the code tree or in the code sub-tree below the specific code sequence is used by other mobile stations.

As presented in figure 6.1, each layer contains groups of code sequences. Each group of code sequences corresponds to a branch (a line) in the code tree having a member of 64 code sequences. Therefore, layer 1 (SF = 64) contains one group of code sequences, layer 2 (SF = 128) contains two groups of code sequences where group 1 corresponds to first branch (first line) and group 2 corresponds to second branch (second line) in that layer, and more groups for higher spreading factor (if a layer has SF value twice that of another layer, then the layer with higher SF will have twice the number of groups having lower SF).

Orthogonal Gold code sequence and orthogonal m-sequence can also be made to support multi rate data transmissions by adapting the method demonstrated by Adachi et. al., 1997. Since the minimum code sequence length of the orthogonal Gold code sequence and orthogonal m-sequence is 8, various spreading factors that can be generated using the code tree are 8, 16, 32, 64, etc. The detailed calculation is presented in appendices A and B.

6.2 Implementation and Analysis of The Proposed OVSF HOVLS Code Sequence

The proposed OVSF HOVLS code sequence is implemented in a synchronous CDMA system to analysis its BER performance under different channel conditions namely Rayleigh flat and frequency selective fading channels, via simulation using Simulink/Matlab programming. ACF and CCF of the proposed OVSF HOVLS code sequence are also analysed, and compared to that of the existing OVSF code sequences namely OVSF Gold code sequence and OVSF m-sequence.

6.2.1 Simulation of the proposed OVSF HOVLS code sequence

To simulate the proposed OVSF HOVLS code sequence in a synchronous CDMA system, two kinds of scenarios have been adopted, which are given in section 6.2.1.1, and the assumptions for the simulation are given in section 6.2.1.2. The block diagram and the rationale behind the blocks used to simulate the synchronous CDMA system have been discussed in section 5.2.1.1. Number of Monte Carlo simulations used for this system is five times.

6.2.1.1 Scenario for simulation of the proposed OVSF HOVLS code sequence

Though the proposed OVSF HOVLS code sequence is able to accommodate any number of different bit rates, for simplicity, only two kinds of users namely user $2R$ and R were considered in this scenario. The total number of users in this simulation is 64. User $2R$ transmits information at twice the bit rate than that of user R .

a. Scenario for user $2R$

In order to analysis the BER performance of the proposed OVSF HOVLS code sequence, the system was populated with a total of 64 users of which 16 were with $2R$ bit rate in this simulation. The BER values were measured for an increasing number of users, first by increasing the number of users with $2R$ bit rate from 1 to 16 and then by increasing the number of users with R bit rate until the total number of users in the system were 64. The OVSF Gold code sequence and OVSF m-sequence do not have zero MAI due to non-zero CCF for scenarios with less than 8 users. So, in order to make a fair comparison of the codes sequences, a scenario with more than 8 users has to be considered so that the OVSF Gold code sequence and OVSF m-sequence will have zero MAI. Therefore, 16 user $2R$ s were chosen to evaluate the BER values of the proposed OVSF code sequence when OVSF Gold code sequence and OVSF m-sequence have zero MAI. The BER performance was measured to see

the effect when the desired user is interfered by MAI coming from other users with both 2R and R data rates.

b. Scenario for user R

The scenario for user R is the same as that for user 2R described above, with the users R and 2R interchanged.

6.2.1.2 Simulation assumptions for the proposed OVSF HOVLS code sequence of synchronous CDMA system

The assumptions for the simulations are as follows:

- The input considered is Bernoulli distribution with same probability between bit 0 and 1.
- Sampling time = 0.001 sec.
- The total number of bits for the entire simulation is 300 Kbits for user R and 600 Kbits for user 2R, since user 2R has twice bit rate than user R. In this case, there are 2 bits per frame for user 2R and 1 bit per frame for user R.
- For the proposed OVSF HOVLS code sequence, user 2R is allocated code sequences of layer 2 of group 1 and user R is allocated code sequences of layer 3 of group 3 so that there is no mother-child relationship.
- For OVSF Gold code sequence and OVSF m-sequence, user 2R is allocated code sequences of layer 5 of group 1 to 8 and user R is allocated code sequences of layer 6 of group 17 to 32 so that there is no mother-child relationship.
- Modulation is DBPSK.
- The number of users is 64.
- The average power transmitted by each user's signal at the base station is 1 Watt.

- The receiver is a correlation receiver.
- The desired signal and MAI signals are chip synchronized at the receiver.
- Each signal is assumed to arrive at the receiver with equal average power.
- There is no interference from other cells.
- Rayleigh flat fading channel is modeled by one path with a path gain equal to 0 dB and a Doppler shift of 10 Hz.
- Rayleigh frequency selective fading channel is modeled with four path time delays (0 , 1 chip duration, 2 chips duration, 3 chips duration) and four path gains (0 dB, -3 dB, -6 dB -9 dB), and with 10 Hz Doppler shift. One chip duration = $\frac{0.001}{128} = 0.0000078$ second

As user 2R has twice the bit rate of user R, from the code tree shown in figure 6.1, if SF = 128 is selected for user 2R then SF = 256 will have to be selected for user R. However, code sequences having mother – child relationship between the code sequence sets with SF = 128 and code sequence sets with SF = 256 must not be selected for the group, as these code sequences are non-orthogonal. As seen in the code tree in figure 6.1, the code sequence with SF = 64 for user 2R and SF = 128 user R cannot be selected as all code sequences with SF = 64 and SF = 128 have mother – child relationship.

Therefore, in this simulation the author used code sequences with SF = 128 of group 1 (first line of SF = 128) in the code tree for user 2R and code sequences with SF = 256 of group 3 (third line of SF = 256) for user R.

6.2.2 Simulation results and discussion

The performance of the proposed OVFS HOVLS code sequence is analysed in terms of autocorrelation function (ACF), cross-correlation function (CCF), and BER

under Rayleigh flat and frequency selective fading channel conditions. These parameters will be benchmarked against that of OVSF Gold code sequence and OVSF m-sequence.

6.2.2.1 Autocorrelation function of the proposed OVSF HOVLS code sequence

ACF of the OVSF code sequence proposed by Adachi, et.al, 1997 at some zero time shifts has similar autocorrelation values to that of non-zero time shift. The proposed OVSF HOVLS code sequence, OVSF Gold code sequence and OVSF m-sequence were all generated by adapting the method proposed by Adachi, et.al, 1997. Therefore, they have autocorrelation values at some non-zero time shifts similar to that of at zero time shift, as seen in figures 6.2 to 6.4 and figures 6.5 to 6.7.

As seen in figures 6.2 to 6.4 and figures 6.5 to 6.7, the proposed OVSF HOVLS code sequence has comparable autocorrelation function to those of OVSF Gold code sequence and OVSF m-sequence for 128 and 256 chips lengths respectively, since each of these OVSF code sequences has similar merit factor (MF) as shown in table 1 which are less than 2 (Wieser and Hrudkay, 2002). That is the ratio of the autocorrelation energy at zero time shift ($R_{xx}(0)$) to the total energy of autocorrelation at non zero time shifts ($R_{xx}(\tau)$) for the OVSF code sequences is similar.

Table 6.1 MF of the proposed OVSF HOVLS code sequence

OVSF code sequence	MF for 128 chip lengths	MF for 256 chip lengths
Orthogonal Gold	0.02	0.01
Orthogonal m-sequence	0.02	0.01
The proposed code	0.20	0.08

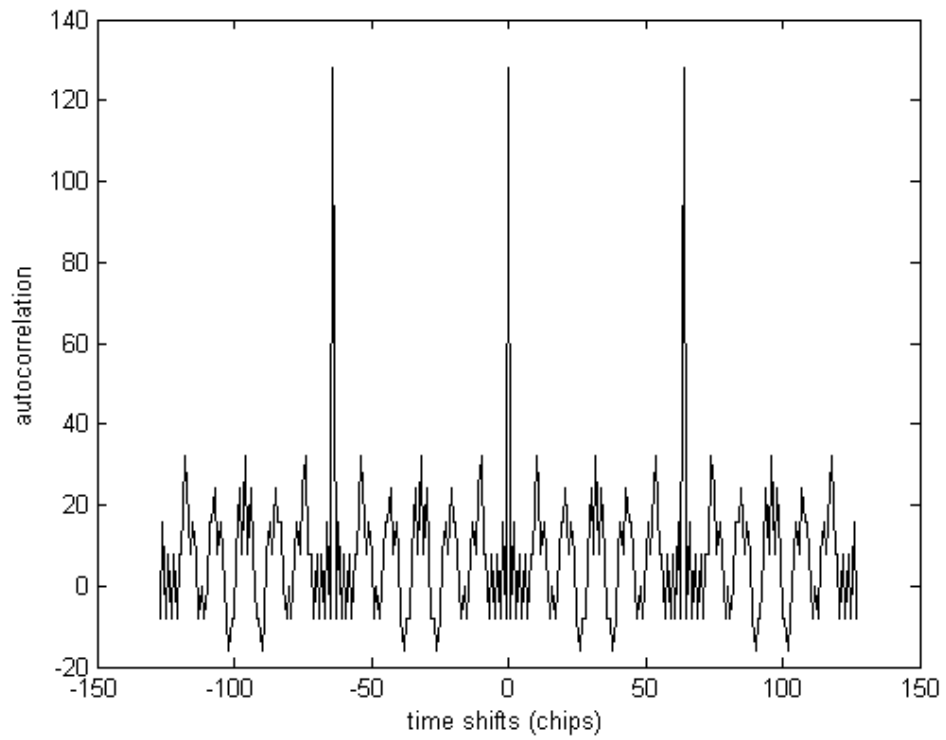


Figure 6.2 ACF of the proposed OVSF HOVLS code sequence for 128 chip lengths

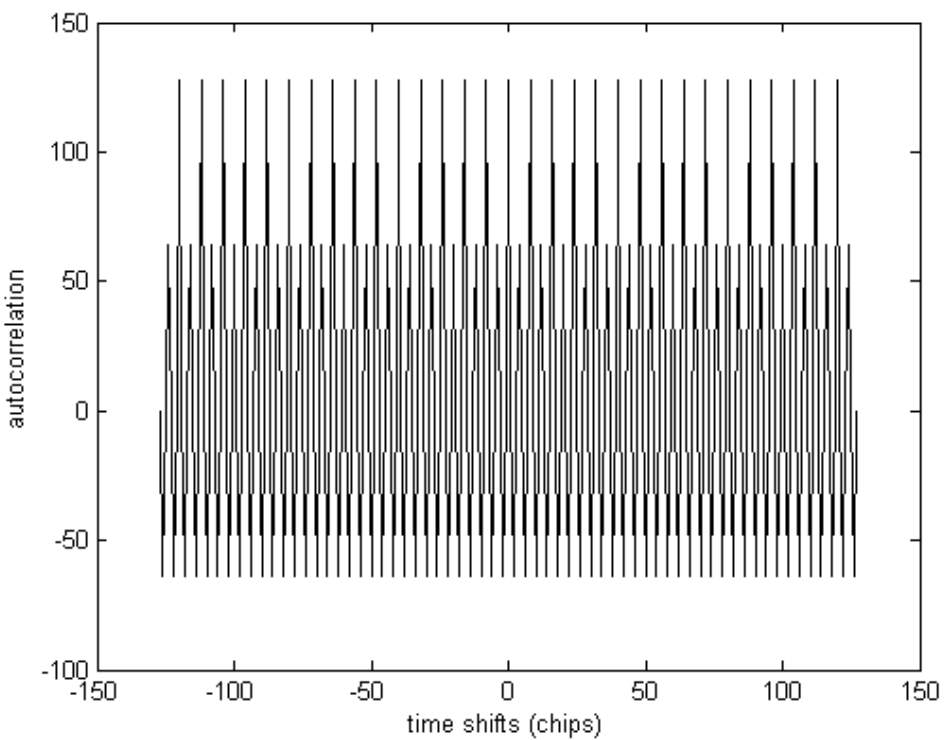


Figure 6.3 ACF of OVSF Gold code sequence for 128 chip lengths

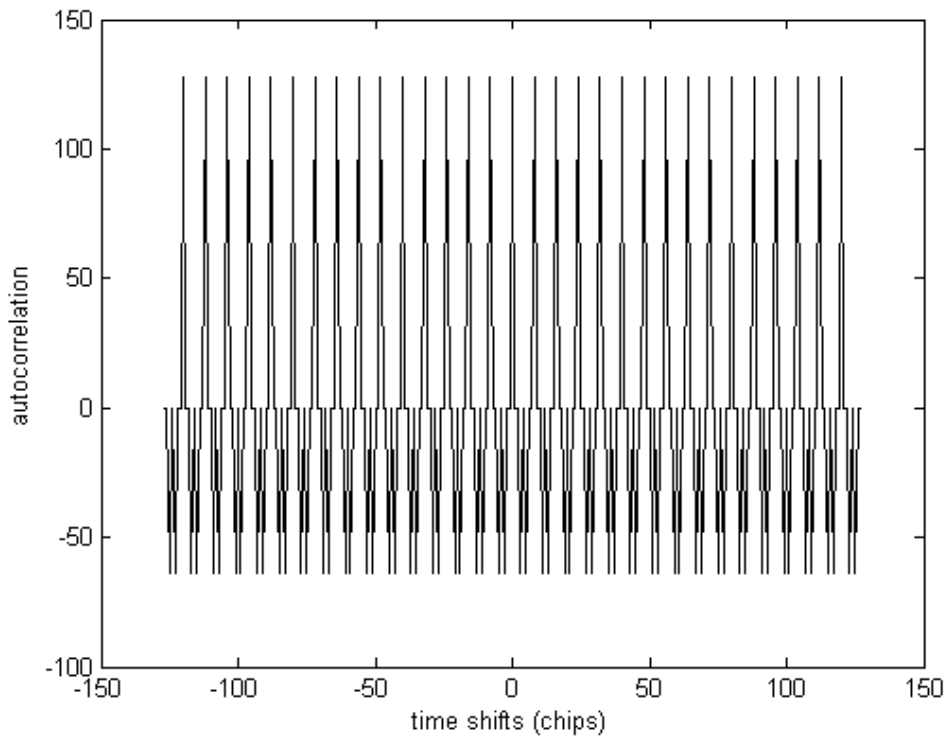


Figure 6.4 ACF of OVSF m-sequence for 128 chip lengths

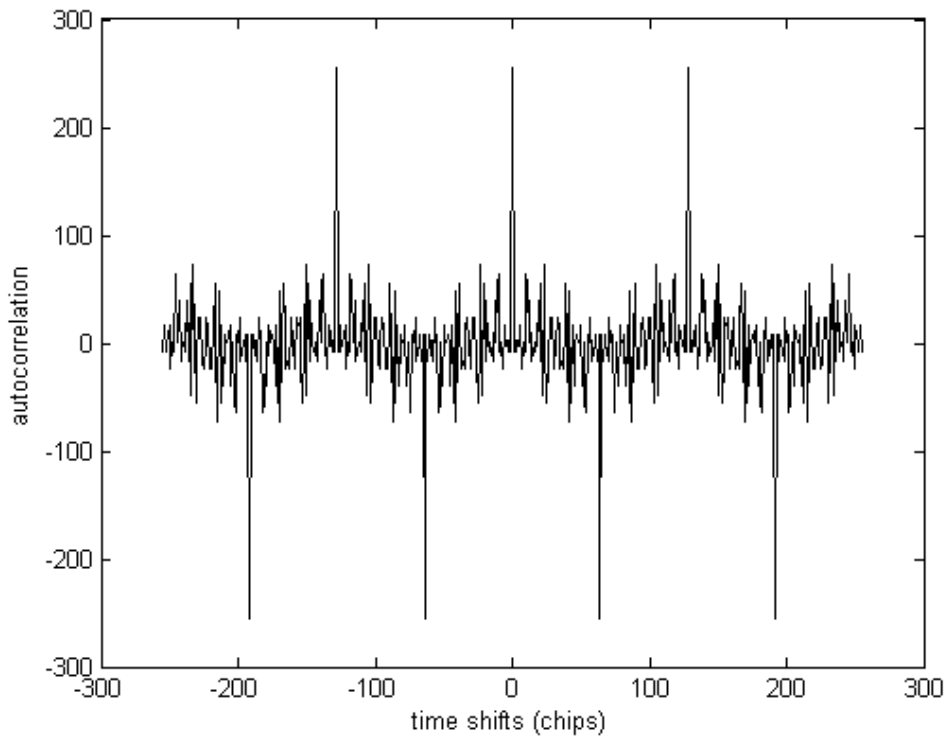


Figure 6.5 ACF of the proposed OVSF HOVLS code sequence for 256 chip lengths

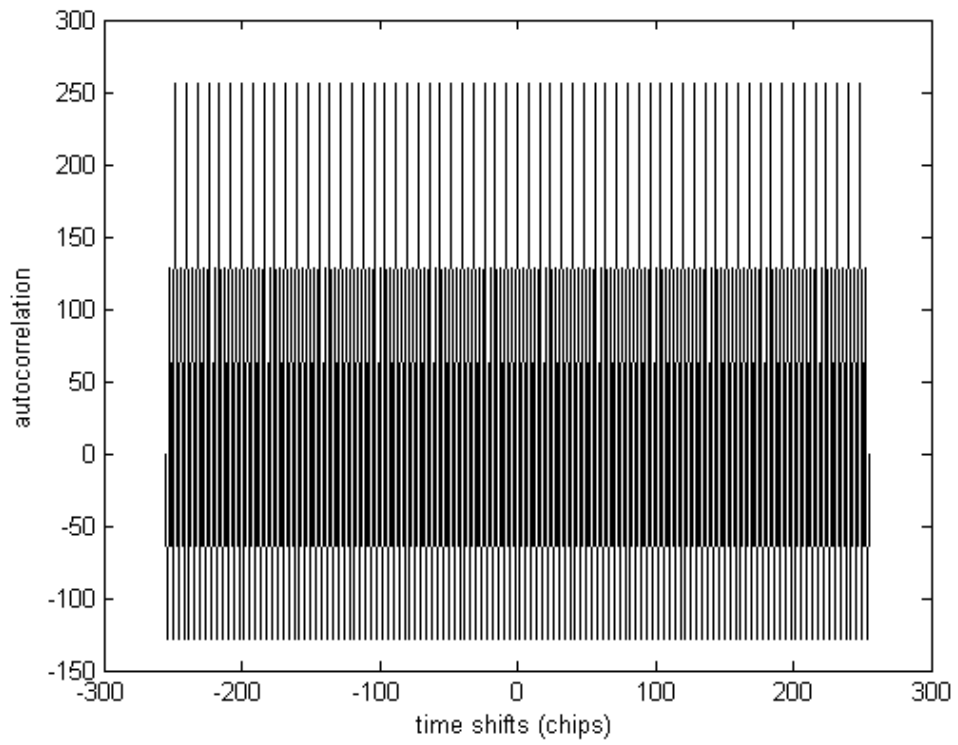


Figure 6.6 ACF of OVSF Gold code sequence for 256 chip lengths

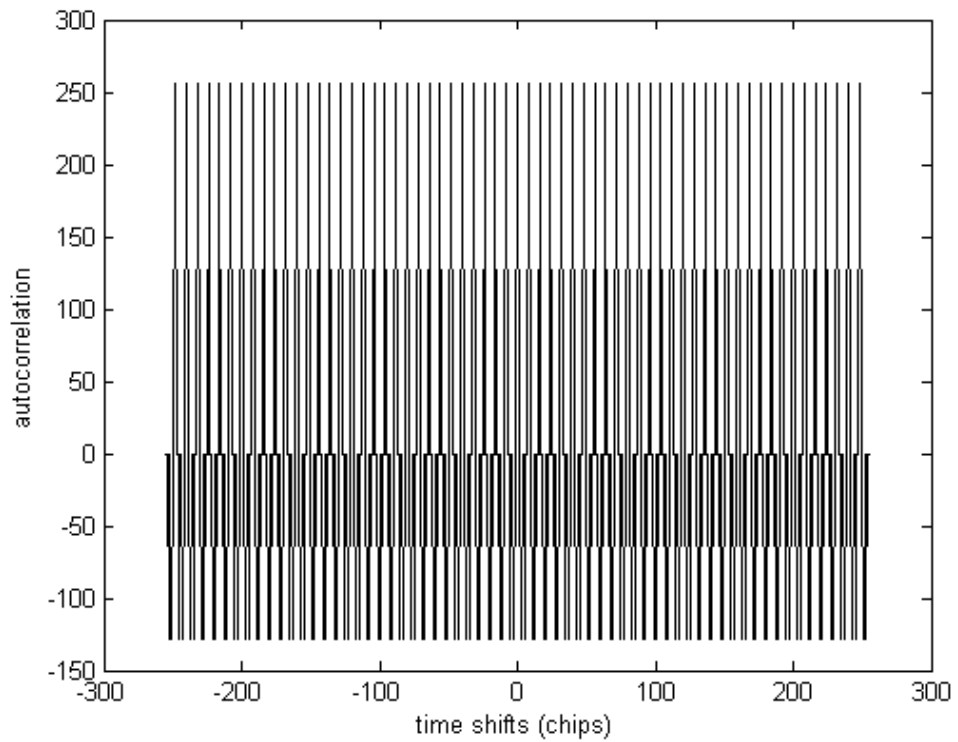


Figure 6.7 ACF of OVSF m-sequence for 256 chip lengths

6.2.2.2 Cross-correlation function of the proposed OVFS HOVLS code sequence in same groups in the code tree

Cross-correlation functions of the proposed OVFS HOVLS code sequence, OVFS Gold code sequence and OVFS m-sequence from the same group in the code tree are shown in figures 6.8 to 6.10 and figures 6.11 to 6.13 for 128 and 256 chips length respectively. The proposed OVFS HOVLS code sequence, OVFS Gold code sequence and OVFS m-sequence belonging to the same group in the code tree, at zero time shifts have zero cross-correlation values, as they are orthogonal code sequences. However, at some non-zero time shifts, cross-correlation values are not zero, since chips structure has been changed by chips shifted at non-zero time shifts.

As presented in table 6.2, the proposed OVFS HOVLS code sequence has slightly higher correlation margin (2.04 dB more tolerant for SF = 128 and 2.50 dB for SF = 256 in multi users environment) than that of OVFS Gold code sequence and OVFS m-sequence. Whereas CM of OVFS Gold code sequence is similar to that of OVFS m-sequence. Therefore, in terms of CM, the proposed OVFS HOVLS code sequence has slightly better CCF than that of OVFS Gold code sequence and OVFS m-sequence, and CCF of OVFS Gold code sequence is comparable to that of OVFS m-sequence. Cross-correlation functions of the proposed OVFS HOVLS code sequence, OVFS Gold code sequence and OVFS m-sequence from the same group in the code tree are shown in figures 6.8 to 6.10 and figures 6.11 to 6.13 for 128 and 256 chips length respectively.

Table 6.2 CM of the proposed OVSF HOVLS code sequence

OVSF code sequence	CM for 128 chip lengths (dB)	CM for 256 chip lengths (dB)
Orthogonal Gold	-18.06	-21.07
Orthogonal m-sequence	-18.06	-21.07
The proposed code	-16.02	-18.57

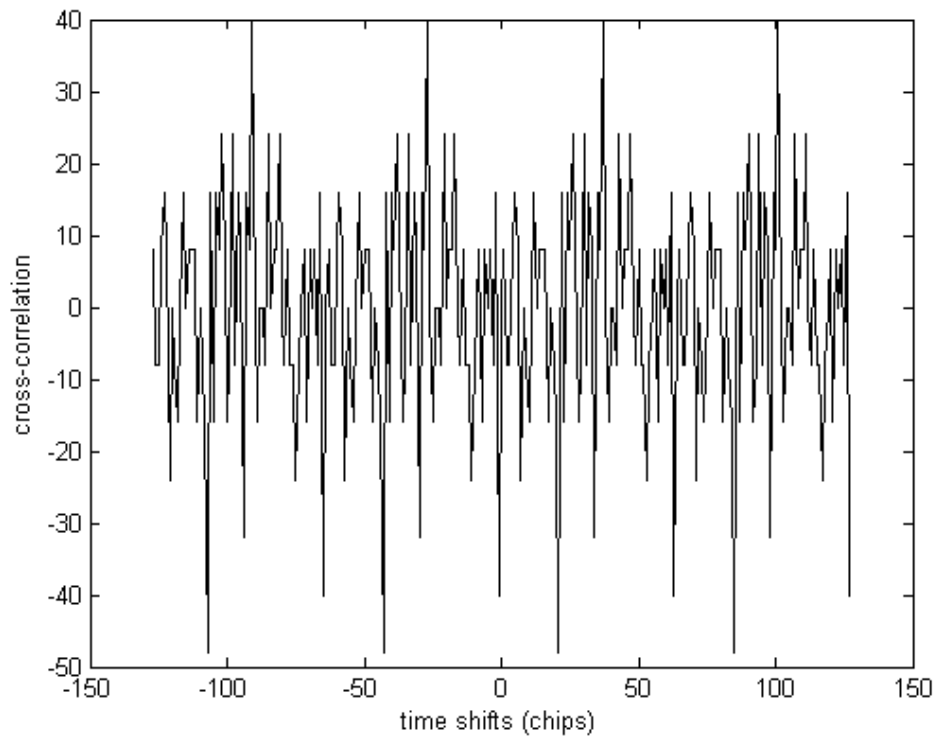


Figure 6.8 CCF of the proposed OVSF HOVLS code sequence in the same groups in the code tree for 128 chip lengths

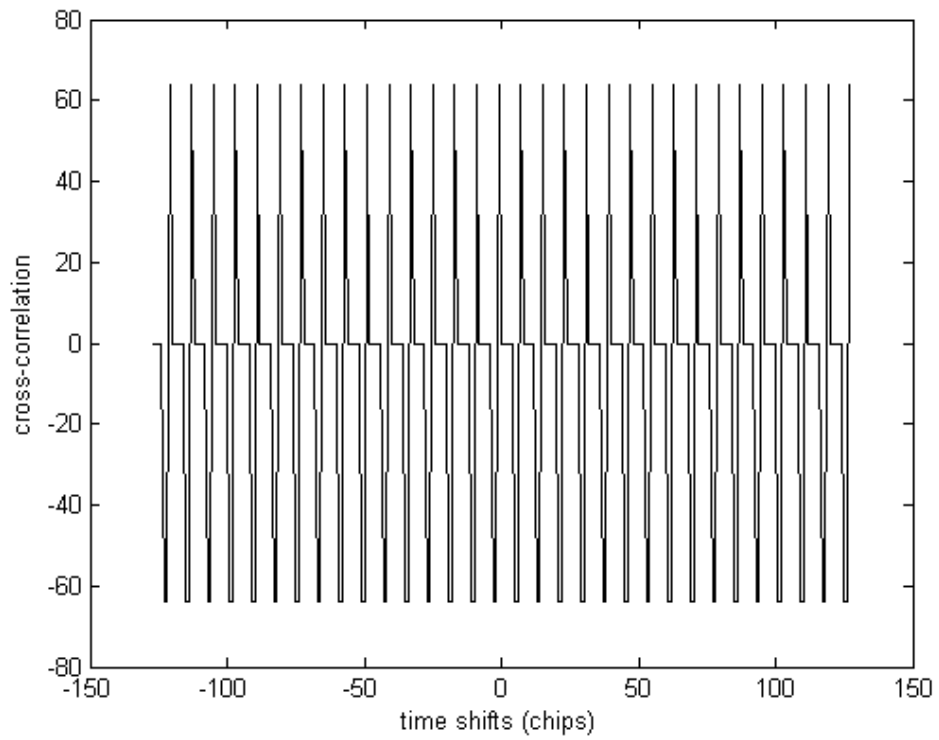


Figure 6.9 CCF of OVSF Gold code sequence in the same groups in the code tree for 128 chip lengths

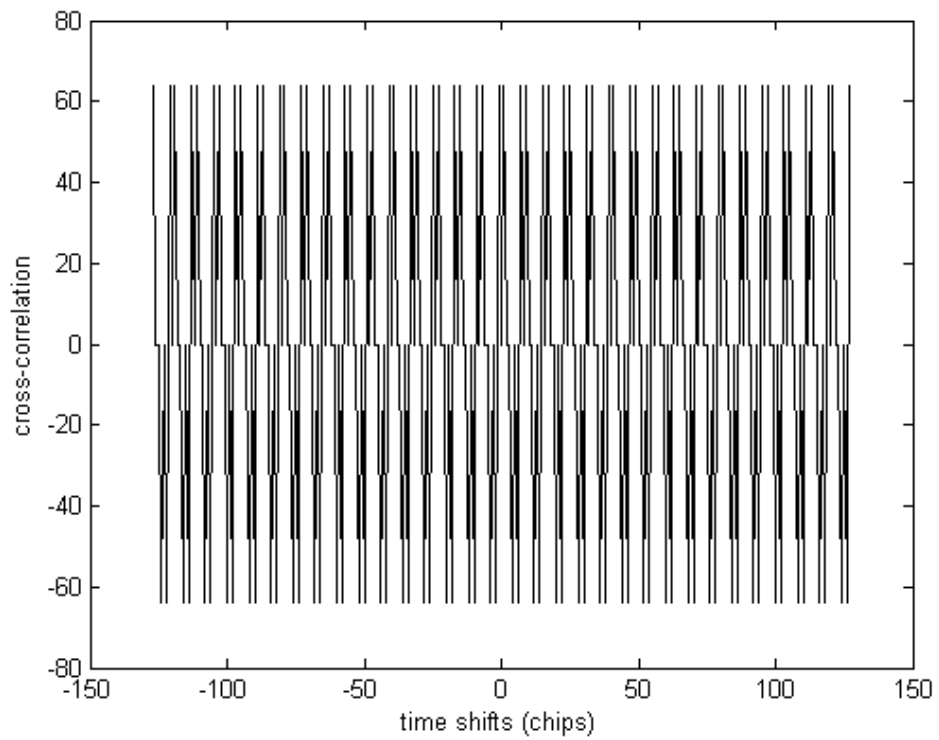


Figure 6.10 CCF of OVSF m-sequence in the same groups in the code tree for 128 chip lengths

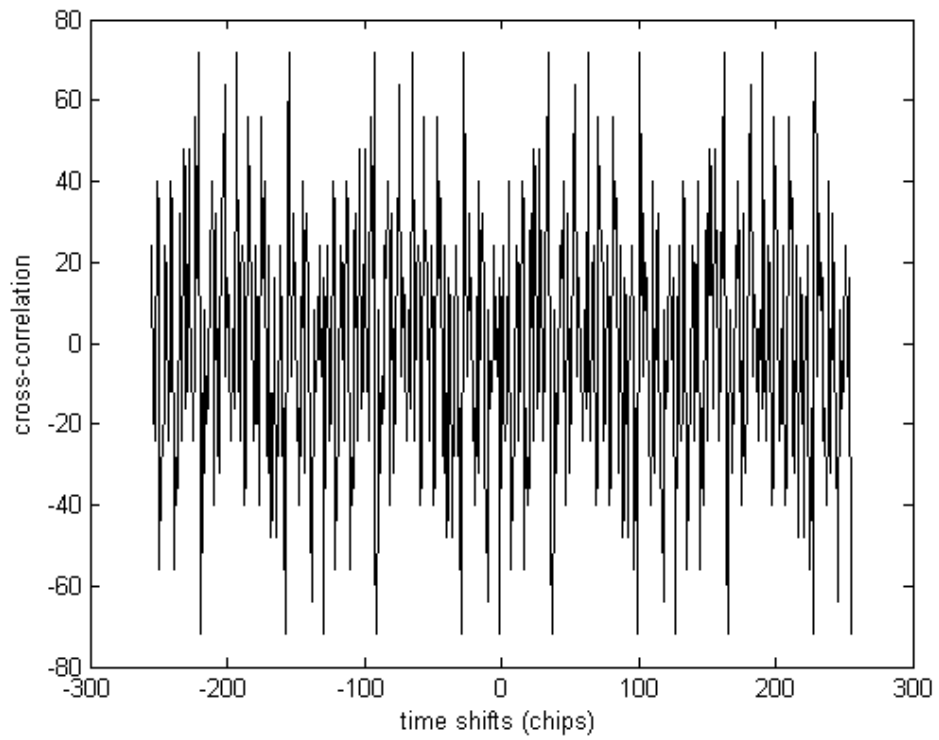


Figure 6.11 CCF of the proposed OVFS HOVLS code sequence in the same groups in the code tree for 256 chip lengths

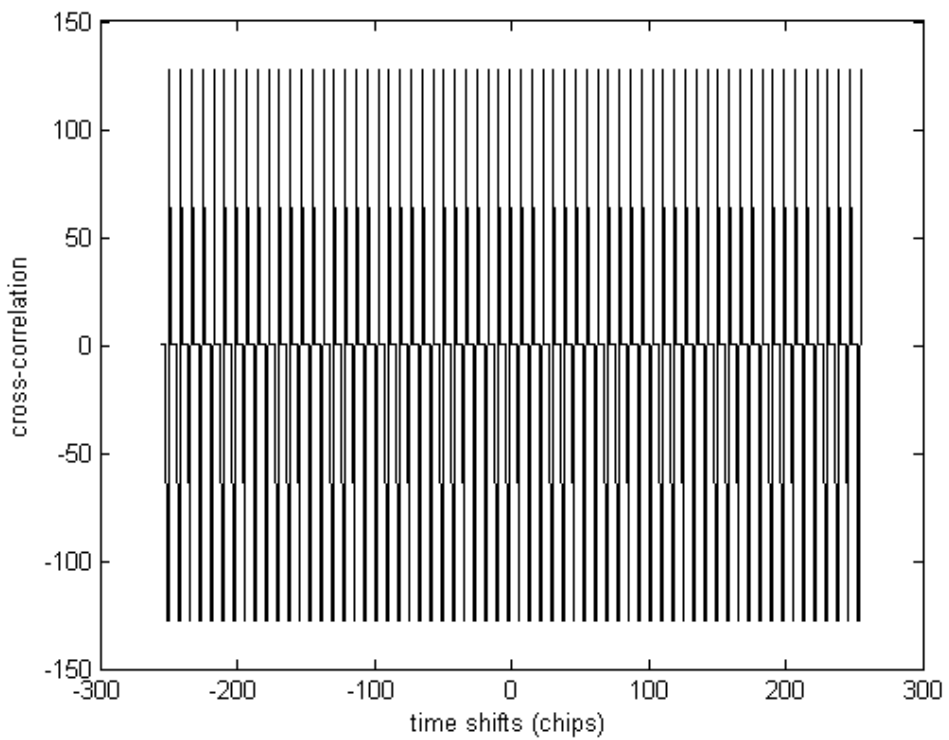


Figure 6.12 CCF of OVFS Gold code sequence in the same groups in the code tree for 256 chip lengths

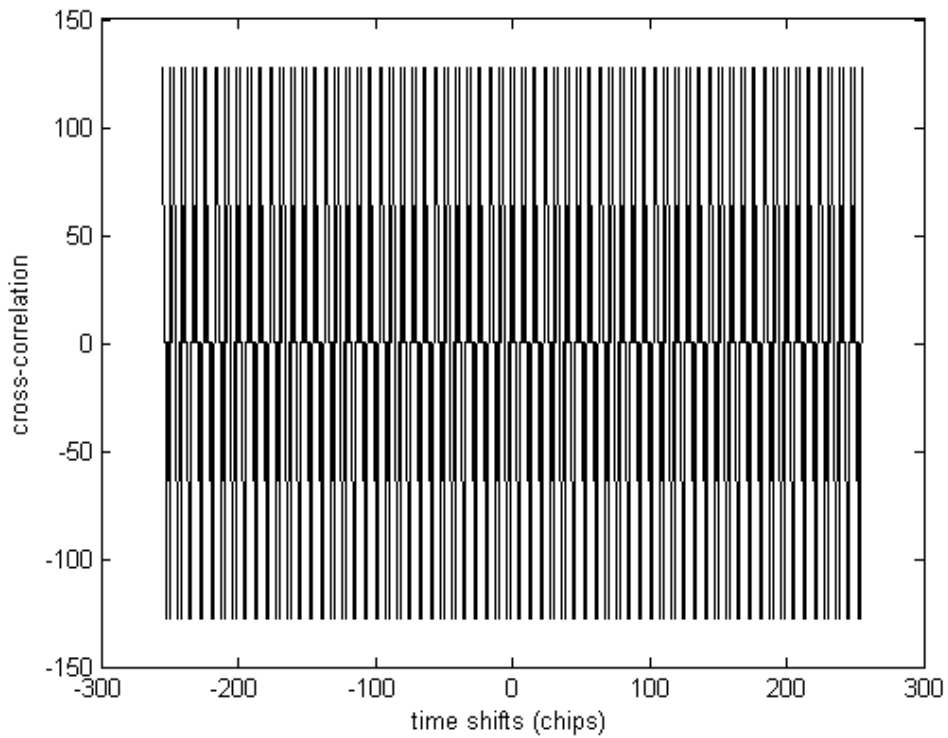


Figure 6.13 CCF of OVFSF m-sequence in the same groups in the code tree for 256 chip lengths

6.2.2.3 Cross-correlation function of the proposed OVFSF HOVLS code sequence from different groups in the code tree

The OVFSF code sequence proposed by Adachi, et.al, 1997 has zero CCF between any two code sequences that are from different groups in the code tree. Since the proposed OVFSF HOVLS code sequence, OVFSF Gold code sequence, and OVFSF m-sequence were generated by adapting the method proposed by Adachi, et.al, 1997, CCFs between different groups in the code tree of the proposed OVFSF HOVLS code sequence, OVFSF Gold code sequence, and OVFSF m-sequence are zeroes.

Cross-correlation function between a user 2R using code sequence of 128 chip lengths and a user R using code sequence of 256 chip lengths has been derived by repeating the code sequence of length 128 chips twice before correlating the code

sequences. In this case we correlate two code sequences of length 256 chips. Since code sequences used by users 2R or R must not be of mother-child relationship, correlation between a user 2R (128 chips length) and a user R (256 chips length) means correlation between different groups of two code sequences of length 256.

6.2.2.4 BER performance of the proposed OVFS HOVLS code sequence under Rayleigh flat fading channel

Figure 6.14 shows BER performance of the proposed OVFS HOVLS code sequence, OVFS Gold code sequence and OVFS m-sequence under Rayleigh flat fading channel condition. As can be clearly seen from figure 6.14, the proposed OVFS HOVLS code sequence has similar BER performance to that of OVFS Gold code sequence and OVFS m- sequence in synchronous CDMA system under Rayleigh flat fading channel. The reasons for this performance behaviour are discussed in the following paragraphs.

Since there is only one version of the transmitted signal arriving at the receiver under flat fading channel condition, inter symbol interference (ISI) does not exist on desired user's signal and there is no interfering signal from other users (no MAI). Under this condition, the OVFS code sequences can maintain the orthogonality of the code sequences; therefore BER value is constant for increasing number of users. However, as seen in figure 6.14, BER value decreases for increasing SNR value, therefore under flat fading channel condition the OVFS code sequences are noise limited or the receiver has only to cope with the noise introduced by the channel.

Under Rayleigh flat fading channel condition, the proposed OVFS HOVLS code sequence, OVFS Gold code sequence and OVFS m-sequence are under same condition that is under noise limited condition (no MAI) and there is no ISI on the desired received user's signal and hence have similar signal strength due to same

value on zero time shift on ACF. Therefore the proposed OVFS HOVLS code sequence, OVFS Gold code sequence and OVFS m-sequence have similar BER performance.

BER performance of the proposed OVFS HOVLS code sequence, OVFS Gold code sequence and OVFS m-sequence are also similar for user R under Rayleigh flat fading channel condition as seen in figure 6.15 for the same reason as discussed above for user 2R.

So, BER performance of the OVFS code sequences under flat fading channel condition does not depend on user with higher bit rate (2R) or user with lower bit rate (user R) in downlink CDMA systems. Therefore, BER performance of these OVFS code sequences between user 2R and R under Rayleigh flat fading channel is similar.

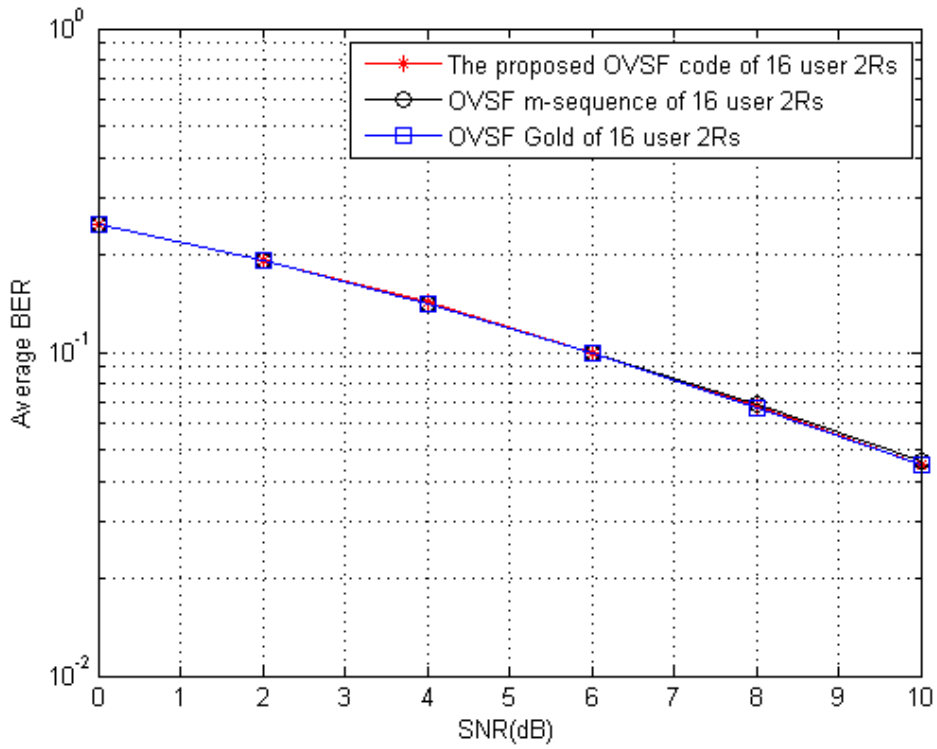


Figure 6.14 BER versus SNR of the OVSF code sequences under Rayleigh flat fading channel for user 2R

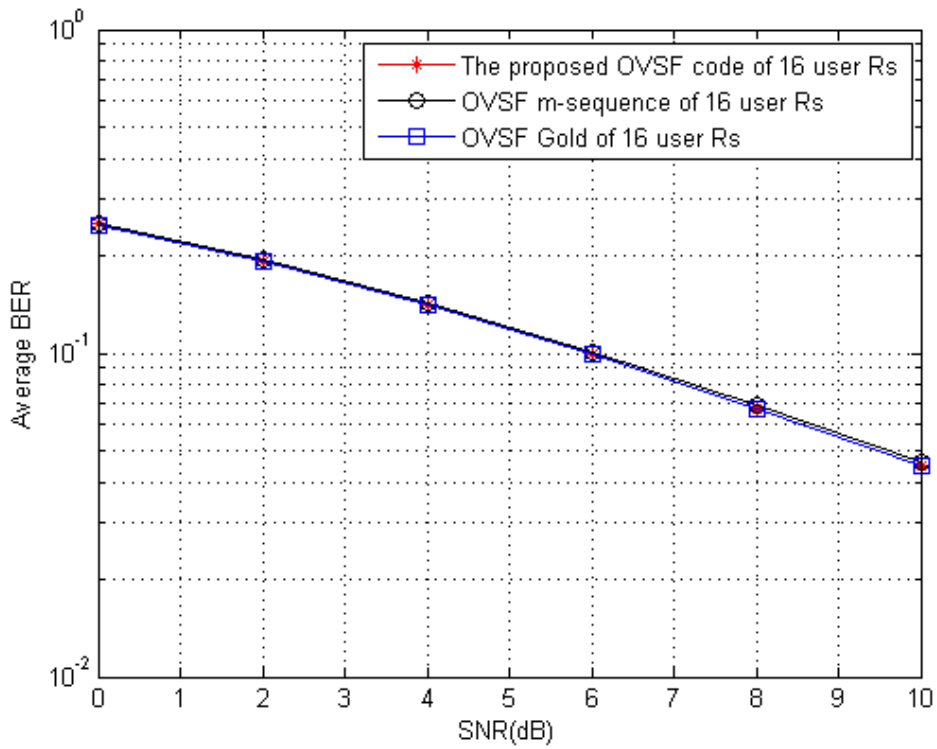


Figure 6.15 BER versus SNR of the OVSF code sequences under Rayleigh flat fading channel for user R

6.2.2.5 BER performance of the proposed OVFS HOVLS code sequence under Rayleigh frequency selective fading channel for user 2R

As seen in figure 6.16, the proposed OVFS HOVLS code sequence has slightly better BER performance than those of OVFS Gold code sequence and OVFS m-sequence. Besides, BER performance of OVFS Gold code sequence is slightly better than that of OVFS m-sequence. The reason is discussed in the following paragraphs.

Under frequency selective fading channel, received signal is multiple versions of the transmitted signal which are attenuated and delayed in time. When de-spreading the received signal, correlation between the first multipath component (not just delayed and attenuated) and the desired user's code sequence is the desired signal. Whereas, the correlation between the desired user's code sequence and other multipath components (delayed and attenuated) are undesired signals that will interfere with the desired signal. These correlation values are determined by ACF of the code sequences where correlation value at zero time shift represents desired user's signal strength while at non-zero time shifts represents undesired signals strengths (ISI).

As shown in figures 6.2 to 6.4, the proposed OVFS HOVLS code sequence, OVFS Gold code sequence and OVFS m-sequence have similar ACF for code sequence of length 128 chips. Therefore, BER values of the proposed OVFS HOVLS code sequence, OVFS Gold code sequence, and OVFS m-sequence for one user 2R are similar to others, as seen in figure 6.17. However, when there is more than one user in CDMA system, the desired user's signal is not only interfered by ISI but also by interfering signals coming from others users. Interfering signal strengths coming from other users are determined by cross-correlation values at non-zero time

shift in the CCF, since correlation values at non-zero time shifts in CCF for orthogonal code sequences represent signal strengths from other users.

As seen in figures 6.8 to 6.10, CCF of the proposed OVSF HOVLS code sequence is slightly better in terms of CM than that of OVSF Gold code sequence and OVSF m-sequence for code sequence of length 128 chips. Therefore, the proposed OVSF HOVLS code sequence has slightly lower BER values for increasing number of users than those of OVSF Gold code sequence and OVSF m-sequence as shown in figure 6.17, and hence BER performance of the proposed OVSF HOVLS code sequence for user 2R that has 128 chip lengths is slightly better than those of OVSF Gold code sequence and OVSF m-sequence.

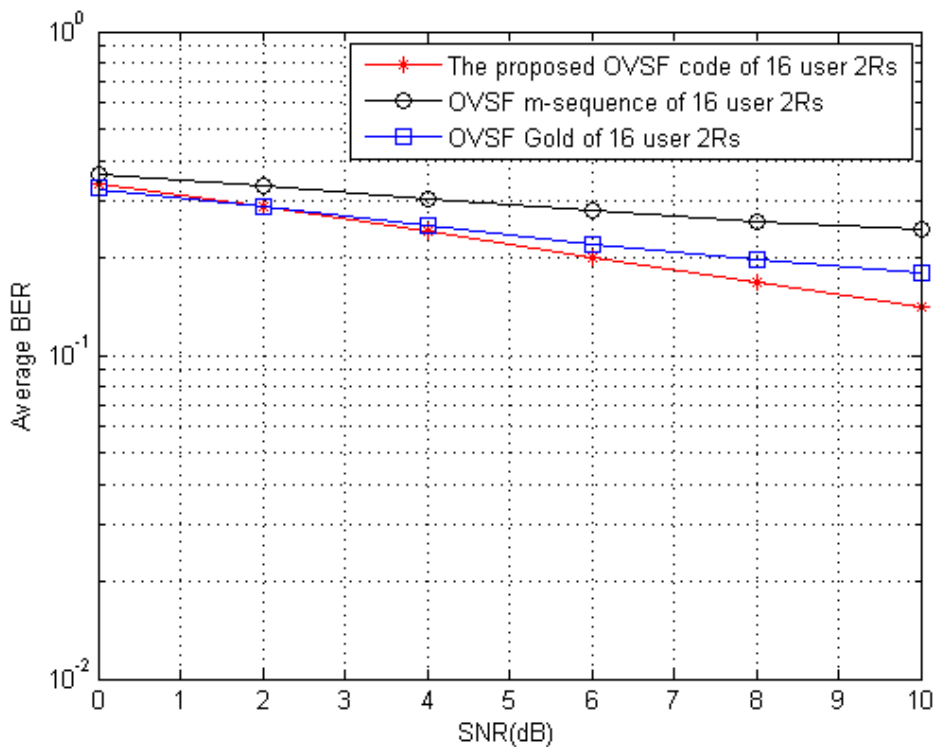


Figure 6.16 BER versus SNR of the OVSF code sequences under Rayleigh frequency selective fading channel for user 2R

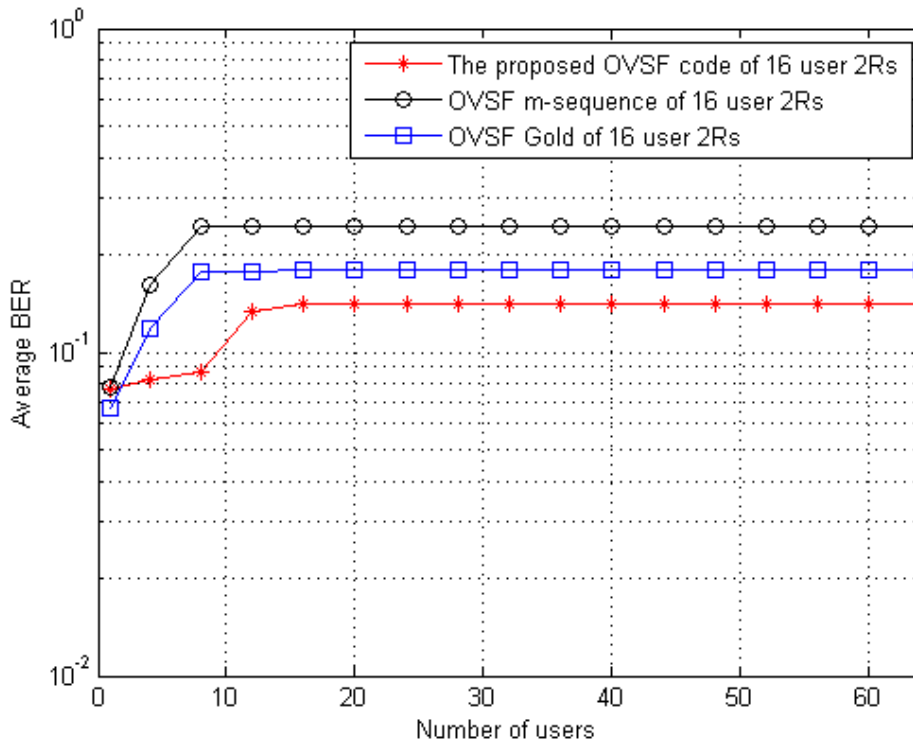


Figure 6.17 BER versus number of users of the OVSF code sequences under Rayleigh frequency selective fading channel for SNR = 10 dB for user 2R

The OVSF Gold code sequence and OVSF m-sequence have similar CCF in terms of CM (correlation margin). However, OVSF Gold sequence for code sequence of length 128 chips has zero cross-correlation value at non zero time shift that happens more frequently than that of OVSF m-sequence as seen in figures 6.9 and 6.10. So, the BER values for increasing number of users of OVSF Gold code sequence are slightly lower than that of OVSF m-sequence as seen in figure 6.17. Therefore, this results in a slightly better BER performance as shown in figure 6.16.

As can be seen in figure 6.17, OVSF Gold code sequence and OVSF m-sequence have constant BER values when the number of users is more than 8. However, the proposed OVSF HOVLS code sequence has a constant BER value when the total number of users 2R and R is more than 16 due to zero CCF.

6.2.2.6 BER performance of the proposed OVFS HOVLS code sequence under Rayleigh frequency selective fading channel for user R

As presented in figures 6.5 to 6.7, the proposed OVFS HOVLS code sequence, OVFS Gold code sequence and OVFS m-sequence all have similar ACF for 256 chip lengths, and hence the BER performance for one user of the proposed OVFS HOVLS code sequence, OVFS Gold code sequence and OVFS m-sequence is similar, as seen in figure 6.19. However, as seen in figures 6.11 to 6.13, the proposed OVFS HOVLS code sequence has slightly better CCF than those of OVFS Gold code sequence and OVFS m-sequence in terms of CM for code of length 256 chips. Therefore the proposed OVFS HOVLS code sequence has slightly lower BER values for increasing number of users than those of OVFS Gold code sequence and OVFS m-sequence, as shown in figure 6.19. The proposed OVFS HOVLS code sequence for 128 chip lengths has similar BER performance to that of 256 chip lengths code sequence. This is presented in figure 6.18.

OVFS Gold code sequence and OVFS m-sequence as presented in figures 6.12 and 6.13 respectively have similar CCF in terms of CM, and the occurrence of zero cross-correlation values are almost similar for these OVFS code sequences. Therefore, BER values for increasing number of users of OVFS Gold code sequence are similar to that of OVFS m-sequence as shown in figure 6.19. Hence, both OVFS code sequences possess similar BER performance as presented in figure 6.18.

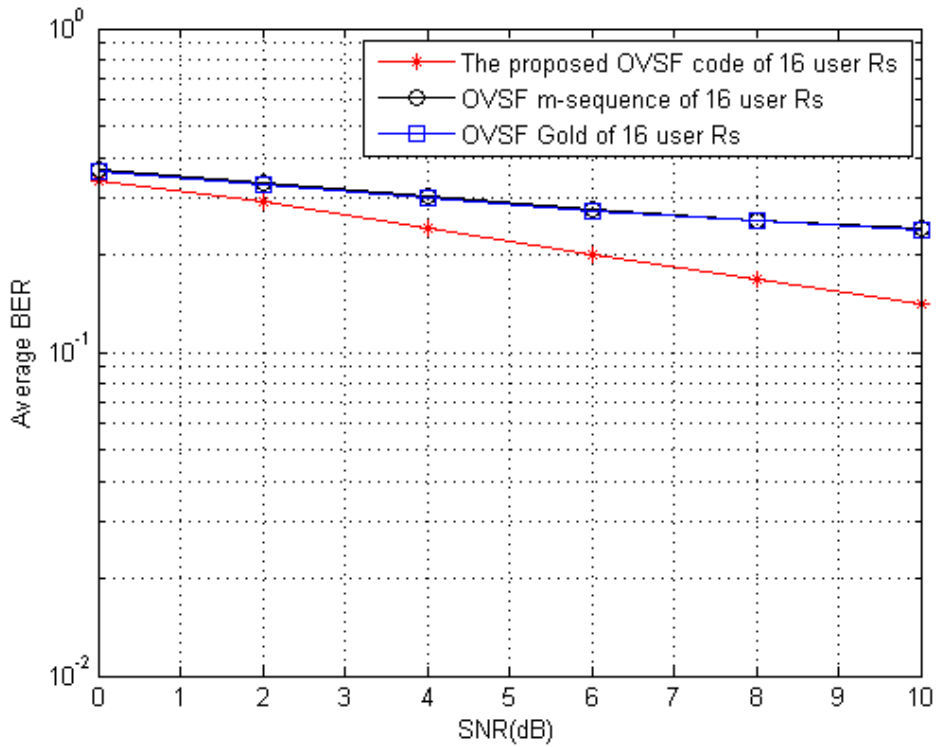


Figure 6.18 BER versus SNR of the OVSF code sequences under Rayleigh frequency selective fading channel for user R

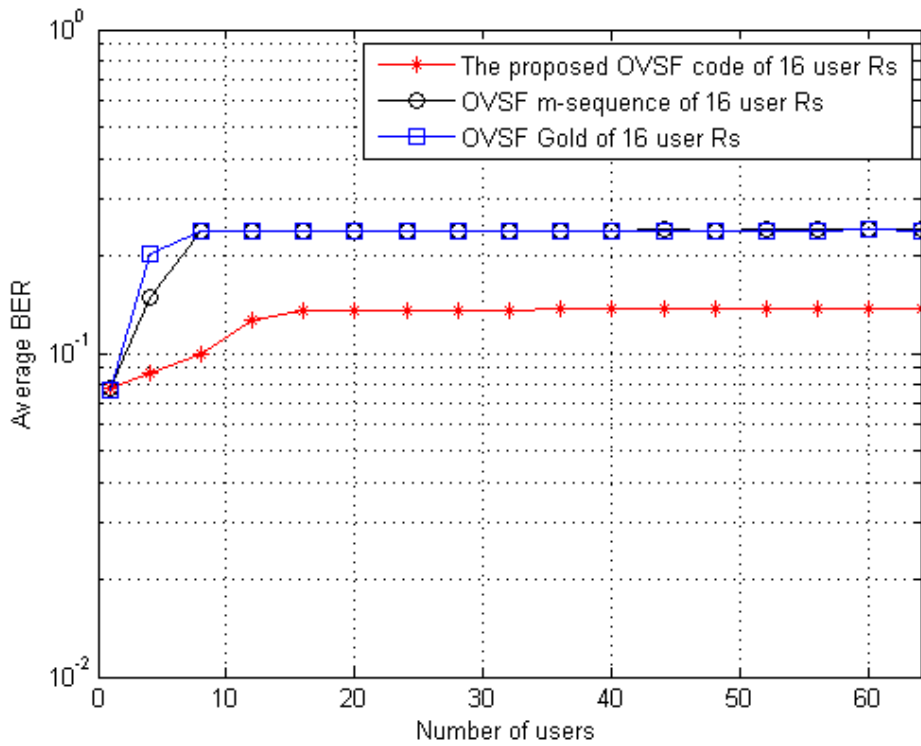


Figure 6.19 BER versus number of users of the OVSF code sequences under Rayleigh frequency selective fading channel for SNR = 10 dB for user R

6.2.2.7 Comparison of BER performance of the proposed OVFS HOVLS code sequence between user 2R and user R under Rayleigh frequency selective fading channel

In this section, BER performance of the proposed OVFS HOVLS code sequence between user 2R and user R under Rayleigh frequency selective fading channel is compared. The BER performance of the proposed OVFS HOVLS code sequence for user R is similar to that of user 2R as presented in figure 6.20. This is because the proposed OVFS HOVLS code sequence for 256 chip lengths used by user R has similar ACF and CCF to that of 128 chip lengths used by user 2R.

The BER performance of OVFS Gold sequence for user 2R is slightly better than that of user R as shown in figure 6.21. This is due to the CCF values of OVFS Gold sequence for 128 chip lengths used by user 2R being similar to that of 256 chip lengths used by user R in terms of CM. However, the CCF of OVFS Gold sequence for 128 chip lengths has occurrence of zero cross-correlation values more than that of 256 chip lengths, and ACF between 128 and 256 chip lengths is similar. Therefore, the BER performance of OVFS Gold sequence for user 2R is slightly better than that of user R.

The ACF and CCF values of OVFS m-sequence for 128 chip lengths used by user 2R are similar to that of OVFS m-sequence for 256 chip lengths used by user R. Therefore, BER performance of OVFS m-sequence for user 2R is similar to that of user R as seen in figure 6.22.

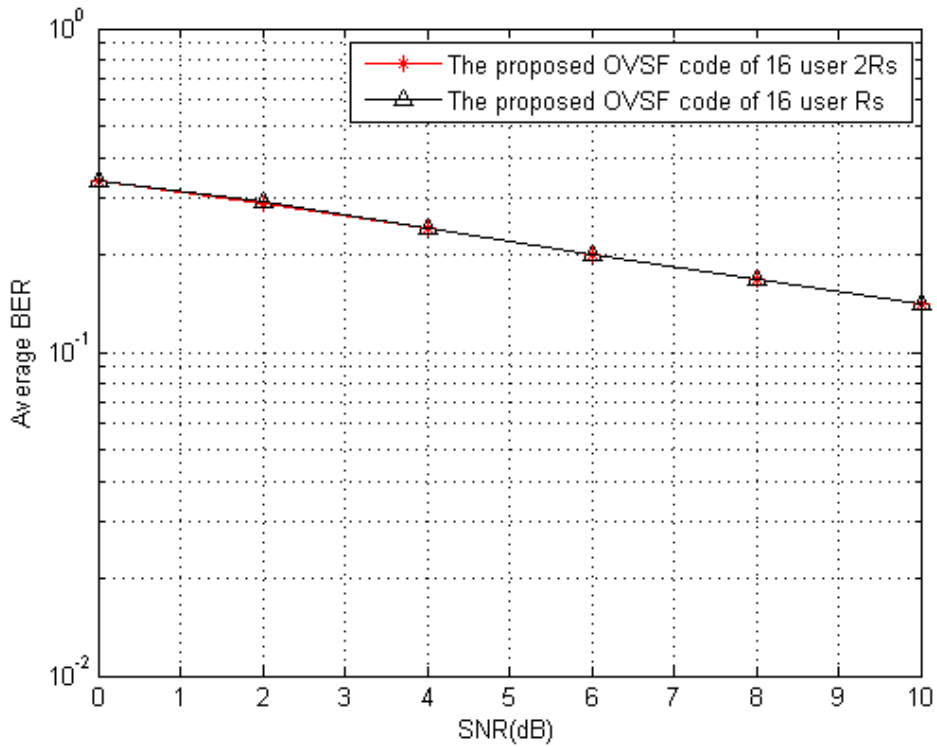


Figure 6.20 BER versus SNR of the proposed OVFS HOVLS code sequence under Rayleigh frequency selective fading channel between 16 user 2Rs and 16 user Rs

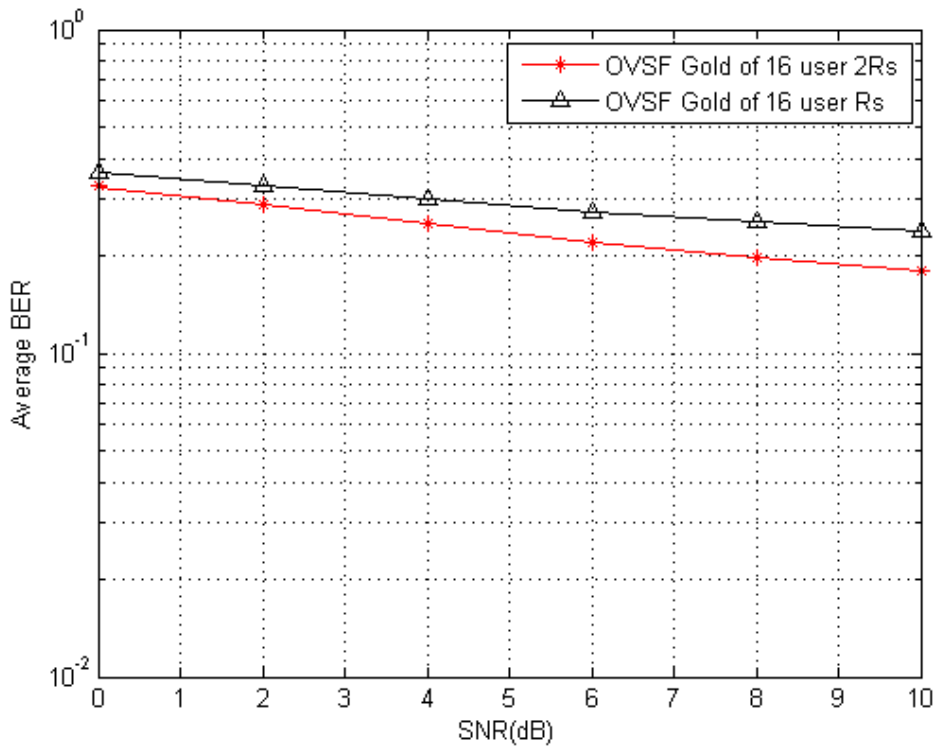


Figure 6.21 BER versus SNR of OVFS Gold code sequence under Rayleigh frequency selective fading channel between 16 user 2Rs and 16 user Rs

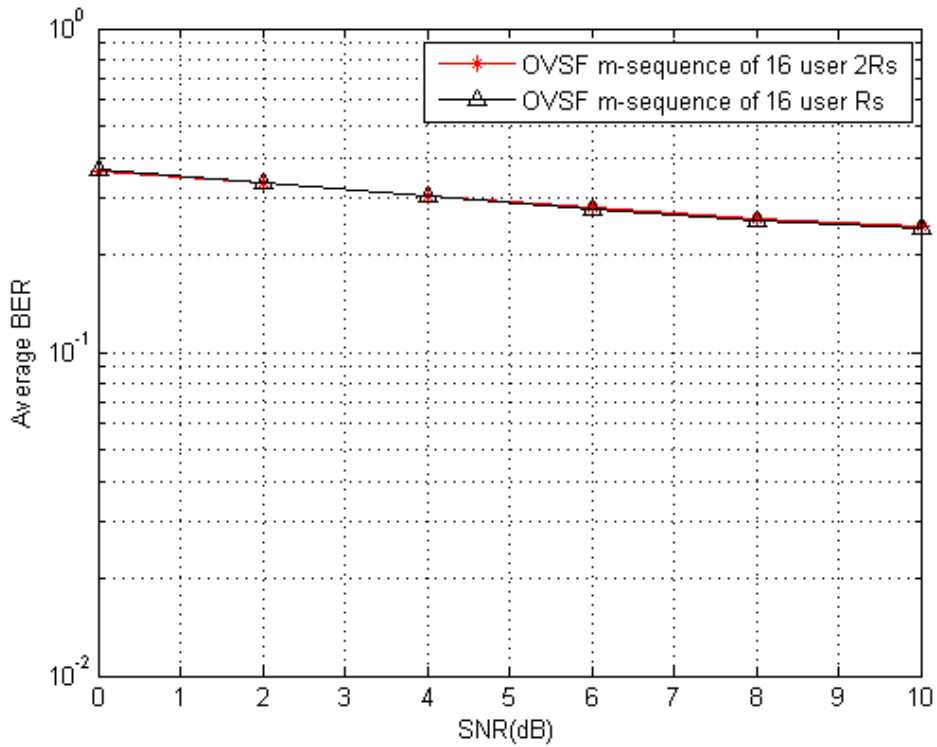


Figure 6.22 BER versus SNR of OVSF m-sequence under Rayleigh frequency selective fading channel between 16 user 2Rs and 16 user Rs

As highlighted in subsections 6.2.2.5 and 6.2.2.6, the proposed OVSF HOVLS code sequence has slightly better performance than those of OVSF Gold code sequence and OVSF m-sequence under Rayleigh frequency selective fading channel in a CDMA system. It is because the proposed OVSF HOVLS code sequence has lower BER values for increasing number of users than those of OVSF Gold code sequence and OVSF m-sequence. This means in a CDMA system, the proposed OVSF code sequence has lower MAI signal strength than that of OVSF Gold code sequence and OVSF m-sequence indicated by lower BER values for increasing number of users. In this case, the proposed OVSF code sequence is more tolerant towards MAI signals than those of OVSF Gold code sequence and OVSF m-sequence for both types of users with higher and lower bit rates.

Besides, users with higher bit rate are not disadvantaged by users with lower bit rate or vice versa, while using the proposed OVFS code sequence as their code sequences. This is substantiated by the similar BER performance between users with higher bit rate and users with lower bit rate (figure 6.20). Whereas, this is not true for OVFS Gold code sequences, where users with lower bit rate are disadvantaged by the users with higher bit rate, which is indicated by slightly better BER performance of users with higher bit rate than that of users with lower bit rate as shown in figure 6.21.

This means that a CDMA system using the proposed OVFS HOVLS code sequence will have lower impact due to MAI introduced by other users, compared to the systems using OVFS Gold code sequence and OVFS m-sequence.

Chapter 7

CONCLUSION AND FUTURE WORK

In this research work, design of novel hybrid orthogonal very large set (HOVLS) code sequence has been proposed for CDMA based high density mobile networks. As the name hybrid indicates, this set of HOVLS code sequence is generated from two different non-orthogonal spreading code sequences namely large set Kasami code sequence and m-sequence. The combination of large set Kasami code sequence and m-sequence, by adaptating the method proposed by Donelan and O'Farrel, 1999 can generate a novel orthogonal code sequence set that possesses larger family size than any existing orthogonal code sequences (orthogonal Gold code sequence and orthogonal m-sequence).

Design of this HOVLS code sequence is divided into two phases. The fixed spreading factor code sequence is developed during the first phase, followed by the variable spreading factor orthogonal code sequence design phase. Orthogonal variable spreading factor (OVSF) code sequence was developed from orthogonal fixed spreading factor code sequence by adapting the method proposed by Adachi, et.al., 1997.

Evaluation of orthogonal fixed and variable spreading factor code sequences includes evaluating the family size, autocorrelation function (ACF), cross-correlation function (CCF), and BER performance of the code sequences in synchronous CDMA system under Rayleigh flat fading and frequency selective fading channels. Evaluation of these performance metrics was performed via simulation using Simulink/Matlab programming.

Evaluation of the fixed spreading factor HOVLS code sequence shows that ACF and CCF of the proposed fixed spreading factor HOVLS code sequence are comparable to that of the fixed spreading factor orthogonal Gold code sequence and orthogonal m-sequence. Moreover, BER performance of the proposed fixed spreading factor HOVLS code sequence is similar to that of the fixed spreading factor orthogonal Gold code sequence and orthogonal m-sequence. However, the family size i.e. the capacity of the proposed fixed spreading factor HOVLS code sequence is much larger (more than twice) than that of fixed spreading factor orthogonal Gold code sequence and orthogonal m-sequence. Therefore the proposed fixed spreading factor HOVLS code sequence is more appropriate to be implemented in CDMA based high density mobile networks than the fixed spreading factor orthogonal Gold code sequence and orthogonal m-sequence.

Similarly, the evaluation of variable spreading factor code sequences shows that the proposed OVSF HOVLS code sequence has slightly better CCF than the OVSF Gold code sequence and m-sequence in terms of correlation margin. Whereas, the ACF of the proposed OVSF HOVLS code sequence is similar to that of OVSF Gold code sequence and m-sequence. BER performance of the proposed OVSF HOVLS code sequence in synchronous CDMA system is similar to that of OVSF Gold code sequence and OVSF m-sequence under Rayleigh flat fading channel. However, under Rayleigh frequency selective fading channel, the BER performance of the proposed OVSF HOVLS code sequence in synchronous CDMA system is slightly better than that of OVSF Gold code sequence and OVSF m-sequence. Therefore, the proposed OVSF HOVLS code sequence is more appropriate code sequence for variable rate applications in synchronous CDMA systems than the OVSF Gold code sequence and OVSF m-sequence.

So, the proposed HOVLS code sequence is appropriate code sequence in CDMA systems than those of orthogonal Gold code sequence and orthogonal m-sequence for both fixed and variable rate high density network applications.

The proposed HOVLS code sequence in this research needs to be studied further. The investigation of the proposed HOVLS code sequence for both fixed and variable spreading factor in this thesis has been carried out in a CDMA system using a simple correlation receiver. The results showed that under Rayleigh frequency selective fading channel condition using CDMA system based-correlation receiver, the BER performance of the proposed HOVLS code sequence is worse than that of Rayleigh flat fading channel due to ISI and MAI present in the Rayleigh frequency selective fading channel. As a further extension of this research work, I would like to suggest evaluation of the proposed HOVLS code sequence using more complex receivers such as Rake and Multi User Detection (MUD) receivers. It would be a worthwhile exercise to evaluate whether these receivers are better in mitigating the effects of ISI and MAI under Rayleigh frequency selective fading channel of the proposed HOVLS code sequence due to non-zero correlation values at non-zero time shifts in the ACF and CCF, and if so how much better.

Besides, CDMA systems used to evaluate the performance of the proposed HOVLS code sequence in this thesis are single carrier CDMA systems, therefore it would be useful to investigate the proposed HOVLS code sequence in a multi-carrier CDMA system. This would allow us to see whether the performance of the proposed HOVLS code sequence improves for both fixed and variable spreading factor.

In addition to the step improvements suggested above, application of the proposed code could be viable in the rapidly developing areas such as Internet of Things and Data security. Internet of Things (IoT) is poised to take over CDMA

based mobile networks. With the proposed system where every device within a geographical location to be connected to the internet with an IP address, time has come to develop new system of generating unique ids for devices within a geographical location. The proposed HOVLS code sequence is a spreading code sequence and could support more than 8000 users in an area. So, it is quite interesting to visualise using the proposed code as the form of identification within the IoT scenario. Spreading code sequence is intended for data security and multi users environment. With the ability to generate such a large number of unique orthogonal codes, the proposed code is an ideal candidate for data provenance and security applications. Therefore, I would like to suggest embedding the proposed code within data, in order to track provenance and provide secure transportation of the same.

According to the development of mobile communication system to the fourth generation, it would be useful to investigate the suitability of the proposed HOVLS code sequence in fourth generation of mobile networks. The investigation could be along the lines of collaboration between CDMA and multi input multi output-orthogonal frequency division multiplexing (MIMO-OFDM) used in fourth generation mobile network so that the proposed HOVLS code sequence can be used in that technology. The implementation of the proposed HOVLS code sequence in that collaboration could be performed using scrambling code and without scrambling code between different cells, and the BER performances are measured and compared to see whether the proposed HOVLS code sequence needs scrambling code between different cells in that collaboration. The same research could also be extended to the proposed OVSF HOVLS code sequence.

References

- Adeola, F.A., Adekunle, A.S. and Peter, A.O. (2011) 'Direct sequence CDMA system using finite-time altered sinusoidal signals as orthogonal signatures', *IEEE 3rd International Conference on Adaptive Science and Technology (ICAST 2011)*, pp.174 – 177
- Akansu, A.N. and Poluri, R. (2007) 'Walsh-like nonlinear phase orthogonal codes for direct sequence CDMA communications', *IEEE Transactions on Signal Processing*, Vol. 55, No. 7, pp. 3800-3806
- Akansu, A.N. and Poluri, R. (2007) 'Design and performance of spread spectrum Karhunen–Loeve transform for direct sequence CDMA communications', *IEEE Signal Processing Letters*, Vol. 14, No. 12, pp.900-903
- Adachi, F., Sawahashi, M. and Okawa, K. (1997) 'Tree-structured generation of orthogonal spreading codes with different lengths for forward link of DS-SS mobile radio', *Electronic Letters*, Vol. 33
- Abu-Rgheff, M.A. (2007) *Introduction to CDMA wireless communications*, Elsevier
- Babadi, B., Ghassemzadeh, S.S, and Tarokh, V. (2011) 'Group randomness properties of pseudo-noise and Gold sequences', *12th IEEE Canadian Workshop on Information Theory (CWIT)*, pp.42-46
- Chandra, A. and Chattopadhyay, S. (2009) 'Small set orthogonal Kasami codes for CDMA system', *4th IEEE International Conference on Computers and Devices for Communication*, pp.1-4
- Cheng, H., Ma, M. and Jiao, B. (2009) 'On the design of comb spectrum code for multiple access scheme', *IEEE Transactions on Communications*, Vol. 57, No. 3, pp.754-763
- Cho, Y.S., Kim, J., Yang, W.Y., and Kang, C.G. (2010) *Mimo-ofdm wireless communications with matlab*, John Wiley & Sons (Asia) Pte Ltd
- Donelan, H. and O'Farrell, T. (1999) 'Method for generating sets of orthogonal sequences', *Electronic Letters*, Vol. 35
- Dinan, E.H. and Jabbari, B (1998) 'Spreading codes for direct sequence CDMA and wideband CDMA cellular networks', *IEEE Communication Magazine*, Vol. 36, pp.48-54
- Dongwook, L., Hun, L., and Milstein, K.B. (1998) 'Direct sequence spread spectrum Walsh-QPSK modulation', *IEEE Transactions on Communication* Vol.46, pp.1227-1232

- Fazel, K. and Kaiser, S. (2008) *Multicarrier and spread spectrum systems*, John Wiley & Sons, Ltd
- Feng, L., Fan, P., and Tang, X. (2007) 'A general construction of OVVSF codes with zero correlation zone', *IEEE Signal Processing Letters*, Vol.14, pp.908-911
- Golomb, S.W. (1967) '*Shift Register Sequences*', San Francisco, Holden-Day. ISBN 0-89412-048-4
- Gold, R. (1967) 'Optimal binary sequences for spread spectrum multiplexing', *IEEE Transactions on Information Theory* Vol.13, pp.619-621
- Gold, R. (1968) "Maximal recursive sequences with 3-valued recursive cross-correlation functions", *IEEE Trans. Inform. Theory*, vol. 14, pp.154-156
- Hoshyar, R., Wathan, F.P., and Tafazolli, R. (2008) 'Novel low-density signature for synchronous CDMA systems over AWGN channel', *IEEE Transactions on Signal Processing*, Vol. 56, pp.1616-1626
- Jatunov, L. and Madisetti, V.K. (2006) 'Computationally-efficient SNR estimation for band limited wideband CDMA systems', *IEEE Transaction on Wireless Communications*, Vol. 5, pp.3480-3491
- Jeruchim, M.C., Balaban, P., and Shanmugan, K.S. (2002) *Simulation of communication systems, 2nd edition*, Kluwer Academic
- Korhonen, J. (2001) *Introduction to 3G mobile communications*, Artech House Sons, Ltd
- Kedia, D., Duhan, M. and Maskara, S.L. (2010) 'Evaluation correlation properties of orthogonal spreading codes for CDMA wireless mobile communication', *IEEE International Advance Computing Conference (IACC)*, pp.325-330
- Kasami, T. (1966) '*Weight Distribution Formula for Some Class of Cyclic Codes*', Tech. Report No. R-285, University of Illinois
- Lee, J.S. and Miller, L.E. (1998) *CDMA system engineering hand book*, Artech House
- Luna-Rivera, J.M. and Campos-Delgado, D.U. (2009) 'Transmitter pre-filtering for the downlink of a time-division-duplex/direct sequence-code division multiple access system over time varying multipath fading channels', *IET Communications*, vol.3, pp.1533-1543
- Lathi, B.P. (1998) *Modern digital and analog communication systems, 3rd edition*, Oxford University Press

- Masouros, C. and Alsusa, E. (2010) ‘Soft linear precoding for the downlink of DS/CDMA communication systems’, *IEEE Transaction on Vehicular Technology*, vol.59, no.1, pp.203-215
- Mollah, M.B. and Islam, Md.R. (2012) ‘Comparative analysis of Gold codes with PN codes using correlation property in CDMA technology’, *IEEE International Conference on Computer Communication and Informatics (ICCCI)*, pp.1-6
- Nikjah, R. and Beaulieu, N.C. (2008) ‘On antijamming in general CDMA systems—Part I: Multiuser capacity analysis’, *IEEE Transactions on Wireless Communications*, Vol. 7, No. 5, pp. 1646-1655
- Oberg, T. (2001) *Modulation, detection and coding*, John Wiley & Sons, Ltd
- Proakis, J.G. and Salehi, M. (1998) *Contemporary communication using MatLab*, PWS Publishing Company
- Pal, M. and Chattopadhyay, S. (2010) ‘A novel orthogonal minimum cross-correlation spreading code in CDMA system’, *IEEE International Conference on Emerging Trends in Robotics and Communication Technologies*, pp.80-84
- Proakis, J.G. (2000) *Digital communications, 4th edition*, McGraw Hill
- Rao, R. and Dianat, S. (2005) *Basic of Code Division Multiple Access*, SPIE Press
- Rappaport, T.S. (1996) *Wireless Communications Principles and Practice*, Prentice Hall PTR
- Shanmugam, K.S. (1979) *Digital and analog communication systems*, John Wiley and Sons
- Sklar, B. (1994) *Digital communication fundamental and application*, Prentice Hall
- Tachikawa, S. (1992) ‘Recent spreading codes for spread spectrum communication systems’, *Electron. Commun. Jpn.*, pp. 4149
- Thompson, A. R.; Moran, J. M.; and Swenson, G. W. Jr. (1986) ‘*Interferometry and Synthesis in Radio Astronomy*’, New York, Wiley
- Tse, D. and Viswanath, P. (2005) *Fundamentals of wireless communication*, Cambridge University Press
- Tsai, Y.R. and Li, X.S. (2007) ‘Kasami code-shift-keying modulation for ultra-wideband communication systems’, *IEEE Transaction on Communication*, vol.55, no.6, pp.1242-1252
- Turkmani, A.M.D. and Goni, U.S. (1993) ‘Performance evaluation of Maximal-length, Gold and Kasami codes as spreading sequences in CDMA systems’, *IEEE International Conference on Universal Personal Communications*, vol. 2, pp. 970-974

Tarek K. H., Richard M. D., and Mohamed E.T. (2010) 'Analysis of BER performance in presence of nonlinear distortion due to PD-HPA in downlink DS-CDMA signals', *IEEE Communication Letters*, vol. 14, pp.273-275

Van-Houtum, W.J. (2001) 'Quasi-synchronous code-division multiple access with high-order modulation', *IEEE Transactions on Communications*, Vol. 49, No. 7, pp.1240-1249

Wang, C.L and Chen, C.H (2011) 'On the selection of partial cancellation factors for a two stage hard decision PPIC scheme in DS-CDMA systems' *IEEE Transaction on Wireless Communications*, vol. 10, pp.4008-4017

Wang, M.M., Brown, T., Fleming, P., and Xu, H. (2008) 'Walsh code assignment and data structure for variable data rate communications', *IEEE Transactions on Communications*, Vol. 56, No. 3, pp.339-343

Wieser, V. and Hrudkay, K. (2002) 'Mutual interference models for CDMA mobile communications networks', *Radio Engineering*, vol.11, No.4, pp.34-38

Woo, T.K. (2002) 'Orthogonal variable spreading codes for wide-band CDMA', *IEEE Transactions on Vehicular Technology*, vol.55, pp.700-709

Xinyu, Z. (2011) 'Analysis of m-sequence and Gold sequence in CDMA system', *IEEE 3rd International Conference on Communication Software and Networks (ICCSN)*, pp. 466-468

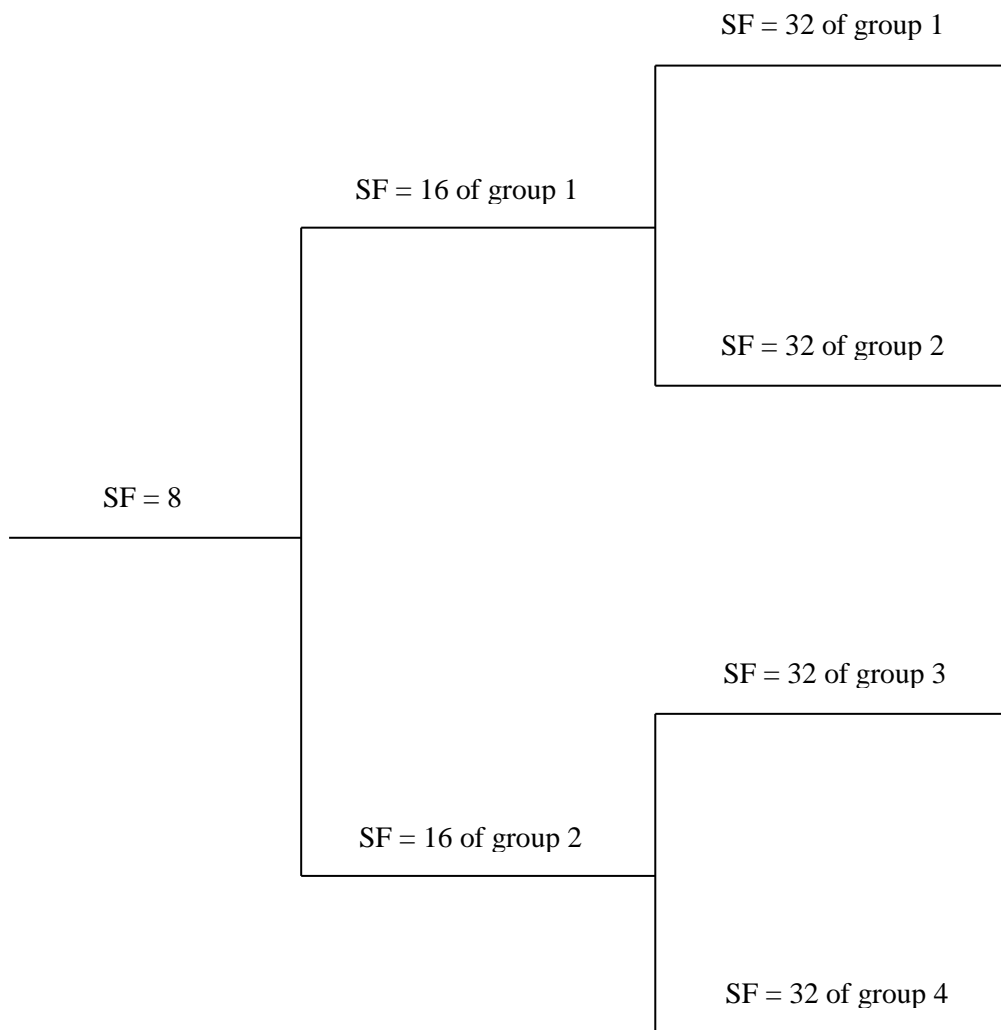
Ziani, A. and Medouri, A. (2012) 'Analysis of different pseudo-random and orthogonal spreading sequences in DS-CDMA', *IEEE International Conference on Multimedia Computing and Systems (ICMCS)*, pp.558-564

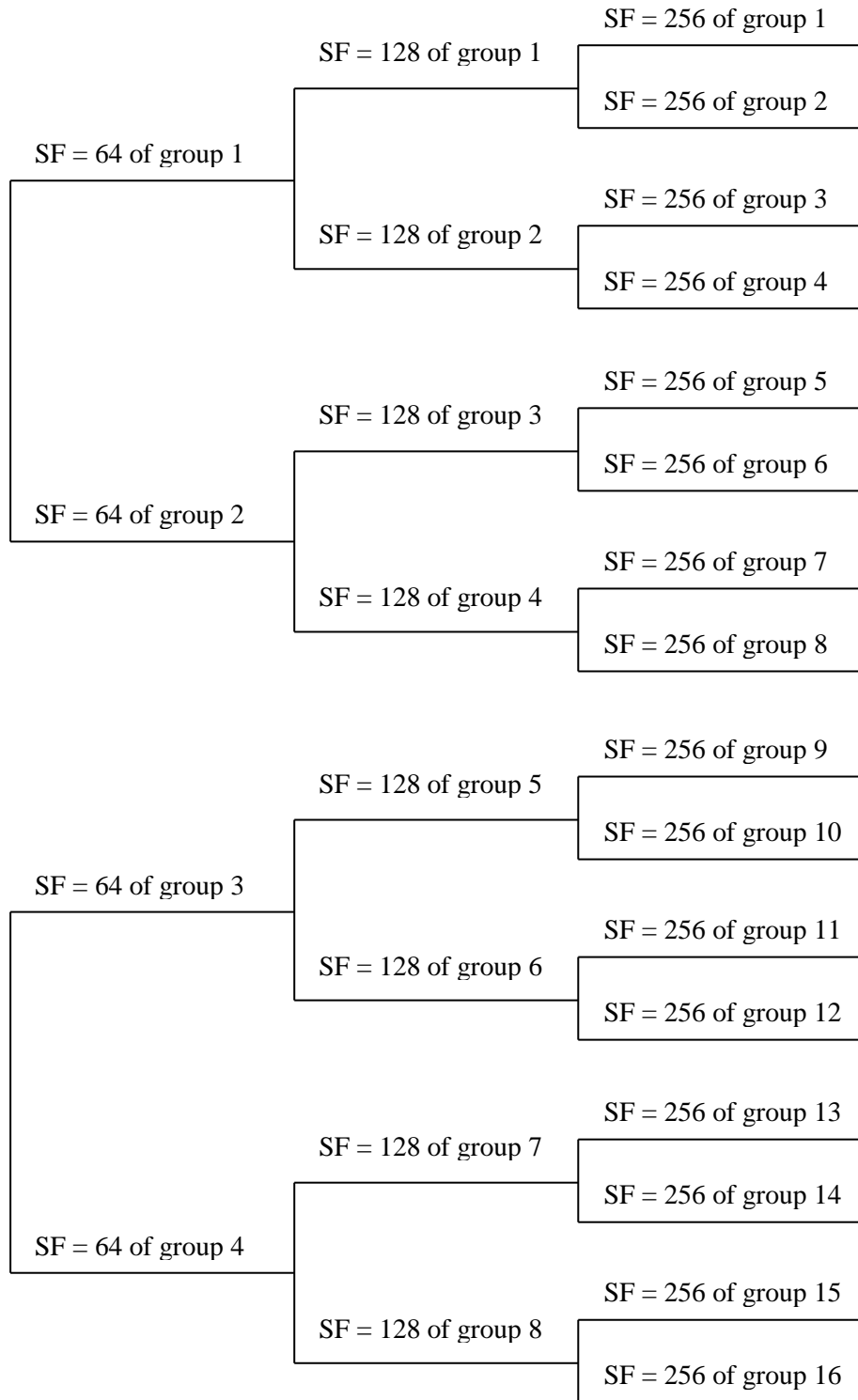
List of Conferences and Journal Submitted

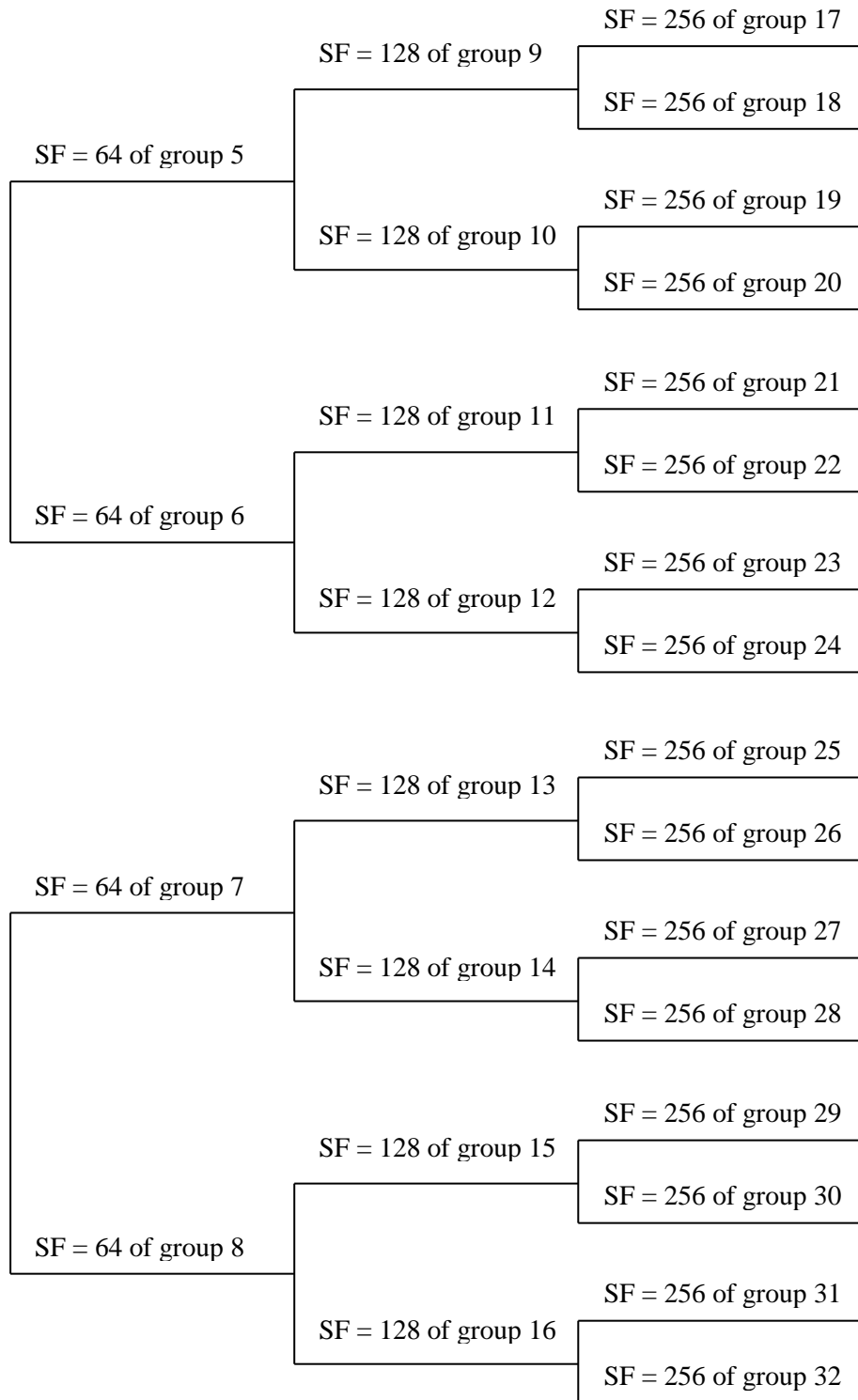
1. Pramaita, N. and Johnson, P.L. (2012) 'Performance evaluation of non-orthogonal and orthogonal spreading codes in synchronous CDMA system over Rayleigh flat and frequency selective fading channels', *GERI 7th Annual Research Symposium*, Liverpool John Moores University, Liverpool, UK, poster presentation
2. Pramaita, N. and Johnson, P.L. (2013) 'Hybrid orthogonal large set code sequence' *Fourth International Conference on Applied Technology, Science, and Arts*, Institut Teknologi Sepuluh Nopember, Surabaya, Indonesia
3. Pramaita, N. and Johnson, P.L. (2013) 'A Novel hybrid orthogonal very large set (HOVLS) code sequence for high-density mobile networks', *IEEE Transactions on Wireless Communications*

APPENDICES

A. The Code Tree for Generation of OVSF Gold Code Sequence and OVSF m-Sequence







B. Notation for OVSF Gold Code Sequence and OVSF m-sequence in the code tree

OVSF code sequence	Notations
SF = 8	OG_8
SF = 16 of group 1	OG_8OG_8
SF = 16 of group 2	$OG_8\overline{OG_8}$
SF = 32 of group 1	$OG_8OG_8OG_8OG_8$
SF = 32 of group 2	$OG_8OG_8\overline{OG_8}\overline{OG_8}$
SF = 32 of group 3	$OG_8\overline{OG_8}OG_8\overline{OG_8}$
SF = 32 of group 4	$OG_8\overline{OG_8}\overline{OG_8}OG_8$
SF = 64 of group 1	$OG_8OG_8OG_8OG_8OG_8OG_8OG_8OG_8$
SF = 64 of group 2	$OG_8OG_8OG_8OG_8\overline{OG_8}\overline{OG_8}\overline{OG_8}\overline{OG_8}$
SF = 64 of group 3	$OG_8OG_8\overline{OG_8}\overline{OG_8}OG_8OG_8\overline{OG_8}\overline{OG_8}$
SF = 64 of group 4	$OG_8OG_8\overline{OG_8}\overline{OG_8}\overline{OG_8}\overline{OG_8}OG_8OG_8$
SF = 64 of group 5	$OG_8\overline{OG_8}OG_8\overline{OG_8}OG_8\overline{OG_8}OG_8\overline{OG_8}$
SF = 64 of group 6	$OG_8\overline{OG_8}OG_8\overline{OG_8}\overline{OG_8}OG_8\overline{OG_8}OG_8$
SF = 64 of group 7	$OG_8\overline{OG_8}\overline{OG_8}OG_8OG_8\overline{OG_8}\overline{OG_8}OG_8$
SF = 64 of group 8	$OG_8\overline{OG_8}\overline{OG_8}\overline{OG_8}OG_8\overline{OG_8}OG_8\overline{OG_8}$
SF = 128 of group 1	$OG_8OG_8OG_8OG_8OG_8OG_8OG_8OG_8OG_8OG_8OG_8OG_8OG_8OG_8OG_8OG_8$
SF = 128 of group 2	$OG_8OG_8OG_8OG_8OG_8OG_8OG_8OG_8\overline{OG_8}\overline{OG_8}\overline{OG_8}\overline{OG_8}\overline{OG_8}\overline{OG_8}\overline{OG_8}$
SF = 128 of group 3	$OG_8OG_8OG_8OG_8\overline{OG_8}\overline{OG_8}\overline{OG_8}\overline{OG_8}OG_8OG_8OG_8OG_8\overline{OG_8}\overline{OG_8}\overline{OG_8}\overline{OG_8}$
SF = 128 of group 4	$OG_8OG_8OG_8OG_8\overline{OG_8}\overline{OG_8}\overline{OG_8}\overline{OG_8}\overline{OG_8}\overline{OG_8}\overline{OG_8}OG_8OG_8OG_8OG_8$
SF = 128 of group 5	$OG_8OG_8\overline{OG_8}\overline{OG_8}\overline{OG_8}\overline{OG_8}OG_8OG_8\overline{OG_8}\overline{OG_8}\overline{OG_8}\overline{OG_8}OG_8OG_8\overline{OG_8}\overline{OG_8}$
SF = 128 of group 6	$OG_8OG_8\overline{OG_8}\overline{OG_8}\overline{OG_8}\overline{OG_8}\overline{OG_8}\overline{OG_8}\overline{OG_8}OG_8OG_8\overline{OG_8}\overline{OG_8}\overline{OG_8}\overline{OG_8}OG_8OG_8$
SF = 128 of group 7	$OG_8OG_8\overline{OG_8}\overline{OG_8}\overline{OG_8}\overline{OG_8}OG_8OG_8OG_8OG_8\overline{OG_8}\overline{OG_8}\overline{OG_8}\overline{OG_8}OG_8OG_8$
SF = 128 of group 8	$OG_8OG_8\overline{OG_8}\overline{OG_8}\overline{OG_8}\overline{OG_8}\overline{OG_8}\overline{OG_8}\overline{OG_8}OG_8OG_8OG_8OG_8\overline{OG_8}\overline{OG_8}\overline{OG_8}\overline{OG_8}$
SF = 128 of group 9	$OG_8\overline{OG_8}OG_8\overline{OG_8}\overline{OG_8}\overline{OG_8}\overline{OG_8}OG_8\overline{OG_8}\overline{OG_8}\overline{OG_8}\overline{OG_8}OG_8\overline{OG_8}\overline{OG_8}\overline{OG_8}$
SF = 128 of group 10	$OG_8\overline{OG_8}OG_8\overline{OG_8}OG_8\overline{OG_8}\overline{OG_8}\overline{OG_8}\overline{OG_8}OG_8\overline{OG_8}\overline{OG_8}\overline{OG_8}\overline{OG_8}OG_8\overline{OG_8}\overline{OG_8}$
SF = 128 of group 11	$OG_8\overline{OG_8}\overline{OG_8}\overline{OG_8}\overline{OG_8}\overline{OG_8}\overline{OG_8}\overline{OG_8}OG_8OG_8\overline{OG_8}\overline{OG_8}\overline{OG_8}\overline{OG_8}OG_8OG_8$
SF = 128 of group 12	$OG_8\overline{OG_8}\overline{OG_8}\overline{OG_8}\overline{OG_8}\overline{OG_8}\overline{OG_8}\overline{OG_8}OG_8OG_8OG_8OG_8\overline{OG_8}\overline{OG_8}\overline{OG_8}\overline{OG_8}$

C. Matlab code/Simulink for HOVLS code sequence

C1. Generation of HOVLS code sequence

```
clc, clear all, close all;

%Code generation
n = 6;%number of register
N = 2^n - 1;%length of the code

sim('L_Kas');
y1 = out_L_Kasami; %element of L Kasami

sim('PN_Out')
y2 = out_PN; %element of m-sequence
M=N-1;

for k = 1:N
    B1(1,k)=y1(M+1)
    for i=1:M
        j=i+1;
        B1(j,k)=y1(i);
    end
    for l=1:(M+1)
        y1(l) = B1(l,k);
    end
end

w = 0;
x = N;
for i = 1:N
    for j = 1:(M+1)
        M1(i,j) = B1(j,x);
    end
    w=w+1;
    z=abs(1-w);
    x=N-(M-z);
end

M1_Box = M1;

for i = 1:N
    for j = 1:N
        M11(j,:,i)=M1_Box(i,:);
    end
end

for zz = 1:N
    if zz == 1
        for k = 1:N
            B2(1,k)=y2(M+1);
            for i=1:M
                j=i+1;
                B2(j,k)=y2(i);
            end
            for l=1:(M+1)
                y2(l) = B2(l,k);
            end
        end
    end
end
```

```

        end
    end
    w = 0;
    x = N;
    for i = 1:N
        for j = 1:(M+1)
            M2(i,j,zz) = B2(j,x);
        end
        w=w+1;
        z=abs(1-w);
        x=N-(M-z);
    end
    M2_Box = M2;
else
    y2 = M2_Box(zz)
    for k = 1:N
        B2(1,k)=y2(M+1);
        for i=1:M
            j=i+1;
            B2(j,k)=y2(i);
        end
        for l=1:(M+1)
            y2(l) = B2(l,k);
        end
    end
end

w = 0;
x = N;
for i = 1:N
    for j = 1:(M+1)
        M2(i,j,zz) = B2(j,x);
    end
    w=w+1;
    z=abs(1-w);
    x=N-(M-z);
end
end
end

M12 = [];
for i = 1:N
    M12(:, :, i) = bitxor(M11(:, :, i), M2(:, :, i));
end

for i = 1:N
    M12_aksen(:, :, i) = [M12(:, :, i); M11(i, :, i)];
end
for i = 1:N
    Buffer_M12_aksen(:, 1, i) = ~(M12_aksen(:, 1, i));
end

MA = ones([(N+1) 1]);
for j = 1:N
    for i = 1:(N-1)
        MB(:, i, j) = M12_aksen(:, (i+1), j);
    end
end

for i = 1:N

```

```

        M12_bintang_1(:, :, i) = [MA MB(:, :, i)];
    end

    for i = 1:N
        M12_bintang_2(:, :, i) = [M12_bintang_1(:, :, i)
        Buffer_M12_aksen(:, :, i)];

    end

    for j = 1:N
        HOVLS_Code(:, :, j) = 1 - (2.*M12_bintang_2(:, :, j));
    end

```

C2. Generation of orthogonal Gold code sequence

```

clc, clear all, close all;

%Code generation
n = 6;%number of register
N = 2^n - 1;%length of the code
sim('Gold_1');
y1 = out_Gold_1;
sim('Gold_2');
y2 = out_Gold_2;
M=N-1;

for k = 1:N
    B1(1,k)=y1(M+1);

    for i=1:M
        j=i+1;
        B1(j,k)=y1(i);

    end
    for l=1:(M+1)
        y1(l) = B1(l,k);

    end
end

w = 0;
x = N;
for i = 1:N
    for j = 1:(M+1)
        M1(i,j) = B1(j,x);
    end
    w=w+1;
    z=abs(1-w);
    x=N-(M-z);
end

M1_Box = M1;
for i = 1:N
    for j = 1:N
        M11(j, :, i)=M1_Box(i, :);
    end
end

```

```

for zz = 1:N
    if zz == 1
        for k = 1:N
            B2(1,k)=y2(M+1);
            for i=1:M
                j=i+1;
                B2(j,k)=y2(i);
            end
            for l=1:(M+1)
                y2(l) = B2(l,k);
            end
        end

        w = 0;
        x = N;
        for i = 1:N
            for j = 1:(M+1)
                M2(i,j,zz) = B2(j,x);
            end
            w=w+1;
            z=abs(1-w);
            x=N-(M-z);
        end
        M2_Box = M2;
    else
        y2 = M2_Box(zz,:);
        for k = 1:N
            B2(1,k)=y2(M+1);
            for i=1:M
                j=i+1;
                B2(j,k)=y2(i);
            end
            for l=1:(M+1)
                y2(l) = B2(l,k);
            end
        end

        w = 0;
        x = N;
        for i = 1:N
            for j = 1:(M+1)
                M2(i,j,zz) = B2(j,x);
            end
            w=w+1;
            z=abs(1-w);
            x=N-(M-z);
        end
    end
end

M12 = [];
for i = 1:N
    M12(:, :, i) = bitxor(M11(:, :, i), M2(:, :, i));
end

MA = ones([N 1]);

for i = 1:N
    U(1, :, i) = [M11(1, :, i) 1];
end

```

```

for i = 1:N
    M12_Gold(:, :, i) = [M12(:, :, i) MA];
    goldn(:, :, i) = [U(1, :, i); M12_Gold(:, :, i)];
end

for j = 1:N
    Orthog_Gold(:, :, j) = 1 - (2.*goldn(:, :, j));
end

```

C3. Generation of orthogonal m-sequence

```

clc, clear all, close all;

%Code generation
n = 6;%number of register
N = 2^n - 1;%length of the code

sim('m_sequence_1');
y1 = out_m_sequence_1;

sim('m_sequence_')%
y2 = out_m_sequence_2;
M=N-1;

for k = 1:N
    B1(1,k)=y1(M+1);

    for i=1:M
        j=i+1;
        B1(j,k)=y1(i);

    end
    for l=1:(M+1)
        y1(l) = B1(l,k);

    end
end

w = 0;
x = N;
for i = 1:N
    for j = 1:(M+1)
        M1(i,j) = B1(j,x);

    end
    w=w+1;
    z=abs(1-w);
    x=N-(M-z);
end

M1_Box = M1;

for i = 1:N
    for j = 1:N
        M11(j, :, i)=M1_Box(i, :);
    end
end

```

```

for zz = 1:N
    if zz == 1
        for k = 1:N
            B2(1,k)=y2(M+1);
            for i=1:M
                j=i+1;
                B2(j,k)=y2(i);
            end
            for l=1:(M+1)
                y2(l) = B2(l,k);
            end
        end

        w = 0;
        x = N;
        for i = 1:N
            for j = 1:(M+1)
                M2(i,j,zz) = B2(j,x);
            end
            w=w+1;
            z=abs(1-w);
            x=N-(M-z);
        end
        M2_Box = M2;
    else
        y2 = M2_Box(zz,:);
        for k = 1:N
            B2(1,k)=y2(M+1);
            for i=1:M
                j=i+1;
                B2(j,k)=y2(i);
            end
            for l=1:(M+1)
                y2(l) = B2(l,k);
            end
        end

        w = 0;
        x = N;
        for i = 1:N
            for j = 1:(M+1)
                M2(i,j,zz) = B2(j,x);
            end
            w=w+1;
            z=abs(1-w);
            x=N-(M-z);
        end
    end
end

M12 = [];
for i = 1:N
    M12(:, :, i) = bitxor(M11(:, :, i), M2(:, :, i));
end

for i = 1:N
    M12_aksen(:, :, i) = [M12(:, :, i); M11(i, :, i)];
end

```

```

for i = 1:N
    Buffer_M12_aksen(:,1,i) = ~(M12_aksen(:,1,i));
end

MA = ones([(N+1) 1]);

for j = 1:N
    for i = 1:(N-1)
        MB(:,i,j) = M12_aksen(:,(i+1),j);
    end
end

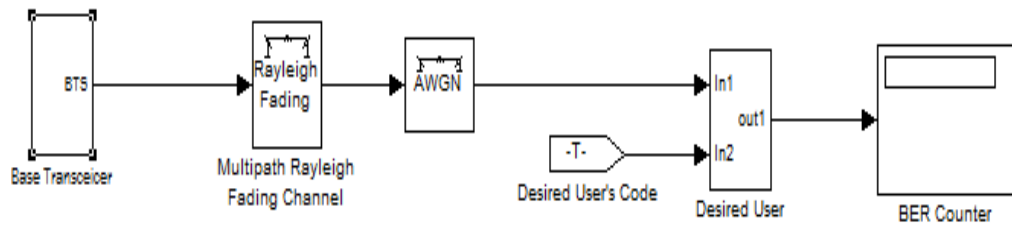
for i = 1:N
    M12_bintang_1(:, :, i) = [MA MB(:, :, i)];
end

for i = 1:N
    M12_bintang_2(:, :, i) = [M12_bintang_1(:, :, i)
    Buffer_M12_aksen(:, :, i)];
end

for j = 1:N
    O_m_seq(:, :, j) = 1 - (2.*M12_bintang_2(:, :, j));
end

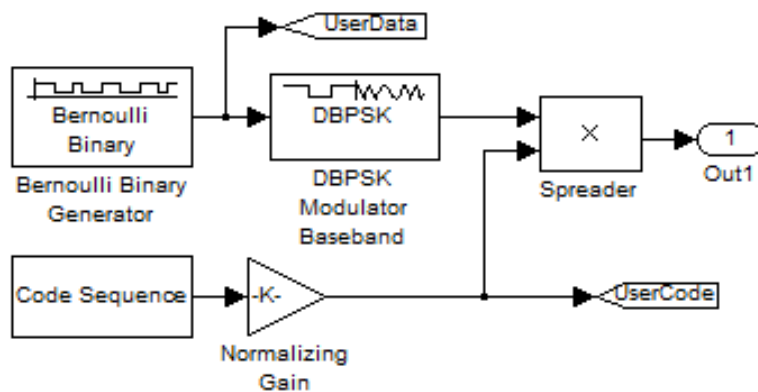
```

C4. Block of Simulink for CDMA system



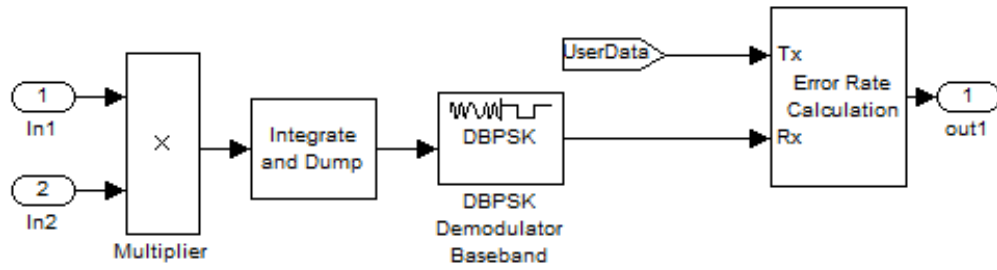
C4.1 Block of Simulink for Base Transceiver

Block of base transceiver (BTS) contains 64 of the following block of Simulink of users in CDMA system. This block was used for simulation of users at BTS of fixed length orthogonal code sequence. The block was also used for users R at BTS for simulation of OVSF code sequences.

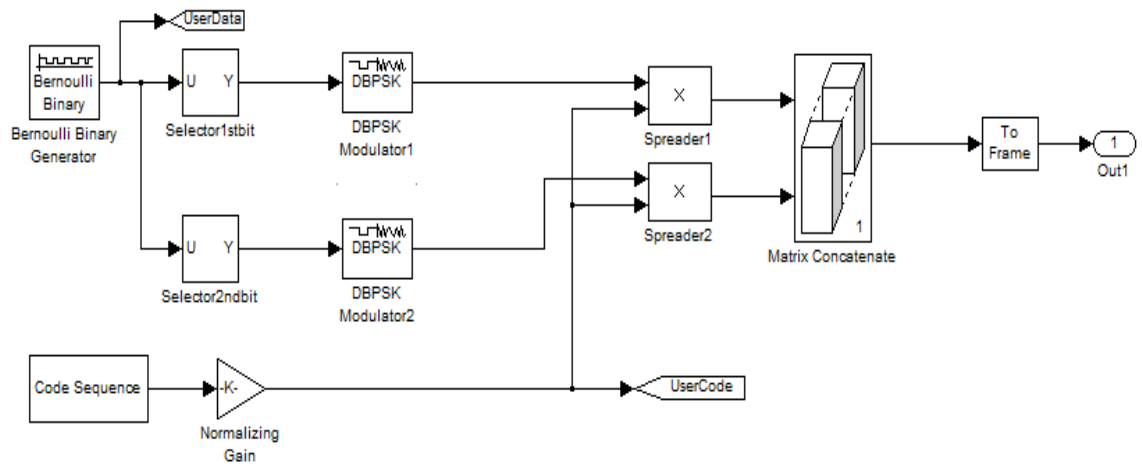


C4.2 Block of Simulink for desired user's receiver

The following block was used for desired user's receiver for simulation of fixed length orthogonal code sequence. The block was also used for desired user R's receiver for simulation of OVSF code sequences.



C4.3 Block of Simulink for users 2R at BTS



C4.4 Block of Simulink for desired user's receiver for user 2R

